Spring 5-15-2017

Factors that Contribute to de novo Protein Misfolding and Prion Formation in Saccharomyces cerevisiae

Kathryn Morgan Keefer
Washington University in St. Louis

WASHINGTON UNIVERSITY IN ST. LOUIS

Division of Biology and Biomedical Sciences
Molecular Genetics and Genomics

Dissertation Examination Committee:
Dr. Heather L. True, Chairperson
Dr. Kendall Blumer
Dr. Barak Cohen
Dr. Sergej Djuranovic
Dr. Chris Weihl

Factors that Contribute to *de novo* Protein Misfolding and Prion Formation in *Saccharomyces cerevisiae*

By
Kathryn Morgan Keefer

A dissertation presented to
The Graduate School
of Washington University in
partial fulfillment of the
requirements for the degree
of Doctor of Philosophy

May 2017
St. Louis, Missouri

Table of Contents

List of Figures

List of Tables

Acknowledgments

I cannot thank Heather enough for being a fantastic boss, mentor, and friend over the last 5 years. She has supported me, encouraged me, and pushed me to be a better scientist and person. Beyond her incredible scientific talent, she is also one of the hardest-working people I have ever met. She inspires the whole lab by her work ethic and her advocacy for graduate students serves as an example for all faculty. I am going to miss our random conversations throughout the day. Again, Heather, thank you so much.

My thesis committee is a group of profoundly thoughtful and intelligent people. Ken, Barak, Chris, and Sergej always created an enjoyable meeting environment, and each committee member provided sound advice and encouraged me to think about my work in different ways. Ken, thank you for serving as Chair and for encouraging me to strive to be the best at whatever I choose to do.

My labmates have been a source of motivation, friendship, and comic relief. Big thanks to the crew who welcomed me to the lab – Laura, Kevin, Jen, Donnel, Siyao, and Vince. I am so glad to have seen Leeran, Ankan, and Melanie join the group, and I appreciate their support and understanding while I locked myself in the break room to write this thesis.

My friends have added so much happiness to my time in St. Louis. Meg and Chung, I love you and our many adventures. Heather, thank you for always being up for a coffee break or a glass of wine, depending on the time of day. Allie, I miss our weekly Bread Co meetings and I am excited that we will soon be neighbors in NYC! A huge “thank you” to everyone in The BALSA Group

for many years of camaraderie -- I have learned something from each one of you and am so proud of what we have accomplished over the course of 150+ Wednesday mornings.

Brian, you came into my life while I was trying to simultaneously finish my first manuscript, take the reins as President of BALSA, interview at numerous consulting firms, get ready to sell my house, and find stability in all the flux. It was the busiest period of my career thus far, but you were in my corner from day one. Your constant support means the world to me, and I am so excited to take on new adventures together. Thank you for everything.

Finally, I would like to thank my family for being my foundation and my rock during years of ups and downs. Mom and Dad, thank you for always being just a phone call away and for your understanding when those calls were spaced too far apart. Grandma and Pappy, you always knew exactly what to say to cheer me up and get me to face another set of experiments. This work is dedicated to my brother, Grant, for making me proud every single day.

Kathryn Keefer

Washington University in St. Louis

May 2017

ABSTRACT OF THE DISSERTATION

Factors that Contribute to *de novo* Protein Misfolding and Prion Formation in *Saccharomyces cerevisiae*

by

Kathryn Keefer

Doctor of Philosophy in Biology and Biomedical Sciences

Molecular Genetics and Genomics

Washington University in St. Louis, 2017

Professor Heather True, Chair

Protein misfolding is a common phenomenon that can have severe consequences on cellular and organismal health. Despite this, the causes of protein misfolding remain poorly understood. Prions are a class of proteins that, when misfolded, can convert other molecules into a heritable, non-native conformation. The yeast *Saccharomyces cerevisiae* naturally harbors several diverse prion-forming proteins; thus, it is an ideal model with which to investigate the factors that influence misfolding and aggregation.

This thesis utilizes the yeast prions [*PSI*+] and [*RNQ*+] to investigate two distinct steps of the protein misfolding pathway: interactions with chaperones and their cofactors, and heterologous templating by other misfolded proteins. Chaperones are proteins that help other proteins fold correctly, yet we have found that chaperones can have non-intuitive effects upon cells that harbor the prion [*PSI*+]. An overabundance of the Hsp70 chaperone Ssa1 relative to the Hsp70 Ssb1 exacerbates [*PSI*+]-related toxicity. This toxicity can be rescued by overexpressing a Hsp70 nucleotide exchange factor, Sse1, that may improve Ssb1 functionality in the presence of excess

available Ssa1. Our results imply that the balance of molecular chaperones is finely tuned and is crucial to maintaining protein homeostasis.

Interestingly, the [*PSI*+] prion cannot form without the presence of an inducing factor, which is most commonly the [*RNQ*+] prion. The nature of the interaction between [*PSI*+] and [*RNQ*+] was previously unknown. Here, we have demonstrated that the two proteins undergo cross-seeding reaction, wherein the prion-forming proteins bind to one another to template the formation of [*PSI*+]. Blocking or restoring a binding site can have significant impacts upon the frequency of prion formation. As cross-seeding has been implicated in several human pathologies, these results may inform key principles that can be utilized to research disease prevention.

Chapter 1: Introduction

1.1 Overview

Proteins perform diverse roles within all cells and are essential for maintaining life. From unicellular bacteria to multi-systemed mammals, all living things depend on proteins to provide cellular structure, perform metabolic reactions, act in signaling cascades, and function in material transport. The proper function of these molecules is dependent upon proteins achieving their proper secondary and tertiary folds, or conformations. Errors in protein folding can have disastrous results on protein homeostasis, or proteostasis, and can lead to death at the cellular, tissue, or organismal level (1). In humans, misfolded proteins are implicated in pathologies such as Alzheimer's Disease, muscular dystrophy, type II diabetes, and Huntington's Disease (2). Despite the prevalence of these diseases and the knowledge of the proteins involved, there are major questions that have yet to be answered about the cause of such protein misfolding. This thesis seeks to address two questions that are broadly summarized as follows: What factors influence the initiation of aggregation, and how is misfolding propagated from molecule to molecule?

1.2 Cellular responses to protein misfolding

Protein misfolding is a phenomenon wherein a polypeptide adopts a conformation other than its functional native state. Misfolding can occur co-translationally, while still emerging from an active ribosome, or post-translationally, in the cytosol or other cellular compartment (3–6). The fates of misfolded proteins vary. They may be refolded through the actions of chaperone proteins, they may accumulate in aggregates, or they may be degraded by the ubiquitin-proteasome system or by the autophagy-lysosome pathway (5,6). These outcomes are not mutually exclusive; for example, a protein may aggregate prior to its eventual degradation.

One of the ways that cells respond to protein misfolding is by producing chaperones. Chaperones are proteins whose role is to assist other proteins in achieving a proper conformation.

Chaperones are present in all known organisms and some chaperone families are highly conserved across kingdoms (7). There is great diversity between chaperone classes. Some chaperones are ATPases that are thought to protect proteins from the crowded cytosolic environment in order to allow independent refolding (e.g. Hsp70s in humans and yeast, DnaK in E. coli). Other chaperones act as cofactors to larger complexes and are responsible for substrate identification and delivery (e.g. Hsp40s in yeast, J proteins in humans). Still others function as hexameric disaggregases (e.g. Hsp104 in yeast, ClpB in bacteria) that actively unfold client proteins. Interestingly, though metazoans do not have a chaperone homologous to this latter class of proteins, chaperone networks are ubiquitously robust. Yeast contain more than 60 distinct chaperones, and human cells contain an estimated 200 distinct chaperone types (8,9).

Chaperone activity is not always sufficient to allow a protein to fold correctly. In some cases, misfolded proteins will form quaternary aggregates that remain within the cell. Broadly, there are two types of aggregation that are relevant to this thesis: prion and non-prion. Prion aggregation is a unique type of protein misfolding that results in the formation of self-propagating, beta sheet-rich amyloids. The generation and structure of prions will be discussed in section 1.3.

Non-prion aggregates are more common and are generally formed from highly-damaged proteins that will eventually be degraded. In yeast, these proteins may be localized to one of three cellular compartments: the juxtanuclear quality control compartment (JUNQ), the insoluble protein deposit (IPOD), or the intranuclear quality control compartment (INQ) (10,11). The proteins in the JUNQ are more immediate targets for degradation by the ubiquitin-proteasome system, while aggregates in the IPOD are stored in the cell for a longer period of time and may eventually be degraded via autophagy (10). In mammalian cells, aggregated proteins also form both juxtanuclear and IPOD-like inclusions. For example, an aggregate storage structure called the

aggresome is surrounded by cytoskeletal filaments and localizes adjacent to the nucleus (12). Overall, these structures serve as holding compartments until proteins can be processed by the cellular machinery.

Some of these misfolded proteins are ultimately degraded by one of two cellular pathways: the ubiquitin-proteasome system (UPS) or autophagy. Both are highly-conserved throughout Eukarya. In the UPS, terminally misfolded proteins are marked for destruction via the attachment of a small protein, ubiquitin, to a lysine within the target protein (13,14). This action is performed by E3 ubiquitin ligases, which also act to form the K48 polyubiquitin chains that are necessary for recognition by the proteasome. The proteasome recognizes the ubiquitin-marked species and subsequently degrades the proteins. The proteasome itself is a multimeric complex comprised of a 20S core and a 19S cap (15). The barrel-shaped core is where degradation takes place, and the cap serves a regulatory function by translocating misfolded proteins and hydrolyzing ATP (16). Due to its specific targeting of polyubiquitinated proteins, the UPS is considered a highly-specific pathway.

In contrast, autophagy is a less-specific, though still regulated, process by which the lysosome degrades cellular components. Autophagy targets include organelles, large protein aggregates, and other bulk macromolecules (17,18). Nutrient starvation is a common cause of autophagy, as are overcrowding, thermal stress, and cellular damage (17,19,20). In brief, the highly conserved process begins with the formation of the double-membraned autophagosome, in which a long membrane called a phagophore randomly envelops cellular components (18). Then, the autophagosome fuses with the lysosome or vacuole (in metazoans or plants/yeast, respectively) to begin degradation (18). Following digestion, amino acids are recycled back into the cytosol in a

process that is poorly understood (21,22). It is unknown whether autophagy is able to recycle carbohydrates and nucleic acids, or whether the process is protein-specific (18).

1.3 Prion aggregation and strains

Prions are a unique class of misfolded proteins that remain incompletely understood. Though every protein can theoretically misfold and aggregate, not every protein can form a prion. When prion-forming proteins aggregate, they form insoluble fibers called "amyloid." Amyloid fibers can vary in width and length, but are characterized by a cross-beta pattern, in which beta strands extend perpendicularly with regards to the fiber axis but form sheets that run parallel to the fiber axis (23–25). Within these beta sheets, variation can exist in the orientation of beta-strands and in the alignment between amino acids within the beta sheets. Beta strands can run antiparallel or parallel to one another (Figure 1.1), and amino acids within parallel sheets can align in-register or be out of register (23). A rare amyloid conformation, β-solenoid, is a "sandwich" structure that can be categorized as containing either β-helices or β-rolls. Notably, the Alzheimer's-related Aβ protein is thought to form a β-solenoid structure (23).

In addition to Aβ, other non-prion-forming proteins can aggregate in amyloid structures. What, then, sets prions apart from other proteinaceous aggregates? Prions are unique in that their aggregates are self-propagating; that is, they can induce the misfolding of monomeric proteins to replicate structures that join the pre-existing template and form additional prion seeds (Figure 1.2)(26). The basis of this transformation remains poorly understood, and is discussed in greater detail in Chapter 4. This self-propagating characteristic is what leads to the pathogenic nature of some prions; notably, the human prion protein.

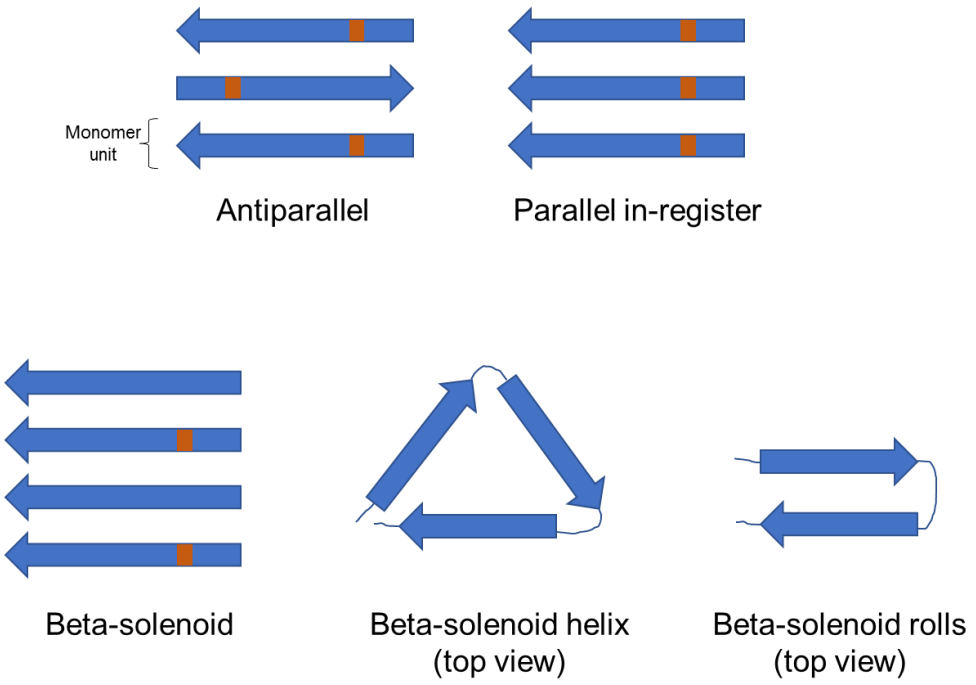

Figure 1.1. Possible orientations of beta sheets within amyloid fibers. All diagrams are of a "side view" perspective of the fiber unless otherwise indicated. Red patches indicate corresponding amino acids from different monomer units. Adapted from Toyama and Weissman, 2011.

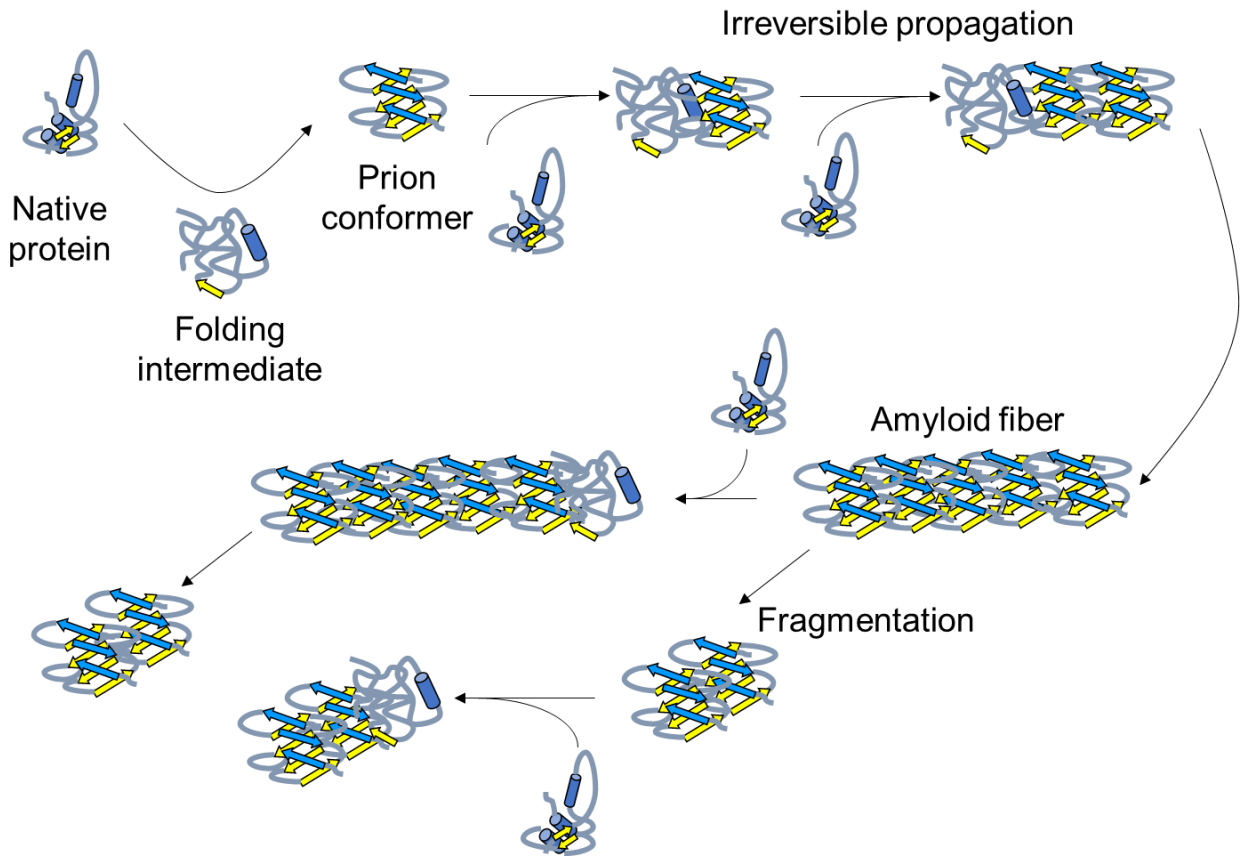

Figure 1.2. The prion life cycle. A native protein misfolds into a prion conformation, forming a prion "seed." The seed can template other monomers to misfold and add onto the end of a growing amyloid fiber. The fragmentation of amyloid fibers, by chaperones or other factors, produce additional seeds that promote prion propagation.

There is only one known prion-forming protein in mammals, PrP (for Prion Protein). This protein is expressed in many tissue types, but is most highly-expressed in the central nervous system (CNS) (27–29). When in its native conformation, denoted PrP^{C}, the protein is glycosyl-

phosphatidylinositol (GPI) anchored to the cell surface and is non-pathogenic. The function of PrP^{C} is unknown, though it has been suggested to play diverse roles in anti-apoptosis pathways, protection against oxidative stress, and transmembrane signaling (30). When PrP misfolds, it is called PrP^{Sc} and its aggregation causes severe, terminal disease that begins in the CNS (31). The cohort of resultant diseases, together called transmissible spongiform encephalopathies (TSEs), include bovine spongiform encephalopathy (BSE) or "mad cow" in cattle, chronic wasting disease (CWD) in deer and elk, and Creutzfeldt-Jakob disease (CJD) and *kuru* in humans (31–33). The TSEs lead to a steady decline in cognition, eventual loss of motor control, and death within a short timescale. Human proteinopathies, including prion diseases, are discussed in further detail in section 1.4.

Interestingly, though all TSEs are caused by the same misfolding prion protein, there is variability between some disease features. The incubation period, rate of disease progression, and specific symptoms may differ between organisms of the same species (34). This is thought to be due to different amyloid conformations that are adopted by PrP^{Sc} when it misfolds (35). In other words, different prion "strains" may exist as a result of amyloid diversity. There is experimental evidence to support the concept of different prion strains in mammals (35,36). When treated with Proteinase K, PrP^{Sc} is digested into different fragment sizes between different aggregates (37). This suggests that the aggregates have adopted distinct conformations that are differentially available to the proteinase (38–40). Further, there are two mink prion strains – hyper (HY) and drowsy (DY) – that are both comprised of PrP^{Sc} but result in differing disease phenotypes (41,42). These two strains show differential susceptibility to protease digestion, differing patterns of sedimentation, and are both propagable over many generations (41,42). However, confounding

factors such as genetic background, the environment, and methodology can hamper discovery of prion aggregate characteristics.

1.4 Human proteinopathies

A variety of human diseases can arise from misfolded and aggregated proteins. These diseases may either be caused by the prion protein PrP or by non-prion aggregation, though the definition of "prion" is becoming blurred as new research suggests infectivity of non-PrP amyloid (43–45).

1.4.1 Transmissible spongiform encephalopathies, a.k.a. prion diseases

All mammalian prion diseases are caused by PrP^{C} conversation into pathogenic PrP^{Sc}, and are collectively called "transmissible spongiform encephalopathies" (TSEs). In humans, these pathologies are called several different names, including Creutzfeldt-Jakob Disease (CJD), *kuru*, fatal familial insomnia (FFI), and Gerstmann-Sträussler-Scheinker syndrome (GSS). Patients suffering from these conditions experience progressive neurodegeneration, loss of motor control, dementia, and eventual death. These diseases also differ in their origins: while most cases of CJD are spontaneous (having no obvious genetic link), FFI is inherited from generation to generation (46,47). On the other hand, *kuru* is most prevalent in cannibalistic tribes in Papua New Guinea, who obtained the disease from eating the neural tissue of afflicted deceased (48). Though this type of inter-organismal infectivity is characteristic of TSEs, there is typically a barrier to inter-species transmission. However, this species barrier can in some cases be overcome, most notably during the "mad cow disease" (bovine spongiform encephalopathy) outbreak in the United Kingdom in the early 1990s (36,49,50). This zoonotic transmission of PrP^{Sc} from cows to humans, via tainted beef, led to variant CJD (vCJD) that was unique in its early age of onset and slow disease progression (50). Similarly, deer afflicted with the TSE known as Chronic Wasting Disease

(CWD) are endemic to parts of the United States and are considered a potential threat to human health if consumed (51). The reasons why some TSEs can overcome the species barrier have yet to be elucidated, though the conformation of the misfolded PrP^{Sc} is thought to be a contributing factor (52).

1.4.2 Pathologies related to protein aggregation

The non-prion proteinopathies of humans show greater diversity in appearance, inheritance, and pathology. Some of the well-known protein misfolding diseases include Alzheimer's disease, Parkinson's disease, Huntington's disease, and amyotrophic lateral sclerosis. These diseases are characterized by neurodegeneration, but the specific types of affected neurons differ from condition to condition. Other diseases that arise from protein aggregation include some forms of muscular dystrophy, several types of dementia, and type-2 diabetes. Further, while TSEs are all caused by the conversion of PrP, there are a diversity of non-prion proteins that contribute to the above pathologies. The detailed etiologies of each disease are diverse and outside the scope of this thesis, but cross-seeding between heterologous proteins have been implicated as factors in several of these pathologies.

Two major types of aggregation occur in Alzheimer's disease: the formation of intracellular amyloid-β (Aβ) peptides, and the accumulation of extracellular tangles of the microtubule-associated protein tau. Mouse studies indicate that Aβ initiates tangle formation, which leads to synaptic dysfunction (53,54). However, the relationship appears to be bidirectional, with the presence of tau being a requirement for Aβ accumulation (55). The conflicting evidence related to which aggregating species is upstream of the other has led to the suggestion of a feedback loop, in which external factors can lead to the misfolding of either Aβ or tau, which then continue to cross-seed each other's aggregation (56). Though the aggregates of Aβ and tau do not localize

to the same region, it has been suggested that Aβ peptides may seed tau into more pathological forms prior to its prion-like spread (57). Interestingly, α-synuclein, the Parkinson's disease-related protein, has also been shown to cross-seed tau aggregation (58). The resulting emergence of separate tau conformers (59) has prompted researchers to posit the existence of multiple α-synuclein "strains," as is seen with prion diseases (58).

Type-2 diabetes (T2D) is a unique proteinopathy because it does not affect the nervous system, unlike many of its related amyloidoses. The aggregating species in T2D is islet amyloid polypeptide, IAPP, which accumulates in pancreatic β-cells and eventually leads to cell death (60). Recently, it was discovered that α-synuclein may be present in β-cells under certain conditions, and an epidemiological study found that T2D was associated with an increased risk for the development of Parkinson's disease (61,62). A similar relationship has been described for T2D and Alzheimer's disease (63). Further, IAPP was found to seed the polymerization of Aβ *in vitro*, suggesting a cross-seeding relationship (64). The connectivity between aggregation-prone proteins of common human diseases highlights the need for greater understanding of the molecular factors that influence cross-seeding, as is described in Chapter 4.

1.5 Functional aggregation of bacteria, fungi, and metazoans

Though amyloidogenic proteins are well-known for causing disease in mammalian systems, functional aggregation exists in bacteria, fungi, and even animals. Further, cross-seeding may play a role in initiating and propagating these functional amyloids.

1.5.1 Curli aggregation of Enterobacteriaceae

In bacteria, the "curli" amyloid is believed to assist in biofilm formation and host invasion. The proteins that comprise these aggregates are encoded by operons that have been identified within *E. coli* and *Salmonella* species. In E. coli, the *csgBA* and *csgDEFG* operons transcribe 6

proteins, two of which play major structural roles (65). These proteins, CsgA and CsgB, share some homology and contain β-strand-forming repeat peptides, as do the non-homologous prion-forming proteins Sup35 and PrP (66,67). Interestingly, the aggregation of CsgA is dependent upon the presence of CsgB: without CsgB, CsgA remains monomeric and soluble (66), suggesting cross-seeding. However, CsgA and CsgB need not be expressed within the same cell for aggregation to take place, as cells expressing CsgB can receive secreted CsgA from a "donor" cell. Once curli has assembled into amyloid fibers, bacterial patches can strongly adhere to smooth surfaces, including stainless steel (68). The role of curli amyloid in pathogenicity is incompletely understood, but curli has been shown to interact with several host proteins (69). In one example, curli binds simultaneously to an inactive protease and its activator, which converts the proenzyme to an active form that can degrade soft tissue (70). The functional role of curli – and its potential to provide an advantage to pathogenic bacteria – highlight the complex utility of amyloid in nature.

1.5.2 [*Het-s*] *prion of Podospora anserine*

Saccharomyces cerevisiae is not the only prion-harboring fungus, as the filamentous *Podospora anserina* contains a well-described prion called [Het-s](71). The HET-s protein plays a role in heterokaryon incompatibility; that is, the relationship between different multinucleate cells. The [Het-s] prion system differs from the *S. cerevisiae* prions, as there is a genetic component that helps to determine the prion state. This system involves two alleles that code for the HET-s protein, these alleles are named *het-s*, which allows formation of the prion [Het-s] or the non-prion state [Het-s*], and *het-S*, which does not allow for prion formation and whose phenotype is denoted [Het-S]. The phenotypic states arising from these two alleles are incompatible. Cell death occurs if a [Het-s] fungus fuses with a [Het-S] partner; however, a genetically identical [Het-s*] strain can successfully fuse with a [Het-S] cell (72). The proteins resulting from the *het-s* and *het-S* alleles

differ by just 13 amino acids, with two non-prion-forming domain residues (23 and 33) playing the largest functional role in heterokaryon incompatibility. Like Sup35 and PrP, HET-s has a prion-forming domain that helps to transition the monomeric protein to a self-perpetuating amyloid, but the protein is far less Q/N-rich than the *S. cerevisiae* prions (73,74). The specific nature of the toxic reaction between [Het-s] and [Het-S] cells is unknown, but dimerization between a prion seed and a non-prion HET-s molecule is thought to be an important molecular switch (72). Thus, the HET-s system is an example of not just functional prion formation, but functional cross-seeding as well.

1.5.3 CPEB3 aggregation in metazoan memory formation

The mouse cytoplasmic polyadenylation element-binding protein 3 (CPEB3) is a conserved, amyloid-forming protein that displays prion-like characteristics. Its invertebrate orthologs, notably CPEB in the slug *Aplysia* and Orb2 in *Drosophila*, have been implicated in long-term memory storage via helping to direct synaptic connections (75,76). As with other amyloid-forming proteins, CPEB3 contains a Q-rich domain that has been described as a functional prion (77). Following synaptic activity, CPEB3 is upregulated and forms SDS-resistant aggregates in murine hippocampi. Cortical and hippocampal knockout of the CPEB3 gene led to mice that were impaired in long-term, but not short-term, memory formation in a variety of learning tests (78). Functionally, CPEB3 acts through the AMPA receptor pathway by binding to the mRNAs of receptor subunits GluA1 and GluA2 (79,80). This binding represses their translation. Following activation of neurons, CPEB3 is ubiquitinylated and translation of GluA1 and GluA2 is activated, leading to a new synaptic spine (79). During this process, a steric inhibitor of CPEB3 is removed, allowing for its subsequent aggregation (81). It has been suggested that aggregation of CPEB3 serves as a mechanism for strengthening long-term memory by providing

a seed template for the rapid aggregation of new CPEB3 upon re-activation of the synapse (78). Though more experimentation will be necessary to clarify CPEB3's role in memory (82), its aggregates have been demonstrated to have a lifespan that could support long-term memory storage (83).

1.6 *Saccharomyces cerevisiae* as a model system to study prion characteristics

There are limitations of mammalian organisms that prevent the elucidation of basic principles of prion generation. Questions such as how prions form *de novo,* how they are propagated between cells and organisms, and how misfolded proteins may interact with native proteins, are time-consuming and difficult to parse when working in a multicellular system. Techniques have been developed to biochemically assess mammalian prions via seeding protocols that attempt to detect conformational changes during aggregation (84,85); however, these provide limited mechanistic insights and are known to yield inconsistent results (84,86). Further, methods of inducing prion conversion *in vivo* often involve cerebral injections that do not recapitulate natural events or disease progression (87). Finally, the lack of understanding about the function of PrP and its interactions with other molecular agents make mammals an insufficient system by which to study prion generation and propagation.

The baker's yeast *Saccharomyces cerevisiae* is an important model system for the study of protein misfolding and prions. Not only does this unicellular Eukaryote have a well-characterized genome and an array of available proteomic tools, but prions are naturally occurring epigenetic elements in yeast. There are approximately eleven identified prions in yeast, and many more phenotypes that exhibit prion-like features (88,89). The yeast prions are diverse in function and consequence, but all share certain characteristics with mammalian prions; namely, they form self-propagating amyloid fibers, are transmitted cytoplasmically between cells, and can form different

strains (88). However, yeast prions are generally not cytotoxic, and can even have benefits to cells that harbor aggregates (90). Further, there are well-established *in vivo* and *in vitro* techniques that have been developed to facilitate the investigation of prions in yeast.

1.6.1 Yeast prion overview

Yeast prions, like mammalian prions, are the amyloid aggregates of misfolded proteins. The monomeric protein that constitutes a prion is referred to by its protein name, while its prion form is specified by an uppercase denotation within brackets, which indicates its epigenetic transmission. For example, the protein Sup35 aggregates to form the prion state called [*PSI*+]. The non-prion state of Sup35 is then denoted as [*psi*-]. Since misfolded proteins often lose their native functions, prion aggregation in yeast usually mimics the loss-of-function phenotype of its monomeric constituent. Thus, prion aggregation can serve a regulatory function by controlling the amount of functional protein that is available in the cell. Of the seven best-characterized yeast prions, four are transcriptional regulators, one is a translation termination factor, and one is involved in nitrogen regulation (88). The formation of these prions have diverse consequences upon the phenotype of their host cells without altering the underlying genotype.

1.6.2 Sup35 and [*PSI*+]

[*PSI*+] is the phenotype that results when Sup35 aggregates into its prion form. Sup35 is a translation termination factor (also called eRF3) that forms the Eukaryotic translation termination complex with Sup45 (also called eRF1). Sup35 is comprised of three domains, denoted N (residues 1-123), M (residues 124-253), and C (residues 254-685) (91). Together, the N and M domains act as the prion-forming region of Sup35 and are designated “NM.” The N domain is Q/N rich, has a high proportion of uncharged amino acids and, like PrP, contains oligopeptide repeats

that may contribute to its aggregation (92,93). The M domain is a highly-charged and polar region that is thought to lend stability to the aggregated state and contain chaperone binding sites (94,95). The C-terminal domain is globular and, when Sup35 is soluble, acts as a GTPase that works with eRF1 (Sup45) to release nascent polypeptide chains from the ribosome (96). When Sup35 aggregates to form [*PSI*+], its functionality is reduced and the translation termination complex does not form at wild type (WT) levels (97,98). Thus, stop codon readthrough, or nonsense suppression, occurs at a higher frequency than in the [*psi*-] WT, approximately 1-3% over baseline (99,100). Though high levels of nonsense suppression are toxic due to cofactor sequestration (101), most states of [*PSI*+] involve low levels of readthrough and are well-tolerated by cells (98). In fact, [*PSI*+] can even be advantageous to yeast in certain environments by allowing them to draw upon potentially beneficial genetic information contained within the 3'UTR of mRNA (90). This is discussed in further detail in section 1.4.5.

The nonsense suppression phenomenon makes it possible to easily track the [*PSI*+] status of yeast via a colorimetric assay. Laboratory strains that have been developed for prion research contain a *ade1-14*, a variant allele of the *ADE1* gene that contains a premature stop at codon 244 (88,102). When Sup35 is soluble and cells are [*psi*-], this aberrant stop codon is faithfully recognized by the translation termination machinery and a truncated protein is produced. Following this pioneer round of translation, the transcript is likely degraded by nonsense-mediated decay (NMD) due to the premature stop (103). As a consequence, cells cannot complete the adenine biosynthesis pathway that is reliant upon the full-length product of *ADE1*, called SAICAR synthase. Thus, these cells cannot grow on media lacking adenine. Further, the yeast experience a buildup of an upstream product, P-ribosylamino imidazole, which is nontoxic but confers a red pigmentation to the colonies. Conversely, the formation of [*PSI*+] causes misfolding and

aggregation of Sup35, leaving a reduced pool of functional protein to form the translation termination complex. In yeast containing *ade1-14*, the resulting nonsense suppression leads to the production of sufficient SAICAR synthase to allow cells to grow on media lacking adenine and maintain a white color on rich media. These two assays – growth on adenine dropout plates and coloration on rich media – allow for rapid identification of [*psi*-] vs [*PSI*+] yeast (Figure 1.3).

[*PSI*+] can exist in two well-characterized strains – "strong" and "weak" – though the existence of other strains has been demonstrated (104–106). Strong [*PSI*+] and weak [*PSI*+] are differentiated by their amount of nonsense suppression, which relates to the total amount of functional Sup35 present in cells (107). Strong [*PSI*+] yeast experience higher levels of nonsense suppression than weak [*PSI*+] yeast because there is a lower ratio of aggregated to soluble Sup35 in the weaker variant. This leads to an observably darker pink coloration of weak [*PSI*+] yeast relative to their strong [*PSI*+] counterparts (Figure 1.3). Similar strains can be formed from recombinant Sup35 in an *in vitro* setting by stimulating amyloid polymerization at varying temperatures. The protein conformations favored at 37ºC confer a weaker phenotype when

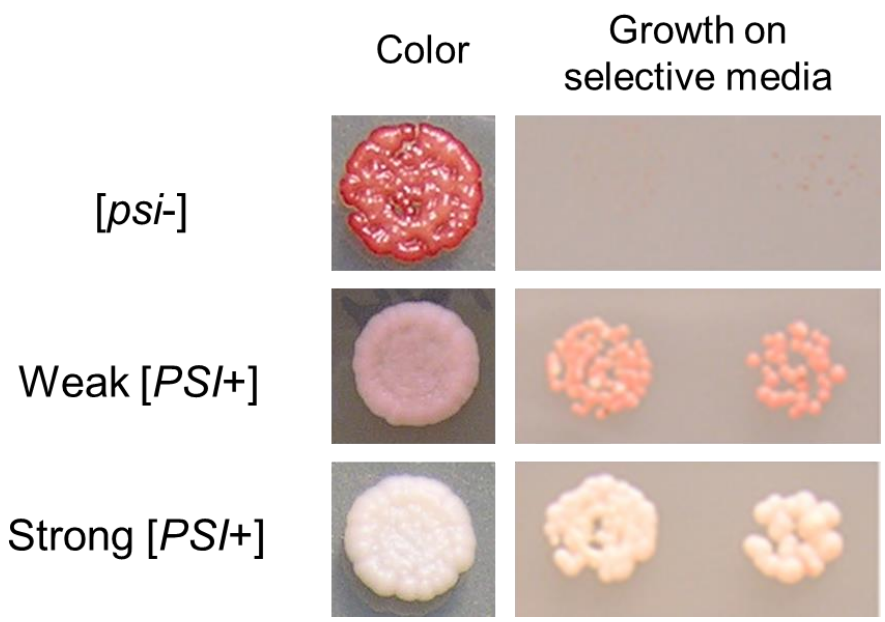

Figure 1.3. Strain variation of the yeast prion [*PSI*+]. In yeast containing the *ade1-14* allele, [PSI+] or [psi-] status can be distinguished by colony coloration and growth on SD-Ade media. Yeast that are [psi-] experience buildup of a red pigment and cannot synthesize their own adenine. Strong [PSI+] yeast are white and grow robustly on SD-Ade, while weak [PSI+] cells exhibit an intermediate pink coloration and weaker growth on selective media.

introduced *in vivo* than fibers formed at 4ºC (108). These new strains of [*PSI*+], respectively called Sc37 and Sc4, highlight the strength of the yeast model system in deciphering prion characteristics.

Studies of Sc4 and Sc37 have led to the discovery of differing properties between prion variants. In an effort to explain the differences in the amount of aggregated Sup35 in weak versus strong [*PSI*+], researchers investigated the physical characteristics of the amyloid aggregates. The stronger strain, Sc4, was demonstrated to be more frequently fragmented, leading to the generation of additional prion "seeds" that could nucleate new aggregates (109). Further biophysical analysis found that the stronger Sc4 strain had a shorter amyloid "core," or a smaller portion of the Sup35 protein making a contribution to amyloid fibers (110).

Though much has been discovered about the prion properties of Sup35, the initial formation of [*PSI*+] is dependent upon another prion factor: the enigmatic element called [*RNQ*+].

1.6.3 Rnq1 and [*RNQ*+]

The [*RNQ*+] prion is formed from the Rnq1 protein, which has no known function in its monomeric state (111). Rnq1 is divided into an N-terminal domain (residues 1-152) and a C-terminal prion-forming domain (PFD, residues 153-405)(112). Within the PFD, four Q/N-rich regions (residues 185-198, 218-263, 279-319, and 337-405) are important to [*RNQ*+] propagation but remain poorly understood (113). Interestingly, [*PSI*+] rarely forms without the presence of [*RNQ*+] (114). Prior to the discovery of [*RNQ*+], the concept of a [*PSI*+] inducing factor, [*PIN*+] had been suggested as a requirement for Sup35 amyloid formation (115). Ultimately, the [*RNQ*+] prion was identified as the most potent [*PIN*+] element, and now the two terms are often used interchangeably (112,114). Following formation of [*PSI*+], the two prions may be propagated or lost independently (116).

There are two models for how [*RNQ*+] induces the formation of [*PSI*+] (114). The first model, the "inhibitor titration model," suggests the presence of a molecular inhibitor of

aggregation that binds to Sup35 in the [*psi*-] state. Upon [*RNQ*+] formation, this inhibitor would be titrated away from Sup35 to the aggregated Rnq1, leaving Sup35 free to form amyloid fibers. Though work has been performed to identify the inhibitor, no molecule has been identified to date (114). The second model, the "cross-seeding model," suggests a binding interaction between misfolded Rnq1 and native Sup35. In other words, the Rnq1 may cause the misfolding of Sup35 by inducing conformational changes that may then be propagated independently by the [*PSI*+] state. This model is supported by co-localization microscopy and the weak *in vitro* polymerization of Sup35 in response to Rnq1, and is confirmed by experiments detailed in Chapter 4 (117,118).

Like [*PSI*+], the [*RNQ*+] prion exists in multiple strains, or "variants." These variants are differentiated by their abilities to induce [*PSI*+] and are accordingly named "low," "medium," "high," and "very high." The "high"-inducing [*RNQ*+] strain is further subdivided based upon its aggregate structure as visualized by fluorescent microscopy with Rnq1-GFP. The "multi-dot high" strain contains multiple Rnq1foci, while "single dot high" is characterized by one large punctum of fluorescence (119). Additional [*RNQ*+] variants have since been described, and it is hypothesized that the existence of a spectrum of conformations is beneficial to cells because it fine-tunes their ability to convert to the [*PSI*+] phenotypic state (120).

1.6.4. Other yeast prions

Beyond [*PSI*+] and [*RNQ*+], there are a multitude of other prion-forming proteins in *Saccharomyces cerevisiae*. The best-characterized of these include [URE3], [*SWI*+], [*OCT*+], [*MOT3*+], and [*ISP*+], which are respectively formed by the proteins Ure2, Swi1, Cyc8, Mot3, and Spf1 (88). All of these proteins have a regulatory function within the cell. Ure2 is a nitrogen uptake

regulator, and the formation of [URE3] allow host cells to take up alternative nitrogen sources, such as ureidosuccinate, in the presence of preferred nitrogen sources (121,122). The other yeast prion-forming proteins play a role in transcriptional regulation of various processes. The aggregation of Swi1 into [*SWI+*] affects the activity of the chromatin remodeling complex SWI/SNF (123); similarly, when Cyc8 converts to form [*OCT+*], it reduces the functionality of the highly-conserved Cyc8-Tup1 transcriptional repressor (124). Mot3 is a transcription factor that regulates genes related to metabolism and stress response (125). Its prion form, [*MOT3+*], displays a gain- and loss-of-function phenotype, via a mechanism that is not understood, that promotes filamentous growth of yeast in response to nutrient challenges (126). The aggregation of these prions mimics the loss-of-function of the monomer protein (88). Further, these prions are all cured by deletion of the chaperone Hsp104 (discussed in section 1.5.1). [*ISP+*] is unique among yeast prions, in that it is Hsp104-independent, localizes to the nucleus, and its aggregation confers a purely gain-of-function phenotype (127).

Other yeast epigenetic elements have been described in the literature as exhibiting prion-like characteristics, yet are incompletely characterized. One of these putative yeast prions, [*GAR+*], is transmitted cytoplasmically but has not been shown to form amyloid structures (128). This element allows *S. cerevisiae* to utilize diverse carbon sources even in the presence of glucose. Another potential prion, [*MOD*], is formed from the Mod5 tRNA isopentenyltransferase. Its amyloid aggregation protects yeast from antifungal compounds (129). Unlike the other prion proteins, it does not have a Q/N-rich prion-forming domain (129). Though much has yet to be learned about these non-canonical prions, their ability to reversibly modify yeast phenotypes, independently from genotypes, makes them an important facet of homeostatic regulation.

Interestingly, even beyond the [*RNQ*+]/[*PSI*+] relationship, prions influence the formation and activities of other prions. The [URE3] and [*SWI*+] prions can act as [*PSI*+]-inducers, albeit more weakly than [*RNQ*+] (114,130). Overproduction of soluble prion-forming proteins, such as Ure2, Swi1, Mod5, and Cyc8, has been shown to increase [*PSI*+] formation when Sup35 is also overexpressed (114,129). Furthermore, [*PSI*+] can reduce the frequency of [URE3] formation, and [URE3] and [*PSI*+] appear to have mutually destabilizing effects when both prions are present in cells (131,132). Additionally, some of these effects may be dependent on the prion strain, or variant, that is in play. The promotion and inhibition of a particular prion by other prions may impact which phenotypic effects are ultimately observed, and is especially significant in light of the fact that many yeast prions may be as-yet undiscovered (89).

1.6.5. Beneficial yeast prions in the lab and in nature

Given the regulatory function that is associated with many prion-forming proteins, yeast can sometimes benefit from the prion state. In the case of [*PSI*+], enhanced nonsense suppression leads to translation of typically silent genetic information in the 3'UTR or in normally silent pseudogenes. Whether these additional polypeptides relay an adaptive advantage to the yeast is dependent upon both the environment and the yeast genetic background (90). This is an example of how yeast prions can decouple genotype from phenotype, as isogenic populations of yeast may have different [*PSI*+] states and thus different levels of nonsense suppression. Relative to genetic modification, yeast prions can be easily gained and cured within a few generations of yeast. Further, the rapidity of prion formation could allow yeast to adapt to quickly-changing environmental pressures.

In a laboratory setting, [*PSI*+] has been demonstrated to confer resistance and sensitivity to a variety of environmental conditions. A large-scale study examined the phenotypes of isogenic [*PSI*+] and [*psi*-] colonies from seven different yeast strain backgrounds (90). Neither the [*PSI*+] nor the [*psi*-] state had a consistent nor predictable effect on the robustness of yeast growth across strains. In some instances, [*psi*-] was generally more beneficial to cells: [*psi*-] yeast of the 5V-H19 strain grew well on non-ammonium sulfate nitrogen sources, in contrast to their [*PSI*+] counterparts (90). However, [*PSI*+] 74D-694 yeast generally grew better on certain alternative nitrogen sources than isogenic [*psi*-] cells (90). In other cases, prion status could be of conflicting benefit even within the same class of environment: when grown on non-glucose carbon sources [*PSI*+] 33G-D373 thrived on 3% ethanol relative to [*psi*-] cells, but [*psi*-] yeast grew more robustly on 2% lactate (90). This seeming randomness to [*PSI*+] benefits makes sense because the 3'UTR and retained pseudogenes inactivated by a premature termination codon are not typically under selection.

Other studies have examined the existence of prions in wild yeast. An examination of 690 yeast strains from beer, wine, soil, fruit, plants, medical clinics, and other sources revealed the presence of amyloid Sup35 in 10 samples (89). These aggregates were cured in response to Hsp104 inhibition, and the resulting [*psi*-] phenotypes were generally at a growth disadvantage relative to their isogenic [*PSI*+] isolates (89). In the same study, [*RNQ*+] aggregates were identified in 43 wild strains, in line with previous reports of [*RNQ*+] in 11/70 wild strains (133) and identified in a multitude of variants in 22 different wild yeast (134). These variants, though differing in biochemical properties, were almost all strong inducers of [*PSI*+] (134). The relative frequency of [*RNQ*+] occurrence in the wild, coupled with its high [*PSI*+]-inducing capabilities in these isolates, suggest a robust bet-hedging mechanism in natural environments. In other words, [*RNQ*+] may

prime yeast to rapidly convert from the [*psi*-] to the [*PSI*+] state in response to changing environmental pressures (135).

Though far less is known about the [*MOT3*+] prion relative to the [*PSI*+]/[*RNQ*+] system, the role of monomeric Mot3 as a transcriptional regulator means that [*MOT3*+] has the potential to promote broad changes in the gene expression profiles of its host cells. In a survey of 96 wild yeast strains, six contained Mot3 aggregates indicative of [*MOT3*+] (89). When cured, these strains exhibited reduced tolerance to extreme environmental conditions. Further, Mot3 aggregates to form [*MOT3*+] at a high conversion frequency relative to other fungal prion proteins, 10^{-4} as compared to less than 10^{-6} for [*PSI*+] (136–138). The ability of [*MOT3*+] to regulate filamentous growth and ethanol stress may make it a particularly beneficial epigenetic element for yeast that naturally occur in the wild and in alcoholic fermentation reactions.

1.7 An introduction to molecular chaperones of *Saccharomyces cerevisiae*

Yeast proteins, including prion-forming proteins, interact with molecular chaperones throughout their "life cycles" (9) Chaperones are proteins that assist other proteins in achieving the correct conformation. Yeast have an estimated 63 chaperone proteins and a multitude of cofactors that assist chaperones in performing their functions (9). Certain chaperone classes are conserved across several Eukaryotic systems, while others are specific to unicellular organisms and have no obvious homologs in metazoans. The balance of chaperones, their cofactors, and their substrates is essential in the maintenance of proteostasis.

1.7.1 Hsp104

Hsp104 is a hexameric AAA^{+}-ATPase that is required for the propagation of most known yeast prions (139,140). The deletion of Hsp104 is non-lethal under standard growth conditions.

However, deletion or null mutations of the *HSP104* gene leads to severe growth defects following heat shock and other forms of cellular stress (141). The denaturant guanidine hydrochloride (GdnHCl) inhibits Hsp104 by repressing its activity and reducing its interaction with chaperone cofactors (142,143). Manipulation of Hsp104 is an important tool for the investigation of prions in yeast, and is discussed in section 1.8.1.

The assembled Hsp104 complex is comprised of six identical subunits. Each subunit of Hsp104 contains an N-terminal domain and two ATPase domains, AAA1 and AAA2, separated by a linker (144,145). A regulatory domain (MD) appears as an extension in AAA1 and facilitates binding to other chaperones, communication between AAA1 and AAA2, and modulating the activity of the disaggregase (146,147). The C-terminal domain is important for oligomerization of the complete hexamer (148). When the complex is assembled, six Hsp104 monomers join in a barrel conformation around a central pore. This allows the translocation of protein substrates through the Hsp104 refolding channel via a threading mechanism (145,149,150). Within this hollow center, middle domain pore loops form a spiral pattern to assist with substrate binding and translocation (151).

Hsp104 is capable of dissolving amyloid aggregates under normal conditions, and potentiating mutations allow it to dissolve fibrils of human disease-associated proteins such as FUS, TDP-43, and α-synuclein (152). These mutations can reduce or eliminate Hsp104's reliance on cofactors and prevent the complex from autoinhibitory interactions between monomers (152). This is in contrast to native Hsp104 activity, which is assisted in part by the actions of the Hsp70/40 system. These chaperones are believed to bind to Hsp104 substrates and promote their delivery to the disaggregase (153).

1.7.2 Hsp70s and their nucleotide exchange factors

The Hsp70 chaperones are highly conserved across kingdoms (154). Broadly, the Hsp70s are abundant ATPases that promote the refolding of aberrant proteins. In yeast, the two major families of Hsp70 are the Ssas and the Ssbs. There are four members of the Ssa family (Ssa1-4) and two Ssbs (Ssb1-2). The quadruple-deletion of the *ssa1Δssa2Δssa3Δssa4Δ* is lethal, though the presence of any one of the Ssa-encoding genes is sufficient for survival (155). Of these proteins, Ssa1 is both constitutive and stress-inducible, Ssb1 and Ssa2 are constitutive and non-inducible, and Ssa3-4 are only induced under stress conditions (155).

In contrast, the double *ssb1Δssb2Δ* deletion is non-lethal, though it does confer a slow-growth phenotype (155). Ssb1 and Ssb2 differ by only four amino acids (156). Interestingly, the three substrate binding domain polymorphisms have been shown to be under selective pressure to maintain their divergence across species, indicating a functional role for the differences between Ssb1 and Ssb2 (157). It has been shown that Ssb1 binds to calmodulin (158) and that its overproduction can rescue a mitochondrial defect (159), though the differing functions of Ssb1 and Ssb2 have yet to be completely elucidated.

Both families of Hsp70s contain a three-domain structure: a 40kDa N-terminal nucleotide binding domain (NBD), a 20kDa substrate binding domain (SBD), and a 10kDa C-terminal variable domain (VD) (160,161). In the ADP-bound state, client proteins are trapped within the SBD with a very low off-rate and are protected from cytoplasmic interactions (162,163). Upon binding of ATP, Hsp70s adopt a more open conformation that releases the substrate (164). Though ATP cycling is essential for Hsp70 function, the innate ATPase activity of Hsp70s is low (165). Thus, these proteins require assistance in order to cycle nucleotides. This assistance comes in the

form of Hsp40s (described in further detail in section 1.5.3) and nucleotide exchange factors (NEFs). Hsp40s bind to client proteins and "deliver" them to a partner Hsp70, while simultaneously stimulating the hydrolysis of ATP into ADP so that the client remains bound by the SBD (166). Then, a NEF partners with the Hsp70s to catalyze ADP release. Upon binding of another molecule of ATP, the SBD returns to its open conformation and the substrate is released.

Yeast contain four NEFs: Sse1, Sse2, Fes1, and Snl1 (167). Though required for optimal Hsp70 function, NEFs exist in substoichiometric ratios to their partner chaperones. Indeed, it is estimated that NEFs are present at 1/10 to 1/12 of the total molar concentration of Hsp70s (168,169). It is hypothesized that this balance is essential due to the NEFs' affinity for ATP: an overabundance of NEFs could out-compete Hsp70s for ATP binding (170). Sse1, also called Hsp110, is the most abundant and presumably most active NEF, as it partners with both the Ssa and Ssb chaperone families (168,171,172). Deletion of both Sse proteins is lethal (173). Conversely, Fes1 is known to bind only to Ssa *in vivo* (174), though other studies have suggested a complex regulatory mechanism wherein it inhibits the Ssb ATPase in a ribosome-associated manner (175). Its deletion leads to a heat shock response regardless of environment, as well as a temperature sensitivity phenotype (176). Snl1 is localized to the endoplasmic reticulum membrane via a transmembrane region and associates with both Ssa and Ssb *in vitro* (177,178). Its deletion confers no detectable phenotype and it is thought to be a highly-specialized, predominantly ribosome-associated NEF (177,178). In general, NEFs are thought to have a greater impact on Ssa's nucleotide exchange, while Ssb is believed to act with some independence from NEFs (156). However, both the Ssa and Ssb families rely upon chaperone cofactors known as Hsp40s.

1.7.3 Hsp40s

While nucleotide exchange factors facilitate the ADP release from the Hsp70 NBD, Hsp40s assist with hydrolysis of Hsp70-bound ATP to ADP. The yeast Hsp40s are homologs to the human J-proteins that help drive substrate recognition and client specificity for the larger Hsp70 proteins. This allows for one type of Hsp70 to serve a diversity of clients: humans have 11 Hsp70s that partner with 41 J-domain proteins (179). Yeast have 22 Hsp40s, including Sis1, Zuo1, Ydj1, and Jjj1, of which 13 are cytosolic (179,180). There is variable necessity for the Hsp40s in yeast, as some are required (Sis1, Jjj1, Jjj3, Cwc23) while others are dispensable for survival (180,181). Unlike the Hsp70s, Hsp40s exhibit a high degree of inter-protein diversity, and the proteins are broadly sorted into classes I, II, or III based on their domains. This diversity enables the targeting of Hsp70s to a broad pool of substrates. However, all Hsp40s contain a ~70 amino acid J-domain that stimulates the ATPase activity of Hsp70s (182). Some Hsp40s preferentially interact with specific Hsp70s: Sis1 partners with Ssa1, while Zuo1 binds to Ssb1 as part of its ribosome-associated role (183).

In its canonical function, an Hsp40 will bind to a substrate with the purpose of preventing aggregation and delivering it to an Hsp70 for refolding (179). Upon binding to an Hsp70 partner, the substrate is transferred from the Hsp40 to the Hsp70 SBD; further, the Hsp40 stimulates ATP hydrolysis at the Hsp70 NBD. However, studies have demonstrated a more complex role for the myriad Hsp40s of yeast, including independent Hsp70 stimulation without first binding to a client protein (180). This function appears to rely solely on the J-domain and not on the other motifs within the Hsp40s. Conversely, other Hsp40 functions are J-domain-independent. For example, the protein Cwc23 is necessary for spliceosome disassembly, and deletion of its J-domain had no effect upon this role (184). Domain diversity, client specificity, and Hsp70 interactions all play a

part in directing the activity of the Hsp40s, which highlights the immense complexity in balancing the yeast molecular chaperone system.

1.8 The role of chaperones in yeast prion formation and propagation

Adding to the complexity of the chaperone system, yeast prions have unique and sometimes unpredictable relationships with Hsp104, Hsp70s, and Hsp40s. Intuitively, chaperones exist to restore proper protein folding and should thus ubiquitously inhibit prion formation. However, this is not the case. The overexpression, depletion, or deletion of chaperones can have non-obvious effects upon prion induction and propagation (88,153,179,185); further, these effects are often prion- or even prion strain-dependent.

1.8.1 Yeast prions display varying dependence upon Hsp104

The Hsp104 disaggregase is required for the propagation of most yeast prions (88), with the notable exception of [*ISP*+] (88). This requirement appears to be due to the nature of the mother-to-daughter cell transmission of small prion aggregates (seeds). When Hsp104 is inactivated in a [*PSI*+] cell, the Sup35 aggregates increase in size, which presumably correlates to a decrease in the production of the smaller infectious oligomers that are propagated to budding cells (186,187). Further, there is a bias towards prion seeds remaining with the older "mother" cell during division (188,189). As fewer daughter cells receive Sup35 seeds, the prion is eventually titrated out of the population. This happens at a relatively rapid rate, within 10-14 generations (188). Though the Sup35-Hsp104 relationship remains the best-studied among yeast prions, the general principles of seed generation and propagation likely hold true for the other biochemically-similar aggregates.

However, Hsp104 overexpression has conflicting effects on yeast prions. Cells are cured of the [*PSI*+] state following Hsp104 overexpression, but other prions persist (190,191). It is unknown why [*PSI*+] is uniquely affected by Hsp104 overexpression, but it may be due to Hsp104 binding sites within the middle domain of Sup35 (192). There are competing theories about the mechanism of Sup35 solublization by Hsp104 overexpression. The first model suggests that abundant Hsp104 dissolves Sup35 aggregates to the point that they are no longer propagable prion seeds, either by trimming fiber ends or complete fiber fragmentation (187,190). Alternatively, Hsp104 may inhibit amyloid seed formation by binding to the fiber and preventing its fragmentation into oligomers (193). The final model is based upon asymmetric prion segregation between mother and daughter cell, similar to what is observed upon Hsp104 inactivation (194). This latter hypothesis has been disproven, and the dissolution/trimming model is the paradigm with the greatest experimental support to date (195).

Surprisingly, Hsp104 overexpression can promote the appearance of the [URE3] prion in the presence of the [*RNQ*+] prions (196). In this case, it is thought that Hsp104 remodels semi-soluble Ure2 aggregates into an on-pathway (amyloid-forming) conformation that is templated by [*RNQ*+] (196). The prion-specific effects of Hsp104 may be influenced by the activities of its Hsp70 and Hsp40 cochaperones.

1.8.2 Ssa and Ssb have opposing effects upon [PSI+]

Perhaps the most interesting case of chaperone influence on yeast prions is the relationship between the Hsp70s and [*PSI*+]. The Ssa and Ssb chaperone families, despite their considerable domain and sequence homology, have opposing effects upon [*PSI*+] (185). When overexpressed, Ssa proteins promotes *de novo* [*PSI*+] formation in [*psi*-] cells, and protects [*PSI*+] from curing by

Hsp104 (185,197). A dominant-negative allele of *SSA1*, *ssa1-21*, reduces the propagation of [*PSI*+], and combining this mutant with *ssa2Δ* completely abrogates the prion (198).

Conversely, Ssb overexpression both reduces *de novo* [*PSI*+] formation and enhances prion curing or loss (199,200). The double *ssb1Δssb2Δ* decreases Hsp104-mediated [*PSI*+] curing (199). The substrate binding domain has been implicated as an important region for these chaperones' divergent effects upon [*PSI*+], though substituting any Ssa1 domain for an Ssb1 domain is sufficient to reduce [*PSI*+] induction in Hsp70 chimera experiments (185). Notably, it is not the amount of Hsp70 but the stoichiometric balance between Ssa and Ssb that influences the [*PSI*+] state, as Ssb deletion mimics Ssa overproduction in its positive effects upon [*PSI*+] generation (199). Thus, any event that were to perturb, enhance, or otherwise affect any of the Hsp70s may have consequences for the prion state of the cell. Chapter 2 of this thesis investigates this concept in further detail.

1.8.3 Hsp40s and NEFs can support or antagonize prions

Titration of Hsp70 cofactors can also affect prions, independently or perhaps via their effects on Ssa and Ssb. Deletion of nucleotide exchange factor Sse1 inhibits [*PSI*+] formation and propagation, while overproduction of the NEF enhances *de novo* [*PSI*+] formation (201). A cohort of Sse1 mutants have been identified that impair [*PSI*+] propagation to varying degrees (202). It is possible that this is due to Sse1's Hsp70 interactions, specifically with Ssa1. Ssa1 is believed to be more reliant on NEFs for its activities than are the Ssb proteins (156), and as such,

overexpressing Sse1 may enhance Ssa1's [*PSI*+]-promoting activity to a greater extent than it enhances Ssb's [*PSI*+]-curing role.

The role of the Hsp40 Sis1 in [*PSI*+] propagation has been well-studied relative to other Hsp40s. The maintenance of the "strong" versus "weak" strains of [*PSI*+] relies upon different subsets of Sis1 domains, with weak [*PSI*+] relying more on the C-terminal regions of the protein (203). While both [*PSI*+] variants are supported by a Sis1 construct lacking the glycine/phenylalanine-rich "G/F" domain, the elimination of this region does not allow for the propagation of [*RNQ*+] (203). The five canonical strains of [*RNQ*+] also demonstrate differential requirements for Sis1 domains (204). Downregulation of Sis1 leads to [*PSI*+] and [*RNQ*+] curing, albeit at different rates (205). It is thought that these effects of Sis1 are due to different binding patterns of the Hsp40 to amyloid, resulting in variable delivery of substrate to Hsp70s (206,207).

1.8.4 Other prions have unpredictable chaperone requirements

Chaperone requirements of other yeast prions are less well-characterized. All tested prions – [*PSI*+], [*RNQ*+], [*SWI*+], and [URE3] – require Sis1 for propagation (205,208). Of these, only [*SWI*+] also requires Ydj1, another Hsp40 J-protein (208). Overexpressing Ydj1 leads to [URE3] loss, as well as the curing of some [*RNQ*+] strains (132,191). While Ssa1 overexpression promotes [*PSI*+] formation, it appears to inhibit [URE3] (131). Conversely, Ssa2 mutation or deletion similarly inhibits the propagation of both [*PSI*+] and [URE3], highlighting that the directionality of chaperone effects is unpredictable even within the same protein family (209). Overexpression or depletion of the Sse1 NEF can inhibit [URE3] propagation, which is in contrast to its promotional effects on [*PSI*+] when overexpressed (201,210,211). Of great interest, the unique prion [*ISP*+] is not eliminated by Hsp104 deletion, but is still cured by the Hsp104-inactivating

GdnHcl (127). The mechanism for this has yet to be elucidated, but may involve a chaperone imbalance generated by the inactive Hsp104.

The effects of chaperones on amyloid aggregates are inconsistent between different prions and between different prion strains. Further, chaperones even have distinct mechanisms for recognizing misfolded structures of the same protein (212). Further research into the chaperone systems that influence the aggregation of the full cohort of yeast prions will be necessary to gain a more nuanced understanding of the factors that maintain proteostasis.

1.9 Cotranslational folding factors are incompletely characterized

Chaperone-mediated refolding of proteins in the cytosol and within cellular compartments is only one component of protein homeostasis. The folding of a nascent polypeptide during its synthesis by the ribosome, called "cotranslational folding," is essential to the generation of functional proteins but is a poorly-understood process. There are two protein families that are known to play a role in this folding in eukaryotes: the nascent-polypeptide associated complex (NAC) and the ribosome-associated complex (RAC) (213,214).

1.9.1 The nascent-polypeptide associated complex

The NAC is a highly-conserved heterodimeric complex that is ubiquitous in Eukaryotic organisms from yeast to humans. The NAC is cytosolic and binds to the ribosome near the exit tunnel; as such, it is the first protein complex to bind to emerging polypeptides (215). The purpose of this binding is poorly understood, though it is thought that the NAC helps to protect nascent chains from inappropriate intra- or inter-protein contacts prior to whole-domain folding (215).

The NAC is comprised of two subunits called the α-NAC and the β-NAC (216). Yeast have an additional subunit, the β'-NAC, that can substitute for the β-NAC in some heterodimers, but

β'-NAC has a much lower expression level than the other subunits (217,218). These proteins in yeast are named Egd2, Egd1, and Btt1, respectively. Throughout this thesis, the terms "α-NAC" and "β-NAC" will refer to the Eukaryotic proteins in general, while the Egd2, Egd1, and Btt1 nomenclature will be utilized in discussions of the yeast NAC in particular. All NAC subunits contain sequence homology within their 61-amino acid NAC domains, which are thought to assist in the dimerization of the proteins (219). The α-NAC contains a C-terminal ubiquitin-associated (UBA) domain, which may help to prevent newly-synthesized proteins from being targeted for degradation by competing for ubiquitin ligases (219,220). Ubiquitination of Egd1 and Egd2 by Not4 is required for stability of the NAC complex (221,222). Both the α- and β-NAC are independently capable of binding strongly to nascent chains, and both are able to prevent polypeptides from prematurely interacting with other cytosolic factors (215). In yeast, the NAC is anchored to the ribosome via a short tract of Egd1, within the first 30 residues of the N-terminus (223–225). The location of binding is under debate, with the original evidence pointing to contact on ribosomal subunit Rpl25 (L23), but later research identified Rpl31 as the main site of interaction (223,224). In the absence of Egd1, Btt1 may assist in binding of the NAC heterodimer to the ribosome (218). Ribosomal binding to the whole NAC complex occurs in a 1:1 ratio, and the expression of NAC subunits is associated with ribosome biogenesis (226,227).

The function of the NAC is controversial and poorly understood. It was initially suggested that NAC subunits played a role in protein targeting to the ER and mitochondria, but subsequent *in vivo* studies have disproven these theories (216–218,228–230). However, there is some support for the role of individual NAC subunits as transcription factors (231–233). The α-NAC binds to nucleic acids, though with a stronger affinity for RNA than for DNA (219,234). Early studies suggested that the transcription-related activities of the NAC are more significant than its role in

translation; however, further analysis in model organisms have demonstrated a crucial role for the NAC in proteostasis (213).

Deletion of the NAC is embryonic lethal in multicellular organisms, though its deletion in yeast is tolerable (218,235–237). The *egd1Δbtt1Δ* double-deletion may confer a slight growth defect at 37ºC; however, this effect was not reproducible in other strain backgrounds (218,238). Deletion of the yeast NAC and the Ssb proteins did confer a growth defect and caused aggregation of newly synthesized proteins (227). Re-introduction of Egd1 and Egd2 was sufficient to rescue the phenotype (239). Depletion of NAC subunits in adult organisms has implications for heat shock and stress response (240,241). SiRNA-mediated knockdown of the *C. elegans* β-NAC (ICD-1) in adult nematodes leads to increased apoptosis and UPR induction; however, it increased worms' resistance to heat stress (241). NAC subunits also localized to protein aggregates following heat shock, potentially to assist in their resolubilization, which concurrently reduces the translational capacity of ribosomes (240). As such, it has been suggested that the NAC is a sensor of protein homeostasis and plays a role in linking translation to the chaperone network (240). Chapter 2 demonstrates the effects of NAC subunit deletion upon chaperone balance and prion-related toxicity in yeast.

1.9.2 The ribosome-associated complex includes the Hsp70 Ssb

The RAC is the second protein complex to bind to nascent chains, at approximately 58 amino acids (242). In yeast, the RAC is composed of the atypical Hsp70 Ssz1 and a J-protein called Zuo1 (226,243,244). Ssz1 is a unique chaperone that lacks the C-terminal domain that is characteristic of Hsp70s (244). Further, its nucleotide binding domain is divergent from other ATPases and is not thought to hydrolyze ATP *in vivo* (245,246). The Hsp70 Ssb often associates

with these subunits, and thus this system is commonly referred to as "RAC-Ssb." Ssz1 relies upon Zuo1 for ribosomal anchorage, and the proteins bind to ribosomes in a 1:1 ratio (244). Yeast that have been deleted for either or both Ssz1 and Zuo1 display a slow growth phenotype but are viable, and overexpression of Zuo1 partly rescues the phenotype (244). Like the NAC, RAC has been shown to bind to the Rpl31 large ribosomal subunit (183).

The RAC has demonstrated interactions with prion-forming proteins in yeast. Deletion or mutation of Zuo1 increases the frequency of [*PSI*+] formation, including spontaneous formation independent of [*RNQ*+] (247). However, RAC deletion also destabilizes pre-existing Sup35 aggregates, presumably be increasing the cytosolic availability of Ssb (248–250). Because its amyloid remodeling functionality occurs through Ssb, the RAC complex is collectively viewed as a cochaperone that may exert a "holdase" function prior to passing nascent polypeptides to Ssb for processing (248,251).

Relative to the NAC, less is known about RAC homologs in other systems. In humans, the RAC is formed by Hsp70L1 and MPP11, a Zuo1 homolog (252). However, no clear ribosome-associated Ssb homolog has been identified, and it is theorized that other mammalian Hsp70s substitute for this role in metazoans (249). Ultimately, far less is understood about the folding capabilities of human cotranslational chaperones that may play a role in the genesis of protein misfolding disorders.

1.10 Summary and significance

Protein folding is a challenging process, and organisms have evolved myriad mechanisms to create properly-folded proteins (cotranslational folding), rehabilitate misfolded species (molecular chaperones), and degrade structures that are beyond repair (protein quality control). These mechanisms work in concert to maintain protein homeostasis and, more broadly, organismal

health. Pathogenic protein aggregation, prion-like or otherwise, works in opposition to these processes and can cause irreversible damage to hosts. However, little is known about the initial stages of protein misfolding and how misfolded conformations are propagated from one molecule to another. This thesis serves to address both questions by utilizing the yeast prions [*PSI*+] and [*RNQ*+] as models.

Chapter 2 investigates the nascent-polypeptide associated complex and its role in modulating the chaperone network. The balance between Hsp70 chaperones is demonstrated to be an important factor that influences cellular tolerance of a toxic [*PSI*+] state, and this balance is directly affected by the presence or absence of the NAC subunits. Tipping the ratio of available Hsp70s can create a more favorable environment that appears to improve Sup35 folding. Chapter 3 extends the concept of chaperone balance to the nucleotide exchange factor Sse1, and demonstrates how Hsp70 cofactors can act to restore cellular health in an imbalanced system. Finally, Chapter 4 addresses questions of templated prion formation by examining the relationship between Rnq1 and Sup35 *en route* to [*PSI*+] formation, and finds that intermolecular binding is a major contributing factor in the seeding of prion formation. Overall, this work illuminates important principles across several stages of the prion life cycle, and may inform future research that will help to modulate or prevent toxicity associated with protein aggregation.

Chapter 2: Prion-associated toxicity is rescued by elimination of cotranslational chaperones

Keefer KM, True HL. PLOS Genet. 2016;12: e1006431. doi:10.1371/journal.pgen.1006431

2.1 Abstract

The nascent polypeptide-associated complex (NAC) is a highly conserved but poorly characterized triad of proteins that bind near the ribosome exit tunnel. The NAC is the first cotranslational factor to bind to polypeptides and assist with their proper folding. Surprisingly, we found that deletion of NAC subunits in *Saccharomyces cerevisiae* rescues toxicity associated with the strong [*PSI+*] prion. This counterintuitive finding can be explained by changes in chaperone balance and distribution whereby the folding of the prion protein is improved and the prion is rendered nontoxic. In particular, the ribosome-associated Hsp70 Ssb is redistributed away from Sup35 prion aggregates to the nascent chains, leading to an array of aggregation phenotypes that can mimic both overexpression and deletion of Ssb. This toxicity rescue demonstrates that chaperone modification can block key steps of the prion life cycle and has exciting implications for potential treatment of many human protein conformational disorders.

2.2 Introduction

Protein synthesis is an essential process undertaken by all organisms, but its necessity also presents cells with a myriad of challenges. An extensive network of molecular machines is active throughout translation, folding, and degradation in order to preserve protein homeostasis (proteostasis). Perturbations to that machinery can have ripple effects that impact many cellular systems.

Misfolded proteins are one such challenge to proteostasis. Improperly folded proteins are generally non-functional; thus, the correct folding and trafficking of polypeptides is essential to the maintenance of cellular viability (253). Protein misfolding can lead to the induction of cellular stress responses, apoptosis, and cell death. In humans, protein misfolding diseases include Alzheimer's disease, Parkinson's disease, Huntington's disease, and prion diseases such as

Creutzfeldt-Jakob disease (31,253,254). The complexity of protein folding is mirrored by the complexity of these incurable diseases; thus, increased understanding of the molecular basis of folding and misfolding will be crucial to improved treatment of various pathologies.

Prions are a subset of misfolded proteins that are self-templating and stably propagated from cell to cell. In yeast, the intrinsically disordered domain of the translation termination factor Sup35 misfolds and aggregates to form the [*PSI*+] prion, which is cytoplasmically inherited via amyloid seeds (255–257). [*PSI*+] is toxic under certain circumstances, including Sup35 overexpression, due to severe disruption of proteostasis as a consequence of excessive aggregation of Sup35 (258,259).

Nascent polypeptides begin to fold cotranslationally before protein synthesis has been completed by the ribosome (260). Sup35, not unlike other proteins, faces folding challenges immediately upon emergence from the ribosome exit tunnel. Proteins are protected from early misfolding by ribosome-bound protein chaperone families (261). First, the nascent polypeptide-associated complex (NAC) interacts with nascent chains (262), followed by the ribosome-associated complex (RAC) and the Hsp70 Ssb (263–266). Cotranslational chaperone factors are of keen interest in the area of protein aggregation, as they have a bias towards substrates that are intrinsically disordered and amyloidogenic (267). The NAC and Ssb-RAC systems are components of a larger molecular chaperone network within *Saccharomyces cerevisiae* (261,268). However, the interactions between cotranslational folding factors and other players in the chaperone network have yet to be fully elucidated.

Here, we describe a surprising mechanism for preventing aggregation-related cytotoxicity by manipulating cotranslational folding pathways. We utilized the [*PSI*+] prion as a model for protein misfolding and a reporter for the activities of the chaperone network. We screened for

factors that, when disrupted, rescued the prion-dependent toxicity and restored viability. Surprisingly, disruption of β-NAC, a subunit of the NAC chaperone complex, was identified as one of the rescuing mutants in our screen. This counterintuitive result suggests that depletion of chaperones can, in some cases, rescue defects associated with misfolded proteins.

Indeed, we found that deletion of NAC subunits has significant impact on the localization and activity of other cytosolic chaperones, the Hsp70 family in particular. We propose that altered localization and activity of chaperones can aid cells in the ability to maintain proteostasis when faced with severe folding challenges. As such, inhibition of the NAC presents a novel avenue for investigation into therapeutics to treat protein conformational disorders that may slow further aggregation of amyloidogenic proteins and suspend disease progression.

2.3 Materials and Methods

Yeast strains, plasmids, cultures, and transformations

Yeast were cultured and transformed using standard techniques (269). All deletion strains were created from the same 74D-697 [*RNQ*+][*PSI*+] parent. Genetic deletions were made by replacing the coding regions of *EGD1*, *EGD2*, and *BTT1* with *KANMX4*, *loxP-HIS3MX6-loxP*, and *loxP-URA3MX-loxP*; knockouts were confirmed by auxotrophic markers and colony PCR. Strains and plasmids are available in the supplemental experimental procedures.

Fluorescence microscopy

Cells expressing pCUP1-*SUP35NM-GFP* were grown overnight in SD-Ura and Sup35NM-GFP expression was induced by the addition of $CuSO_4$ to a final concentration of 50μM. After 2 hours of induction, cells were washed twice in 1X PBS, resuspended in 1X PBS, transferred to a 12-well

glass slide (Erie), and observed with an Olympus FV1200 laser scanning confocal microscope fitted with a 100x oil immersion objective.

Prion manipulation

SDD-AGE and colorimetric assays were performed as previously described (270). Antibodies utilized in this study are available in the supplemental experimental procedures. Cytoduction was performed similarly to previous studies (271) to transfer a medium strain of [*RNQ*+] into [*rnq*-][*psi*-] strains (S2 Table). Putative cytoductants were selected on SGly-Ura and examined for accuracy by assessing auxotrophic markers. Prion transfer was confirmed by color on YPD and growth on SD-Ade plates. Haploid cytoductants retained the WT nucleus of the recipient strain and the strong [*PSI*+] prion aggregates of the donor strain.

Ribosome profiling and quantification

Ribosome fractions were collected as previously described (272). Protein precipitation of fractions was performed by TCA precipitation, followed by SDS-PAGE and Western blotting for the presence of Ssb and Rpl3. Quantification was performed with ImageJ, and background signal was subtracted from each measurement. The detected protein in the polysome fractions was divided by the detected protein in the monosome fraction as a way of controlling for the total amount of detected Ssb bound to ribosomes. We performed this analysis for Ssb, and scaled the quantification by the same method for the ribosomal protein Rpl3. This controlled for the total amount of protein in the polysome versus the monosome and allowed us to quantify changes in Ssb relative to the total ribosomal protein. The fraction of polysome-associated Ssb was normalized to the amount of polysome-associated Rpl3 from the same blot for both WT and *egd1Δegd2Δ* in triplicate. Thus, the quantification metric was calculated in this manner: $\frac{\left(\frac{Ssb\ in\ polysome}{Ssb\ in\ monosome}\right)}{\left(\frac{Rpl3\ in\ polysome}{Rpl3\ in\ monosome}\right)}$

Joining assay

Yeast strains transformed with pCUP1-*SUP35* were grown overnight in SD-Trp media. At t=0, $CuSO_4$ was added to the media to a final concentration of 50μM. Aliquots were removed at indicated time points post-induction and cells were washed, pelleted, and frozen in liquid N_2 prior to use. Cell lysis and protein extraction was adapted from the ball mill method (273).

Co-Immunoprecipitation

Yeast strains were grown overnight in 10ml YPD or SD media. Cells were lysed in buffer (50mM Tris pH 8, 150mM NaCl, 1mM EDTA, 0.2% Triton X-100, protease inhibitors) with acid-washed glass beads (Sigma) for 2x3 minutes in a multi-tube vortexer (Scientific Industries). Lysates were incubated with 1μl Sup35 antibody at 4ºC for 2 hours, and 40ul of a 50% slurry of Protein G sepharose beads (GE) and lysis buffer was added and tubes were incubated at 4ºC overnight. An unbound fraction was retained and beads were washed 3X in lysis buffer and resuspended in SDS-PAGE sample buffer as the bound fraction. Fractions were boiled in sample buffer for 5 minutes before SDS-PAGE (10% polyacrylamide) and Western blotting with enhanced chemiluminescence (G-Biosciences) and film (GeneMate). Bands were quantified with ImageJ and normalized to immunoprecipitated Sup35.

Sedimentation assay

Yeast were cultured in rich media under homeostatic conditions. Cells were lysed in buffer (100mM Tris pH 7.5, 200mM NaCl, 1mM EDTA, 5% glycerol, protease inhibitors) with glass beads as described above. A “total” fraction was retained, and then lysates were centrifuged at 250,000xg in a TLA100 rotor in an Optima TLX Ultracentrifuge (Beckman Coulter). The supernatant was retained as the “soluble” fraction, and then the pellets were washed in lysis buffer and centrifuged again. Supernatant was discarded and the pellets were resuspended in a 1:1 ratio of lysis buffer to RIPA buffer (50mM Tris pH 7, 200mM NaCl, 1% Triton X-100, 0.5% Na

deoxycholate, 0.1% SDS). Following SDS-PAGE, gels were stained with coomassie blue to visualize the total protein content of each fraction.

2.4 Results

2.4.1 Disruption of NAC subunits rescues toxicity associated with the [PSI+] prion

We set out to identify factors that modulate the toxic misfolding environment associated with the [*PSI*+] prion. Though [*PSI*+] is generally well-tolerated by cells, the overexpression of Sup35 in [*PSI*+] cells is cytotoxic (258). To identify factors that could rescue this toxicity, we overexpressed Sup35 from a copper-inducible promoter and screened for colonies that overcame the toxicity phenotype while retaining the "strong" variant of [*PSI*+] (Figure S.2.1A). Upon sequencing, two toxicity-suppressing candidate colonies contained single gene disruptions of *EGD1*. The *EGD1* gene encodes Egd1, the β-NAC subunit (Figure 2.1A). The NAC is comprised of three subunits: Egd1 (β subunit), Egd2 (α subunit), and Btt1 (β' subunit), which are together known to play an important role in cotranslational folding and protein homeostasis (proteostasis) (274). Our results indicate, for the first time, that deletion of NAC subunits may help to improve cellular health in the face of misfolding stress.

Intrigued by this result, we tested whether deletion of other NAC subunits also rescued the [*PSI*+]-dependent toxicity caused by Sup35 overexpression (258,259). We theorized that double- or triple-deletions, which would not be recovered by our screen, may exhibit stronger phenotypes. We created yeast strains containing combinatorial deletions of all NAC subunits, hereafter referred to as "NAC deletion strains," and tested them for growth in the presence of toxic Sup35 aggregates. We found that two double deletions, *egd1Δegd2Δ* and *egd1Δbtt1Δ*, strongly rescued the toxicity

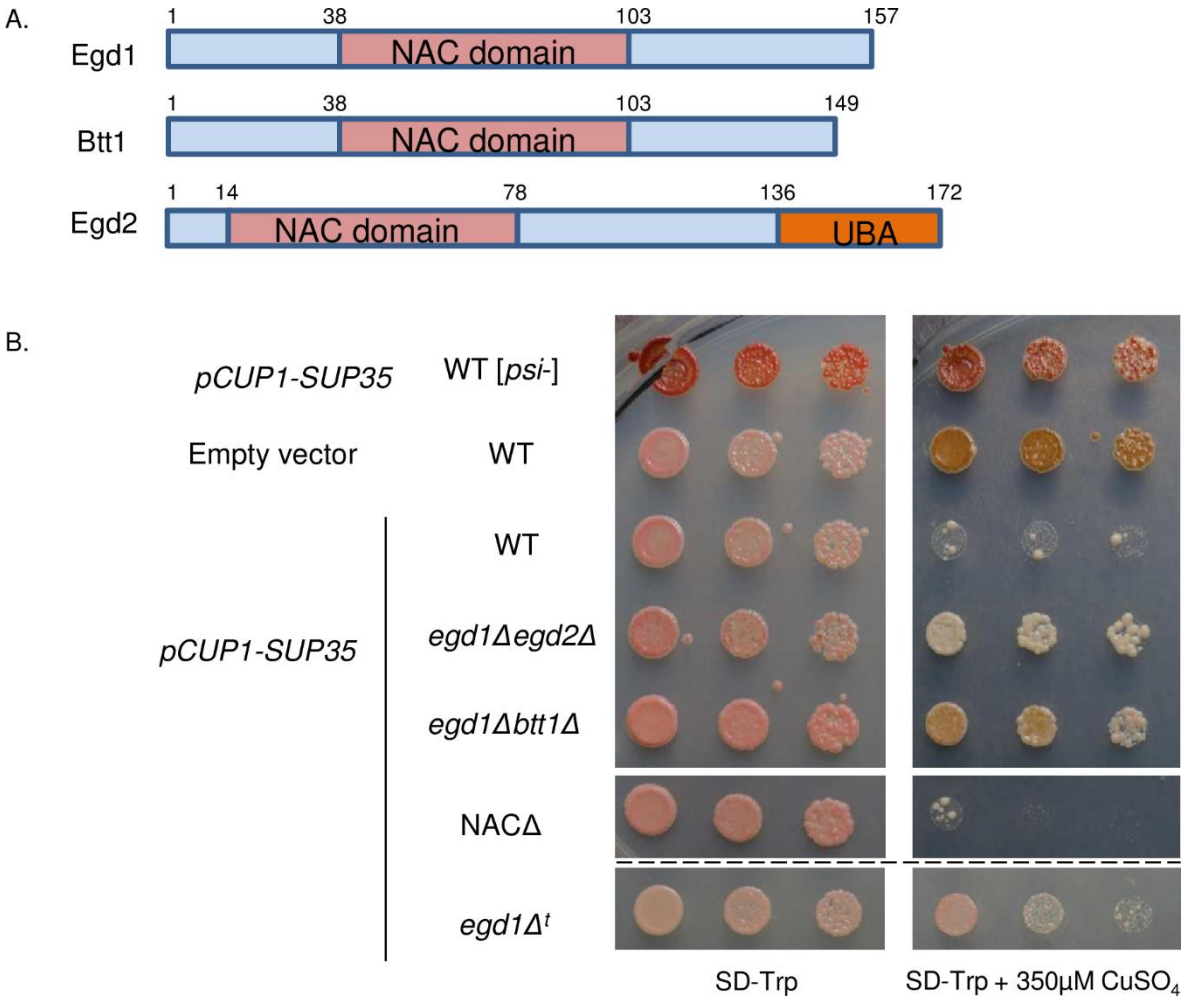

Figure 2.1. Disruption of NAC subunits rescues toxicity associated with the [*PSI*+] prion.
(A) The nascent-polypeptide associated complex consists of the proteins Egd1 (β), Btt1 (β'), and Egd2 (α) that share homology within their NAC domains. (B) Sup35 under control of the copper-inducible promoter CUP1 was induced in [*psi*-] WT, [*PSI*+] WT, and [*PSI*+] NAC deletion strains by growth on selective media containing 350μM CuSO4. The empty vector (EV) control contained the pCUP1 vector. Single horizontal white line separates non-contiguous spots from the same plates. Dashed black line separates spots from different plate of identical media. The "*egd1Δ*^{t}" designation indicates the strain isolated from the transposon screen.

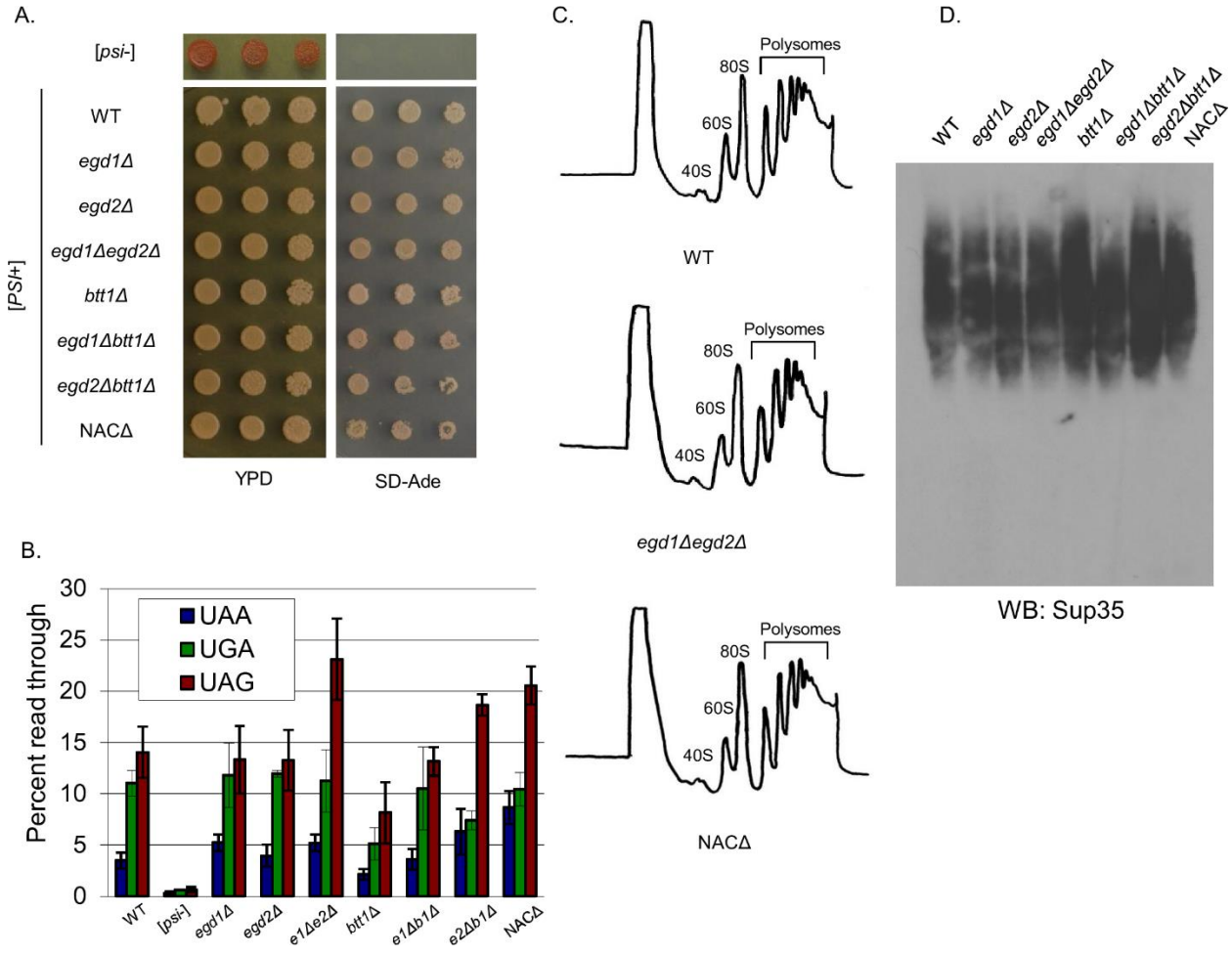

Figure 2.2. Nonsense suppression and prion status are not changed as a result of NAC subunit deletion.

(A) [*PSI*+] NAC deletion strains were tested for growth on YPD and SD-Ade to monitor nonsense suppression of the *ade1-14* allele. (B) Stop codon readthrough is not significantly altered in NAC deletion strains relative to the WT. Expression of PGK(stop)LacZ fusion proteins was monitored by a β-galactosidase assay (275). Data are represented as mean ± SEM. (C) Ribosome profiling revealed no differences in ribosome or polysome formation between the NAC deletion strains. (D) SDD-AGE shows that Sup35 aggregates in the NAC deletion strains are not changed relative to the WT, and all strains retain the "strong" strain of the [*PSI*+] prion.

caused by the overexpression of Sup35 in [*PSI*+] cells (Figure 2.1B). Interestingly, other deletion combinations and deletion of the whole NAC did not detectably overcome the toxicity, potentially due to individual subunit interactions that are not yet understood (Figure S.2.1B).

2.4.2 Nonsense suppression and prion status are not changed as a result of NAC subunit deletion.

It has been previously shown that impaired translation termination is responsible for the toxicity phenotype in [*PSI*+] cells overexpressing Sup35 (258). Therefore, we hypothesized that a decrease in stop codon readthrough may be responsible for the toxicity rescue in the NAC deletion strains.

To test this, we utilized a well-characterized genetic assay: the *ade1-14* allele, which contains a premature stop codon in the *ADE1* open reading frame. Yeast carrying the *ade1-14* allele are unable to complete adenine biosynthesis, resulting in accumulation of a red pigment in cells grown on rich media that have faithful translation termination. The nonsense suppression that occurs in *ade1-14* [*PSI*+] cells leads to completion of the adenine biosynthesis pathway, thus the colonies are white in color and are able to grow on media lacking adenine (SD-Ade) (276). We spotted [*PSI*+] NAC deletion strains onto rich media (YPD) and SD-Ade plates to assess their nonsense suppression phenotypes. All NAC deletion strains formed white colonies and grew strongly on SD-Ade (Figure 2.2A), indicating similar levels of nonsense suppression in all strains in the context of endogenous Sup35.

To assess nonsense suppression quantitatively, we measured stop codon readthrough via the expression of β-galactosidase from a set of reporter plasmids (277). Quantification indicated that there was no significant change in nonsense suppression in any of the NAC deletion strains relative to the WT [*PSI*+] control (Figure 2.2B). We concluded that a decrease in nonsense suppression was not the mechanism by which the NAC deletion strains rescued [*PSI*+]-associated toxicity.

We considered the possibility that a global change in translation was playing a role in toxicity rescue. The quintuple deletion of subunits in a *nacΔssbΔ* strain has been demonstrated to

cause a defect in ribosome biogenesis (278), and fewer translating ribosomes may allow cells to tolerate reduced Sup35 function and withstand toxicity by improving the ratio of translation termination factors. We analyzed ribosome profiles for all NAC deletion strains and found no differences in the peak heights or integrated peak areas (Figure 2.2C), nor did we observe the formation of ribosomal half-mers. Thus, translation is not globally perturbed in the NAC deletion strains relative to WT.

We next questioned whether the toxicity rescue indicated a change in prion variant of the NAC deletion strains. To assess the Sup35 aggregates biochemically, we used semi-denaturing detergent agarose gel electrophoresis (SDD-AGE). We found that the overall distribution of SDS-sensitive population of Sup35 aggregates did not change following growth in media without copper (Figure 2.2D), confirming that all NAC deletion strains retained the strong [*PSI*+] prion variant. Thus, the toxicity rescue phenotype exhibited by the NAC deletion strains was not due to loss or weakening of the [*PSI*+] prion.

2.4.3 Prion aggregates are visibly altered due to NAC subunit deletion

We were surprised that the NAC deletions rescued [*PSI*+]-related Sup35 overexpression toxicity without observable changes to the prion or to nonsense suppression. To further investigate the reduction of Sup35 toxicity, we examined the aggregation and solubility of the Sup35 prion aggregates in all NAC deletion strains. We sought to do so by a method that would allow observation of intact aggregates in cells, rather than simply the SDS-resistant aggregates detected by SDD-AGE (Figure 2.2D). We transformed a copper inducible, GFP-tagged Sup35 (pRS314CUP1 *Sup35GFP*) into the WT and NAC deletion strains. We induced Sup35-GFP expression by the addition of small amounts (V_f=50μM) of $CuSO_4$ to the culture media and monitored GFP localization by fluorescence microscopy. Sup35-GFP exhibited a diffuse pattern

of fluorescence in [*psi*-] cells (Figure 2.3A), consistent with non-aggregated Sup35. By contrast, Sup35-GFP was observed in a single fluorescent focus in the WT [*PSI*+] strain (Figure 2.3A). Most NAC deletion cells also contained one major fluorescent puncta. However, the *egd1Δegd2Δ* strain harbored multiple fluorescent puncta throughout the cytoplasm (Figure 2.3A, Figure S.2.2A). Interestingly, this phenotype was not apparent in the toxicity-rescuing *egd1Δbtt1Δ* deletion, suggesting that a similar change in aggregate distribution was not the rescuing effect. However, it is plausible that there is an altered aggregation pattern that is too subtle to be detected via fluorescence microscopy. Importantly, the WT and all NAC [*PSI*+] deletion strains exhibit insoluble Sup35 at steady-state levels of Sup35 expression (Figure 2.3B), as expected with the presence of the [*PSI*+] prion.

We then asked if the multiple aggregates in the *egd1Δegd2Δ* strain were due to altered joining of monomeric Sup35 to existing amyloid structures. To address this question, we induced the expression of Sup35-GFP and tracked its solubility over time. In lysates of WT [*PSI*+] strains, an abundance of Sup35-GFP appears in the pellet fraction at two hours post-induction of Sup35-GFP expression due to formation of insoluble aggregates (Figure 2.3C, Figure S.2.2B). Remarkably, we did not detect Sup35-GFP in the pelleted fractions of *egd1Δegd2Δ* or *egd1Δbtt1Δ* strains up to four hours post-induction (Figure 2.3C), consistent with at least transiently enhanced solubility of Sup35. The amount of induced Sup35-GFP was consistent between all tested strains (Figure S.2.2C).

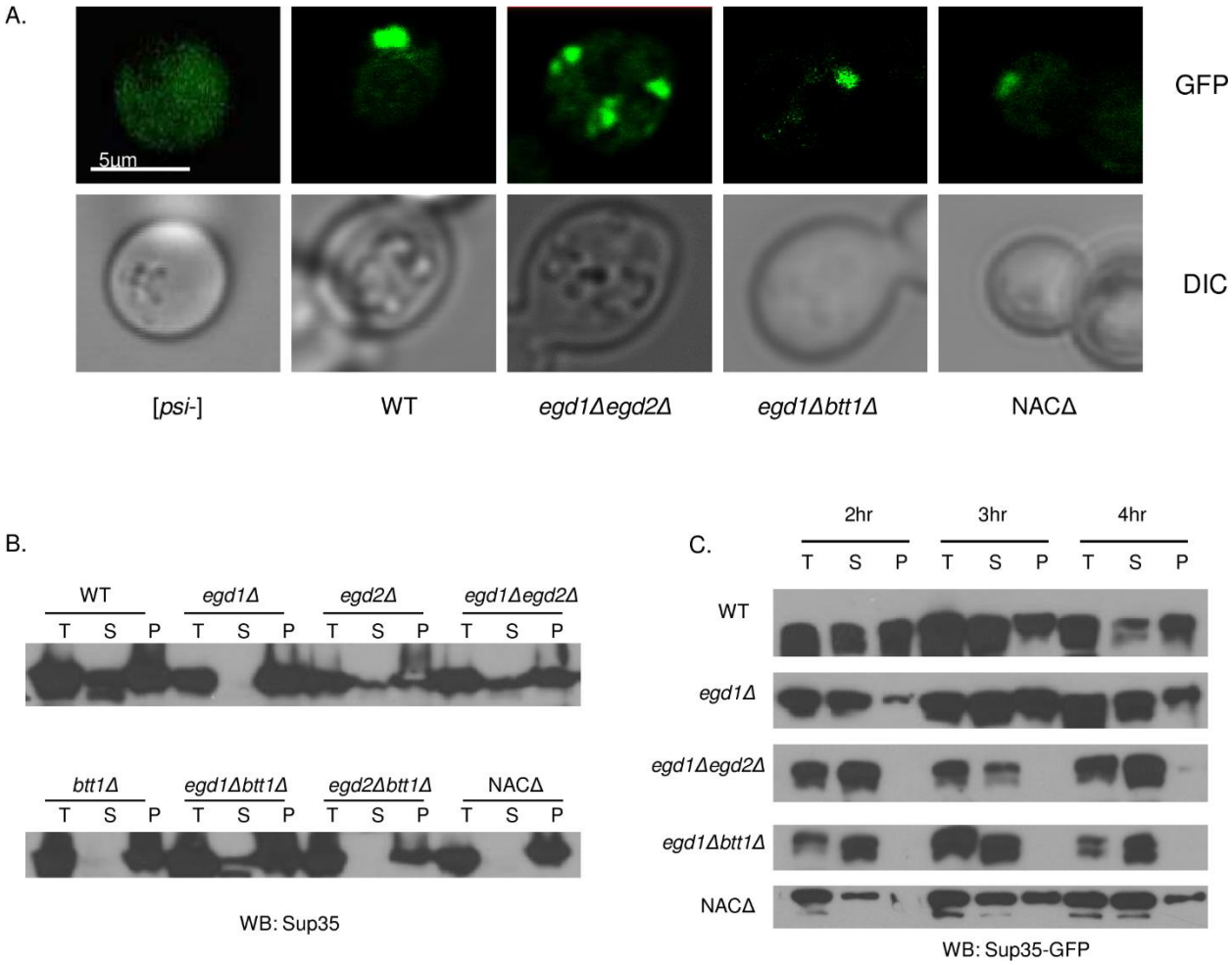

Figure 2.3. NAC deletion strains retain [*PSI*+] despite altered Sup35 solubility.
(A) NAC deletion strains containing pCUP1-*SUP35-GFP* were grown in selective media in the presence of 50µM CuSO4. Two-dimensional images were taken with an Olympus FV1200 laser scanning microscope with a 100X oil immersion objective. The *egd1Δegd2Δ* strain showed a greater population of aggregates than the WT or other NAC deletion strains. (B) Solubility of Sup35 in [*PSI*+] lysates of indicated strains. Total (T), supernatant (S), and pellet (P) fractions were subjected to SDS-PAGE and Western blot. With endogenous levels of protein expression, all NAC deletion strains show insoluble Sup35. The *egd1Δegd2Δ* and *egd1Δbtt1Δ* strains exhibit more soluble Sup35 than the other NAC deletion strains. (C) NAC deletion strains were grown overnight in selective media; Sup35 overexpression was induced by the addition of $CuSO_4$ to a final concentration of 50µM at time= 0. Solubility assays were performed on cells collected at indicated timepoints following Sup35 induction. The *egd1Δegd2Δ* and *egd1Δbtt1Δ* strains exhibited a defect in joining of nascent Sup35 to existing aggregates.

One interpretation of this result is that the joining of newly synthesized Sup35 to prion aggregates is delayed in the *egd1Δegd2Δ* or *egd1Δbtt1Δ* strains. We hypothesize that the structure of nascent

Sup35 in the NAC deletion strains renders Sup35 impaired in joining to pre-existing aggregates due to altered, and possibly improved, folding of nascent Sup35. This is supported by the decrease in *de novo* [*PSI*+] induction in the toxicity-rescuing NAC deletion strains (S2D Fig).

2.4.4 Chaperone balance is altered in NAC deletion strains

We next considered the possibility that the putative changes to Sup35 structure were brought about by altered interactions with chaperone proteins. Sup35 is a client of many cytosolic chaperones (279–281). We reasoned that NAC deletion may spur a compensatory response of other molecular chaperones such that the deletion strains may, in fact, be folding some proteins more efficiently than WT.

When the NAC is depleted, the first major chaperone to interact with nascent chains is the Hsp70 Ssb, in conjunction with the ribosome-associated complex (RAC) (267,278,282). Ssb has dual functions as a ribosome-bound and cytosolic chaperone. In addition, it has a cytosol-only Hsp70 homolog Ssa (280). Both chaperones have been shown to interact with Sup35(283–285). We hypothesized that NAC deletion would impact the abundance, presence, or activity of the Hsp70s. We assessed total levels of Ssa and Ssb in each [*psi*-] and [*PSI*+] NAC deletion strain and found no difference relative to the wild type (S3A Fig).

We theorized that NAC deletion may increase the role of Ssb-RAC in cotranslational folding, as this protein complex is next in line to receive nascent chains following the NAC. This increased folding pressure upon Ssb-RAC as a result of NAC deletion might also localize a larger fraction of Ssb to the ribosome and nascent chains while titrating Ssb away from the available cytosolic pool. The titration would reduce the overall availability of cytosolic Ssb relative to Ssa, thereby creating a chaperone imbalance.

We began by assessing the general effects of imbalanced Hsp70s in strains with intact NAC subunits. We challenged proteostasis by overexpressing Sup35 in a WT [*PSI+*] strain with endogenous Ssa expression and found that the cells grew as expected, with a moderate toxicity phenotype and consistent Sup35 expression (S3B Fig, Figure 2.4A). However, recapitulating an imbalance by deleting Ssb1 from this strain resulted in enhanced toxicity (Figure 2.4A). This indicates that cells are sensitive to chaperone balance in the presence of folding-challenged substrates. We then sought to verify that the balance of Ssb1 relative to Ssa1 was specifically affecting toxicity. To do so, we exacerbated the Hsp70 imbalance by overexpressing Ssa1 in WT and *ssb1Δ* strains. We again challenged proteostasis with overexpression of Sup35, but at a lower level than in the previous experiment. Slightly imbalanced Hsp70s (WT strain with SsaOE) led to poor growth, and severely imbalanced Hsp70s (*ssb1Δ* with Ssa1OE) led to pronounced toxicity (Figure 2.4B). Reintroduction of Ssb1 rescued the phenotype (Figure 2.4B). We concluded that cells are sensitive to the balance between Ssa and Ssb, and that the severity of the toxicity phenotype correlates with the severity of the imbalance.

We then sought to extend our analysis to the NAC deletion strains. As above, we overexpressed Ssa1 from a constitutive promoter in the WT and all NAC deletion strains; we observed no change in either growth or prion phenotype in the absence of Sup35 overexpression (Figure S.2.4 and Figure 2.4C, YPD plates). However, when we subjected the same strains overexpressing Ssa to minor Sup35 overexpression, we observed a severe toxic phenotype in the *egd1Δegd2Δ* and *egd1Δbtt1Δ* strains (Figure 2.4C, selection plates) that mimicked the strong toxicity exhibited by *ssb1Δ* strains under the same conditions. Overexpression of Ssb1 did not

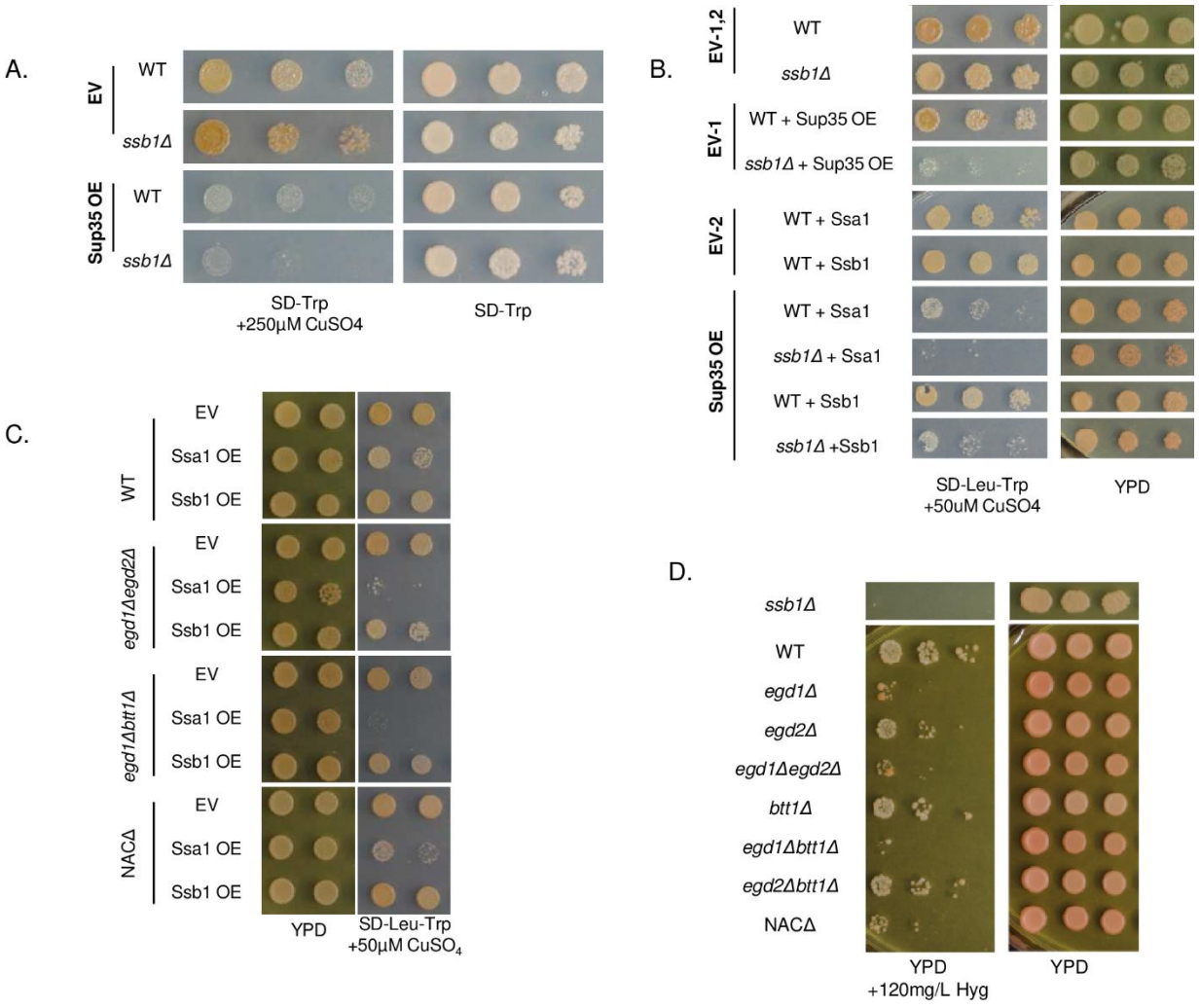

Figure 2.4. Chaperone balance is altered in NAC deletion strains.
(A) WT and *ssb1Δ* strains were transformed with pCUP1-*SUP35* and spotted on plates containing 300μM copper to induce Sup35 overexpression. (B) WT and *ssb1Δ* strains were transformed sequentially with p314CUP-SUP35 and either p415GPD-*SSA1* or p415GPD-*SSB1*; transformants were spotted onto SD-Leu-Trp plates containing 50μM $CuSO_4$. The *ssb1Δ* strain showed increased sensitivity to Sup35 overexpression in conjunction with Ssa1 overexpression. All strains on selective media are overexpressing Sup35. (C) WT and NAC deletion strains were first transformed with p314CUP-*SUP35*, then with either pRS415 (EV), p415GPD-*SSA1*, or p415GPD-*SSB1*. Transformants were spotted onto SD-Leu-Trp plates containing 50μM $CuSO_4$ to induce non-toxic Sup35 overexpression. (D) WT and NAC deletion strains were spotted onto plates containing 120mg/L Hygromycin B. All strains pictured in panels A-D contain [*RNQ*+] and the strong variant of [*PSI*+].

cause cytotoxicity (Figure 2.4C). Ssa1 overexpression in the WT and single deletion strains did not perturb growth as severely (Figure S.2.5), possibly because the chaperone imbalance remained

within a tolerable range. However, the toxicity in the *egd1Δegd2Δ* and *egd1Δbtt1Δ* strains indicates that Ssa1 overexpression pushes an already-imbalanced system into a highly detrimental state. This suggests that NAC deletion mimics Ssb deletion phenotypes despite the unchanged expression levels of all tested chaperones (Figure S.2.3), thereby supporting the concept of cellular localization changes and an imbalance of Ssb relative to Ssa.

We next questioned whether NAC deletion could phenocopy a chaperone imbalance in the absence of Sup35 overexpression. We tested the growth of [*PSI*+] NAC deletion strains under conditions that are disadvantageous to the *ssb1Δ* strain. We spotted the NAC deletion strains onto plates containing 120µg/L HygromycinB (HygB), as it is known that *ssb1Δ* yeast are sensitive to the fungicide (286). Though WT yeast grew on HygB plates, several of the NAC deletion strains, including *egd1Δegd2Δ* and *egd1Δbtt1Δ*, exhibited poor growth consistent with depleted Ssb (Figure 2.4D). The growth similarities between NAC and Ssb deletion strains support the possibility that the NAC-induced chaperone imbalance may be altering the functionality of Ssb in ways that mimic its deletion.

2.4.5 NAC deletion relocalizes Ssb to nascent polypeptides and away from prion aggregates

Though some NAC deletion strains exhibited phenotypes related to Ssb depletion, all strains exhibited WT levels of all tested chaperones (Figure S.2.3). We hypothesized that NAC subunit deletion led to alterations in Ssb localization and availability due to an additional requirement for Ssb at the ribosome. We reasoned that the loss of NAC subunits would cause Ssb to assist in the folding activities that were typically controlled by the NAC. To test this, we returned to our ribosome profile analysis (Figure 2C) and assessed the proteins present in the peak fractions. We theorized that more Ssb would be present in the polysome fractions of the *egd1Δegd2Δ* strain

relative to the WT, because folding-challenged nascent chains would require more extensive cotranslational interactions with Ssb. We probed for the presence of Ssb in the polysome and monosome peaks and normalized to the amount of ribosomal protein Rpl3 detected in the same peaks (Figure 2.5A). The amount of Ssb in the polysome fractions was indeed increased in the *egd1Δegd2Δ* deletion strain relative to the WT, indicating a greater proportion of Ssb comigrating with polysomes. Thus, the localization of Ssb is altered in the NAC deletion strains relative to the WT, potentially modulating nascent Sup35 folding and related cytotoxicity.

To further probe the theory of Ssb relocalization, we sought to assess Ssb binding to aggregated Sup35. We hypothesized that an increase of Ssb binding to nascent chains would lead to a corresponding decrease in the pool of available (non-polysome bound) Ssb. This would cause decreased Ssb binding to Sup35 aggregates. We performed co-immunoprecipitation experiments in [*PSI+*] cells using a Sup35 antibody and probed for the presence of Ssb1/2. We found that the amountof Ssb1/2 that co-immunoprecipitated with Sup35 was reduced in several of the NAC deletions (Figure 2.5B), with the effect being most pronounced in *egd1Δegd2Δ* (50.0% reduction in co-immunoprecipiation, ±8.1%). The steady state levels of Ssb1/2 were not reduced in the NAC deletion strains (Figure S.2.3); thus, the decreased interactions with Sup35 represent a change in the binding between Ssb and its pool of post-translational substrates. This result, in combination with the enhanced presence of Ssb at translating ribosomes, indicates that Ssb localization shifts as a consequence of NAC subunit deletion.

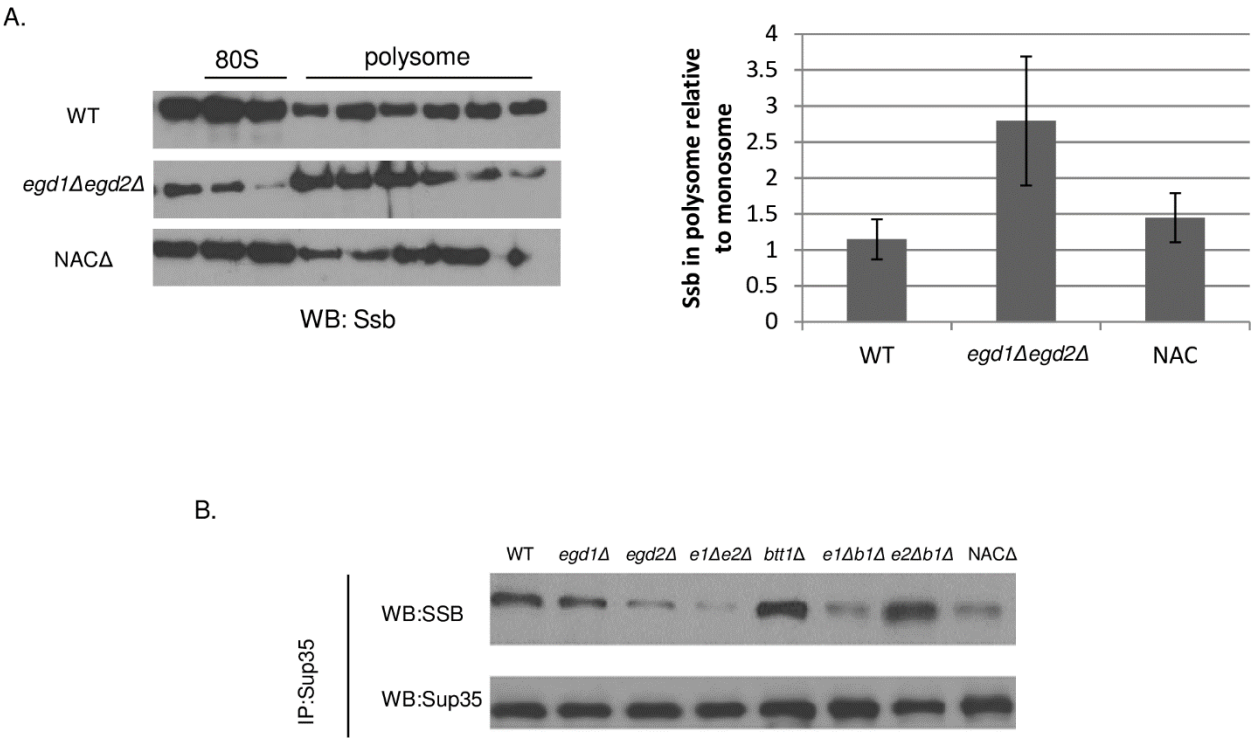

Figure 2.5. NAC deletion relocalizes Ssb to nascent polypeptides and away from prion aggregates

(A) Fractions from the monosome and polysome peaks of ribosome profile experiments were TCA precipitated prior to SDS-PAGE and Western blotting. More Ssb comigrated with polysomes in the *egd1Δegd2Δ* strain relative to the WT or to the whole-NAC deletion. Western blots are of the sucrose gradient fractions that contained the monosome and polysome peaks and are representative images from five independent experiments. Quantifications are from five independent experiments, and data are represented as mean ± SEM. See Materials and Methods for full computational details. (B) WT and NAC deletion strains were subjected to co-immunoprecipitation with an anti-Sup35 antibody. Equal amounts of Sup35 were immunoprecipitated across all strains. "Total" and "unbound" fractions were collected and no differences in Ssb protein expression levels were apparent (Figure S.2.3) Western blots are representative images from three independent experiments. All strains utilized contained [*RNQ*+] and the strong [*PSI*+] variant.

2.4.6 NAC deletion causes [PSI+] to resist curing by Hsp104 overexpression

We hypothesized that the imbalanced Hsp70s may impact other molecular chaperones in the NAC deletion strains. Ssa and Ssb both interact with the disaggregase Hsp104, which is required for the

propagation of all but one of the known yeast prions (276,287). We found no observable difference in steady state levels of Hsp104 (Figure S.2.3). Hsp104 activity was also not different between the WT and NAC deletion strains by thermotolerance tests (Figure S.2.6). Therefore, the observed toxicity rescue was not due to a change in presence or functionality of Hsp104.

Inhibition of Hsp104 is thought to cure prions by preventing fiber fragmentation, which impairs inheritance of seeds (276). Overexpression of Hsp104 specifically cures [*PSI*+], and its curing ability is influenced by the Hsp70s. Ssb overexpression in conjunction with Hsp104 overexpression promotes loss of [*PSI*+], while Ssa1 overexpression prevents Hsp104-mediated curing (280,288,289). Therefore, we predicted that Hsp104 curing efficiency may be altered in the NAC deletion strains due to the imbalance of Ssa and Ssb.

Hsp104 overexpression efficiently cures the [*PSI*+] prion, an effect that is inhibited by simultaneous Ssa overexpression. We wondered whether the Hsp70 imbalance in the NAC deletion strains would mimic this phenotype. We transformed each of the NAC deletion and WT strains with a plasmid that constitutively overexpresses Hsp104 and verified that Hsp104 levels were increased while not altering the growth of the cells or amount of Sup35 expressed (Figure S.2.7). We then phenotypically characterized the transformants by streaking them onto rich media. We again took advantage of the red/white colormetric assay that allowed us to track the presence of the yeast prion: white colonies harbor Sup35 aggregates while red colonies have been cured of [*PSI*+]. Surprisingly, all NAC deletion strains (with the exception of *egd1Δ*) were resistant to Hsp104-mediated curing of [*PSI*+], as a significant proportion of their colonies remained white on rich media on first pass (Figure 2.6A, 2.6B). This result was confirmed by performing an SDD-AGE assay to visualize the SDS-resistant Sup35 aggregates. Following continued growth with Hsp104 overexpression, aggregated Sup35 was still present in the NAC deletion strains but not

the wild type (Figure 2.6C). This demonstrated that prion curing was less efficient in strains where NAC depletion was affecting chaperone balance and mimicked Ssa1 overexpression.

We then hypothesized that a heritable change in [*PSI*+] conformation or structure may have created Sup35 aggregates that were poor Hsp104 binding partners. These altered aggregates may thus be resistant to refolding by Hsp104 activity independent of a chaperone imbalance. We performed cytoduction experiments to test the curing of prions from NAC deletion strains in a WT genetic background (290). We transferred Sup35 aggregates from WT and NAC deletion strains into wild type [*psi*-] strains by cytoplasmic transfer so that the resulting yeast were genetically WT but contained [*PSI*+] from the cohort of NAC deletion strains. We then induced Hsp104 overexpression and found that all of the cytoduced strains were cured as efficiently as WT (Figure 2.6D, Figure S.2.8A). Thus, the heritable Sup35 aggregate structure was not the cause of differential Hsp104 curing; rather, the curing resistance exhibited by the deletion strains was a consequence of the genetic disruption of the NAC.

As the NAC deletion strains exhibited resistance to curing by Hsp104 overexpression, we wondered if they would also resist curing by Hsp104 inactivation. To test this, we passaged the NAC deletion strains on media containing 5mM guanidine hydrochloride (GdnHCl), a strong inhibitor of Hsp104 (291), which cures all known yeast prions. The WT and NAC deletion strains demonstrated equal curability on GdnHCl plates (Figure S.2.8B). Taken together, these results suggest that the differential effects of the NAC interactions between Hsp104 and Sup35 are related the activity of co-chaperones.

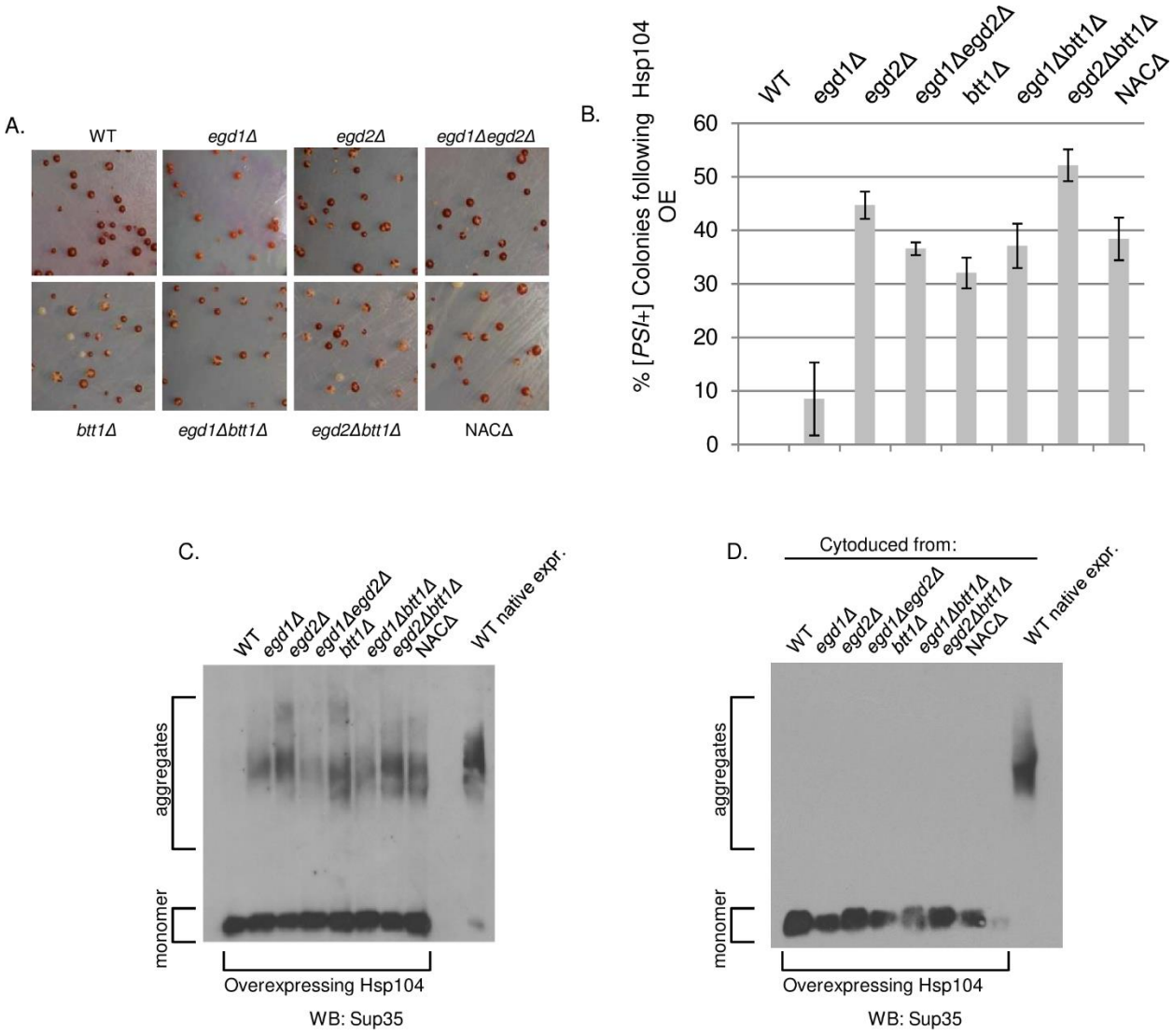

Figure 2.6. NAC deletion causes [*PSI*+] to resist curing by Hsp104 overexpression.
WT and NAC deletion strains were transformed with p426GPD-*HSP104* to overexpress Hsp104 and then grown for 4 days at 30°C. (A) Representative images from transformation plates. Strains were originally strong [*PSI*+]; red color denotes curing of the [*PSI*+] prion. (B) Six independent transformations of NAC strains with p426GPD- *HSP104* were plated on selective media and [*PSI*+] status was quantified via phenotypic analysis of each colony. Data are represented as mean ± SEM. (C) Five colonies per NAC deletion strain, plus WT controls, were picked from transformation plates and grown 16hrs in selective media. SDD-AGE analysis shows the stability of the [*PSI*+] prion in the NAC deletion strains, but not the WT, upon overexpression of Hsp104. (D) Following cytoduction of [*PSI*+] from NAC deletion strains into a WT background, cytoductants did not retain the ability to resist curing by Hsp104 overexpression.

2.4.7 NAC deletion strains are resistant to general protein misfolding

Given the toxicity rescue phenotype resulting from loss of NAC subunits and altered chaperone activity, we considered that NAC deletion may bring about a broader modification to proteostasis and the cellular response to protein misfolding. First, we probed the ability of the NAC deletion strains to manage global protein misfolding. We challenged cells with canavanine, an arginine analog that induces misfolding (292), and found that most NAC deletion strains were able to survive high levels of the compound (Figure 2.7A), indicating that loss of NAC subunits allows cells to better tolerate the adverse effects of misfolding.

To determine how NAC deletion strains tolerate elevated protein misfolding, we asked whether misfolded proteins were differentially acted upon by protein quality control machinery in the NAC deletion strains. We questioned whether the NAC deletion strains resist canavanine-induced misfolding due to increased activity of the ubiquitin-proteasome system (UPS). We assessed the presence of ubiquitinated species in the NAC deletion strains in the presence and absence of canavanine and found no differences between the WT and the most stabilized NAC deletion strains (Figure 2.7B). Additionally, challenging the ubiquitin-proteasome system with heat stress or the proteasome inhibitor MG132 showed no differences between the WT and the NAC deletion strains (Figure S.2.6, Figure S.2.9A). Thus, cellular viability in the presence of canavanine is not related to increased protein degradation as mediated by the UPS.

We considered the possibility that NAC deletion strains may package misfolded proteins into insoluble aggregates, rendering them nonfunctional but nontoxic. We performed solubility assays to visualize total protein aggregation in the NAC deletion strains, and observed no changes relative to the wild type (Figure 2.7C, Figure S.2.9C). Therefore, we concluded that there is no gross global difference in the way proteins are packaged or degraded in the NAC deletion strains relative to the WT, indicating that the toxicity rescue phenotype is not related to enhanced stress

response or turnover of misfolded proteins. Rather, like the prion-dependent effect, the chaperone imbalance renders cells generally resistant to misfolded proteins.

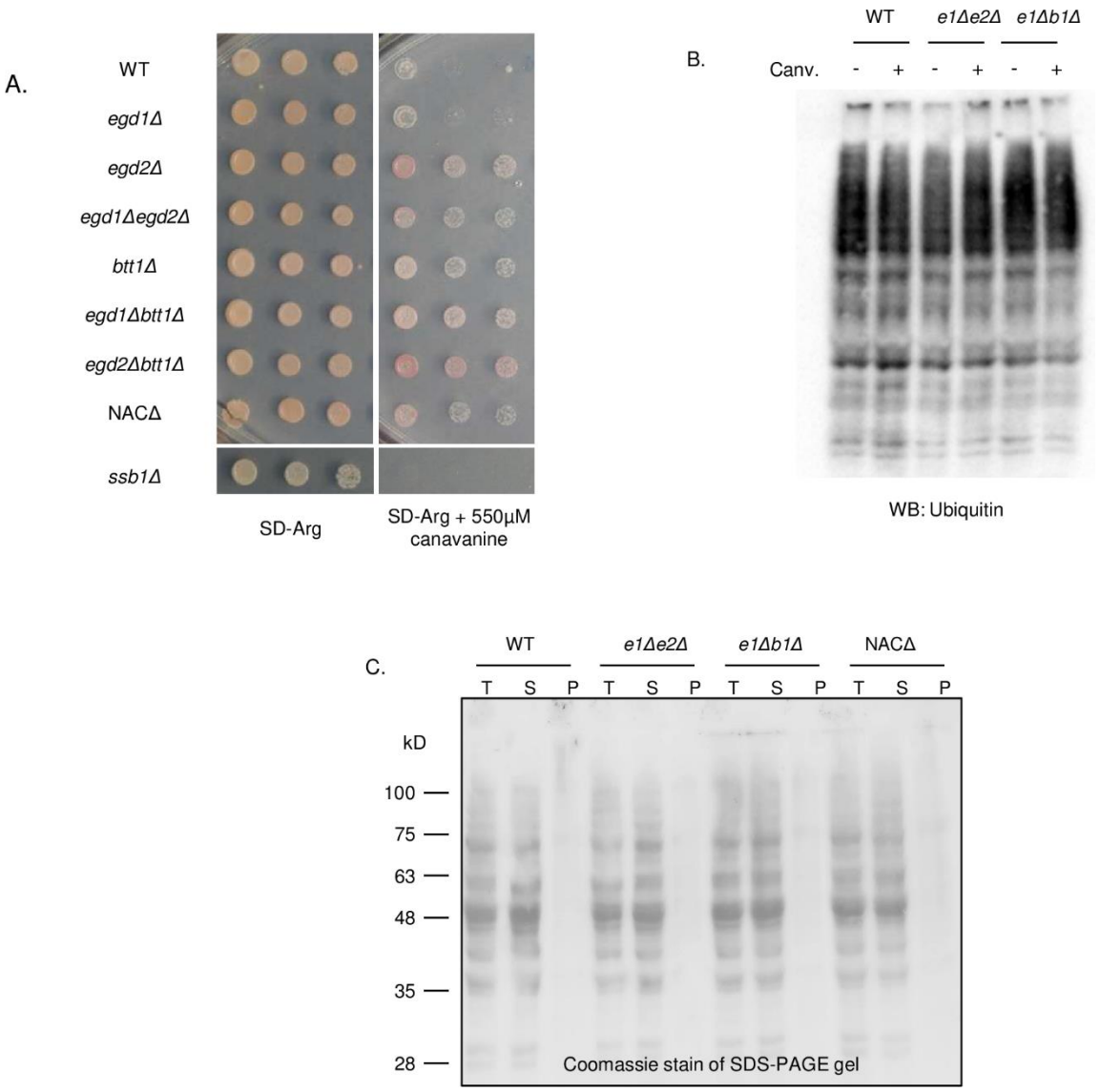

Figure 2.7. NAC deletion strains are able to resist protein misfolding without inducing stress response.

(A) WT and NAC deletion strains were spotted on SD-Arg plates containing 550μM canavanine to induce global protein misfolding. (B) The total ubiquitinated proteins in WT, *egd1Δegd2Δ*, and *egd1Δbtt1Δ* are unchanged in both the presence and absence of canavanine. (C) Total aggregated protein was assessed via a solubility assay followed by SDS-PAGE and Coomassie staining.

2.5 Discussion

Nascent polypeptides are functionally connected to cytosolic chaperones

Here, we show that the NAC affects the localization and activities of other molecular chaperones. Our model (Figure 2.8) suggests that deletion of the α- and β-NAC subunits cause relocalization of the Hsp70 Ssb away from the available pool of cytosolic chaperones and to translating ribosomes, creating an imbalance that mimics Ssb deletion phenotypes. This depletion of Ssb from Sup35 aggregates serves to change the interaction of the [*PSI*+] prion with other chaperones, including Hsp104, which is less able to efficiently cure [*PSI*+] in the NAC deletion backgrounds. The deletion of the NAC does not impact expression levels for any of the proteins examined in this study (Figure S.2.3); thus, the observed phenotypes are due to changes in localization and functionality. These chaperone modifications correspond to an alteration in the aggregation pattern of the [*PSI*+] prion and the reduced ability of newly synthesized protein to join pre-existing aggregates. This alteration can be beneficial when cells are challenged with a toxic prion, presumably due to more active engagement of chaperones with nascent polypeptide chains where there is a high risk for misfolding (267). We suggest a model of cotranslational folding that recruits cytosolic chaperones to nascent polypeptides in a manner that can rescue the toxicity associated with proteins prone to misfolding. Additional mechanistic studies will be necessary in order to determine the extent of Ssb activity on nascent chains in response to NAC deletion and how Ssb may differentially respond to the presence or absence of NAC subunits.

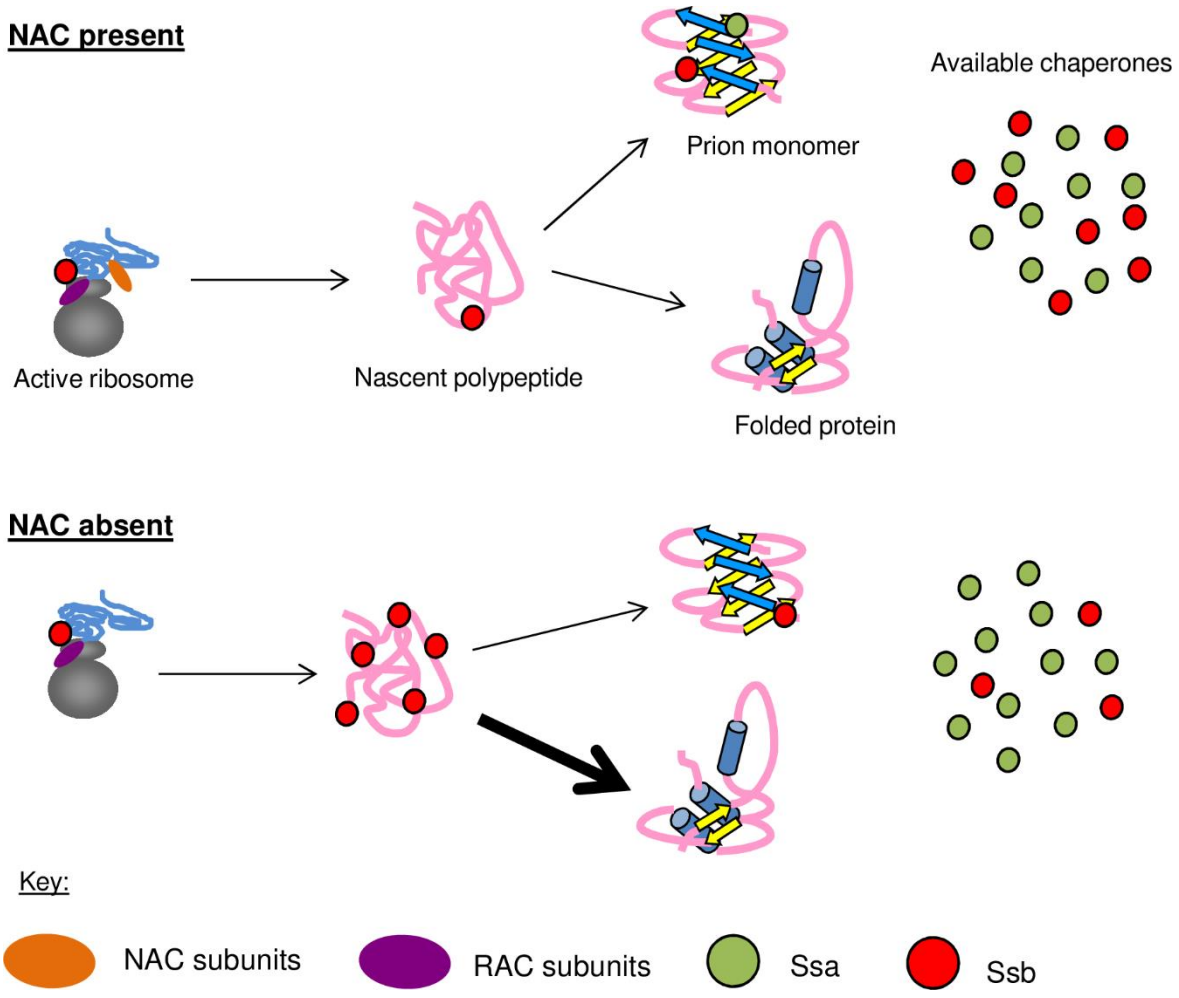

Figure 2.8. NAC subunits affect the yeast chaperone network by altering chaperone pools. In the presence of the NAC, RAC-Ssb receives nascent polypeptides from the NAC and assists with their folding. Both Ssa and Ssb bind to aggregated Sup35 and affect its ability to form and propagate the [*PSI*+] prion. When NAC subunits are deleted, Rac-Ssb becomes the first complete chaperone system to interact with nascent polypeptides. The unfolded state of these proteins requires more extensive interaction with RAC-Ssb, thereby sequestering cytosolic Ssb to the ribosome. Thus, less cytosolic Ssb is available to bind to monomeric or aggregated Sup35. This would lead to a relative increase in Ssa1 binding to Sup35 aggregates, which inhibits efficient monomer joining and reduces the ability of Hsp104 to cure the prion.

Deletion of NAC subunits increases pressure on other cotranslational chaperones

The toxicity rescue effect of NAC subunit deletion was a surprising result. Deletion of cotranslational folding factors would not be expected to rescue toxicity associated with a prion-forming protein. We propose that deletion of NAC subunits creates an environment where the ribosome-associated complex and Ssb (RAC-Ssb) are the first fully-functional chaperones that interact with nascent polypeptides. Nascent polypeptides encountering the RAC-Ssb system in the NAC deletion strains are presumably less protected or folded than in WT cells. The RAC-Ssb system, compensating for loss of NAC subunits, might retain Ssb on nascent polypeptides, thereby reducing free Ssb elsewhere in the cell.

NAC subunits may act independently upon partial deletion of the complex

Interestingly, deletion of the whole NAC did not recapitulate all of the phenotypes associated with the double deletions (summarized in Table S.2.1). In particular, whole-NAC deletion did not rescue [*PSI+*]-related Sup35 overexpression toxicity. Deletion of the entire NAC may exacerbate the chaperone imbalance in such a way that leads to a harmful depletion of the cytosolic pool of Ssb. However, in other cases, the triple NAC deletion did mimic phenotypes associated with the double deletions. For example, NAC deletion confers resistance to hygromycin B and increases resistance to Hsp104-mediated curing. This leads us to hypothesize that there is a function for each of the NAC subunits that can persist independent of the complex. For example, hygromycin B resistance is demonstrated by every strain that has a deletion of *EGD1*, indicating that this subunit may be particularly important in modulating the interaction between nascent chains and molecular chaperones. Further, in the NAC deletion strains, any subunits that remain in the cell might act independently on nascent chains or upon misfolded cytosolic proteins. The

precise function of all of the NAC subunits remains unclear and we look forward to future studies that will shed light on this dynamic complex.

NAC deletion changes chaperone localization, but not functionality

The ability of NAC deletion strains to mimic Ssb deletion phenotypes led us to question Ssb functionality in a NAC-depleted background. However, we have demonstrated that Ssb deletion is toxic in the presence of Sup35 overexpression, indicating that chaperone function is necessary. Further, perturbations that prevent Ssb association with the ribosome have been shown to enhance yeast sensitivity to Sup35 overexpression (293). We suggest that the toxicity rescue observed in the NAC deletion strains is due to a shift in Ssb activity to nascent proteins. This change in localization and/or activity leads to a decrease in available Ssb relative to available Ssa.

Though we suggest an increase in Ssb localization to nascent polypeptides as a result of NAC deletion, we did not observe the distribution of Ssa to be affected. Ssa does not have an established role in cotranslational folding and is not ribosome-associated. Thus, in NAC deletion backgrounds in which Ssb becomes relocalized, the shift in the amount of available cytosolic Ssb relative to Ssa creates local imbalances between the Hsp70s at the ribosome, in the unbound cytosolic pool, and at prion aggregates. Thus, these strains can simultaneously exhibit phenotypes mimicking Ssa depletion (reduced de novo [*PSI*+] formation, Figure S.2.2), Ssa overexpression (resistance to Hsp104-mediated curing, Figure 2.6), Ssb deletion (sensitivity to HygB, Figure 2.4), and Ssb overexpression (prion toxicity rescue, Figure 2.1). This spectrum of effects suggests that neither Ssa nor Ssb has inhibited activity in the NAC deletion strains.

We were surprised that Ssa1 overexpression resulted in a toxicity phenotype in conjunction with slight Sup35 overexpression in [*PSI*+] NAC deletion strains. We hypothesize that Ssa overexpression sequesters an essential cofactor or substrate from Ssb; for example, an Hsp40 or a

nucleotide exchange factor, which would in turn reduce Ssb's folding capabilities. In the NAC deletion strains, the enhanced requirement of Ssb to fold nascent polypeptides would cause any perturbation of Ssb to be harmful to proteostasis and cellular health. Future studies will examine the competition between Hsp70s for multiple cofactors, a relationship that is not fully understood (294,295).

Ssb relocalization prevents new monomer from joining and rescues [*PSI*+]-associated toxicity

Titrating Ssb away from the free pool of molecular chaperones has several effects on the cell and on the [*PSI*+] prion. Increasing the contact between Ssb and nascent polypeptides may cause Ssb to interact earlier with unfolded or misfolding Sup35. This would in turn inhibit the ability of nascent Sup35 to efficiently join aggregates, as Ssb overexpression is known to promote loss of [*PSI*+] (280). In the most extreme case, the *egd1Δegd2Δ* strain, this joining defect manifests as fractured Sup35-GFP aggregates as viewed microscopically. This reorganization of aggregates may either release or reduce interaction with cofactors that are toxically sequestered during normal amyloid formation (258), leading to the rescue phenotype exhibited most strongly by the *egd1Δegd2Δ* strain.

It is likely that other NAC deletion strains undergo similar chaperone reorganization, but to a lesser extent depending on which NAC subunits remain to act upon nascent chains. This slight chaperone imbalance would lead to weaker phenotypes that evade detection. For example, the *egd1Δbtt1Δ* strain does not show altered Sup35-GFP aggregation, yet exhibits a joining defect via solubility assays. This strain also rescues prion-related toxicity, albeit to a weaker extent than the *egd1Δegd2Δ* strain.

Chaperone inhibition is a promising anti-disease mechanism for mammalian systems

The stable propagation of [*PSI*+] by nontoxic Sup35 aggregates indicates that NAC deletion, and the subsequent chaperone imbalance, slows the toxic addition of Sup35 monomer to existing aggregates. Retention of aggregates without toxicity has implications for mammalian protein misfolding disorders that are spread via oligomeric species (296). By reducing monomer joining onto existing amyloid, NAC deletion is blocking a key step in the prion life cycle. The resistance to global protein misfolding induced by canavanine in the NAC deletion strains (Figure 2.7A) indicates that depletion of the NAC, and subsequent functional substitution by other chaperones, can protect cells against non-prion misfolding. Future studies are needed to determine the effects of NAC deletion on the propagation and stability of additional fungal prions and other amyloidogenic proteins. In the context of human disease, amyloid plaque formation may be slowed or stopped if a similar mechanism can be unveiled.

The fact that chaperone deletion can be beneficial to cells, even in the face of protein misfolding stress, is a counterintuitive result. However, there is a growing body of evidence to support chaperone inactivation as a mechanism via which disease progression may be slowed. Many of these studies have focused on cancer (297), but recent research has found that Hsp70 imbalance leads to increased aggregation of the Alzheimer's-related protein tau (298) and that Hsp70 inhibition can promote tau clearance (299). Taken together, these studies highlight the importance of chaperone balance on maintaining cellular health, and implicate genetic and pharmacologic inhibition of chaperones, Hsp70s in particular, as a promising therapeutic avenue.

Our work builds upon the recent discoveries that the NAC can delay protein aggregation and provide feedback to translation machinery (300), assist with general protein folding and ribosome biogenesis (278), and that individual subunits have distinct functionalities related to

protein folding and rescue of aggregation (301). Together with our findings regarding the role of NAC subunits in regulating chaperone balance, this research points to the NAC as a major component in the protein homeostasis network. The NAC's known significance in yeast and its ubiquity in Eukarya should motivate further investigation this multifunctional and essential complex.

2.6 Acknowledgements

We thank Rachel Bouttenout for technical assistance with the transposon screen and strain creation. We are appreciative of Dr. Sergej Djuranovic, Dr. Chris Weihl, and members of the True lab for helpful discussions. We gratefully acknowledge the following for reagents: Drs. E. Craig, M. Funk, J. Glover, S. Lindquist, M. Snyder, M. Tuite, J. Warner, and C. Weihl.

2.7 Supplementary Information

Table S.2.1. Summary of the phenotypes displayed by the NAC deletion strains.
The *egd1Δegd2Δ* and *egd1Δbtt1Δ* strains were able to rescue prion–associated toxicity and had the most severe phenotypes in the remaining assays. Strains that showed variable phenotypes (e.g. *egd2Δ* could resist canavanine but not HygB) may harbor a slight chaperone imbalance that could not produce a detectable readout in our assays.

Strain ***all [PSI+]***	**Robust toxicity rescue**	**Resists canavanine**	**Ssb binding to Sup35** ***relative to WT***	**Sensitive to HygB**	**Sensitive to SsaOE**	**Resistant to Hsp104 curing**	**Altered Sup35 aggregates**	**Joining defect**
WT	*no*	*no*	X	*no*	*no*	*no*	*no*	*no*
egd1Δ	*no*	*no*	*unchanged*	YES	*no*	moderate	*no*	*no*
egd2Δ	*no*	YES	*n.s*	*no*	*no*	YES	*no*	*no*
egd1Δegd2Δ	YES	YES	reduced	YES	YES	YES	YES	YES
btt1Δ	*no*	YES	increased	*no*	*no*	YES	*no*	*no*
egd1Δbtt1Δ	YES	YES	reduced	YES	YES	YES	*no*	YES
egd2Δbtt1Δ	*no*	YES	*unchanged*	*no*	YES	YES	*no*	*no*
NACΔ	*no*	YES	*n.s*	YES	YES	YES	*no*	*no*

Table S.2.2. Strains used in this study.

Strain	**Description**	**Reference**

SL2598	74D-694; Strong [*PSI*+], MATa, ade1-14(UGA), trp1-289(UAG), his3□-200, ura3-52, leu2-3,112	(302)
1271	74D-694; Strong [*PSI*+], MATa, ade1-14 his 3□-200 trp 1-289 ura3-52 leu2-3,112 egd1D::KanMX4	This study
1147	74D-694; Strong [*PSI*+], MATα, ade1-14 his 3□-200 trp 1-289 ura3-52 leu2-3,112 egd2□::loxP	This study
1148	74D-694; Strong [*PSI*+], MATa, ade1-14 his 3□-200 trp 1-289 ura3-52 leu2-3,112 egd1□::KanMX4 egd2□::loxP – clone #1	This study
962	74D-694; Strong [*PSI*+], MATa, ade1-14 his 3□-200 trp 1-289 ura3-52 leu2-3,112 btt1□::HIS5	This study
966	74D-694; Strong [*PSI*+], MATa, ade1-14 his 3□-200 trp 1-289 ura3-52 leu2-3,112 egd1□::KanMX4 btt1□::HIS5	This study
1150	74D-694; Strong [*PSI*+], MATa, ade1-14 his 3□-200 trp 1-289 ura3-52 leu2-3,112 btt1□::loxP egd2□::loxP	This study
1152	74D-694; Strong [*PSI*+], MATa, ade1-14 his 3□-200 trp 1-289 ura3-52 leu2-3,112 egd1□::KanMX4 btt1□::loxP egd2□::loxP	This study
2352	74D-694; [*psi*-],mediuim [*RNQ*+], MATα, ade1-14, trp1-289(UAG), his3□-200, leu2-3,112, □□□□kar1-□□□	(271)
2090	74D-694; [*psi*-],medium [*RNQ*+] MATa, ade1-14, trp1-289(UAG), his3□-200, leu2-3,112, □□□□kar1-□□□	(271)
SL3014	74D-694; [*psi*-], MATα, ade1-14, his 3□-200 trp 1-289 ura3-52 leu2-3,112	(302)
1142	74D-694; Strong [*PSI*+], MATα, ade1-14, his 3□-200 trp 1-289 ura3-52, leu2-3,112, ssb1Δ::loxP	This study
1149	74D-694; Strong [*PSI*+], MATa, ade1-14 his 3□-200 trp 1-289 ura3-52 leu2-3,112 egd1□::KanMX4 egd2□::loxP – clone #2	This study

Table S.2.3. Plasmids used in this study.

Plasmid	Description and use	Reference
5162	pCUP-Sup35-GFP. Copper-inducible expression of Sup35-GFP.	This study
6244	pEMBL-Sup35. Overexpression of Sup35.	(303)
SL6435	pUKC815. Control for nonsense suppression assay. PGK1-LacZ fusion.	(277)
SL6436	pUKC817. Nonsense suppression assay. PGK1(TAA)LacZ fusion.	(277)
SL6437	pUKC818. Nonsense suppression assay. PGK1(TAG)LacZ fusion.	(277)
SL6438	pUKC819. Nonsense suppression assay. PGK1(TGA)LacZ fusion.	(277)
SL7280	p426GPD-Hsp104. Used for the overexpression of Hsp104.	(304)
6221	pCUP-Sup35NM-GFP. Copper-inducible expression of Sup35NM-GFP.	(302)
6765	p424GPD-Hsp104. Used for the overexpression of Hsp104.	This study
6391	p415GPD-Ssa1. Overexpression of Ssa1.	This study
6750	p415GPD-Ssb1. Overexpression of Ssb1.	This study
6751	P415GPD-Ssb2. Overexpression of Ssb2.	This study
EC1219	pRS316K-SSB1. Wild type Ssb1, “BBB.”	(286)
EC1327	pRS316K-SSA1. Wild type Ssa1, “AAA.”	(286)
EC1659	pRS316K-ABB. Chimera of Ssa1 and Ssb1.	(286)
EC1662	pRS316K-BAA. Chimera of Ssa1 and Ssb1.	(286)
EC1695	pRS316K-AAB. Chimera of Ssa1 and Ssb1.	(286)
EC1696	pRS316K-ABA. Chimera of Ssa1 and Ssb1.	(286)
EC1697	pRS316K-BAB. Chimera of Ssa1 and Ssb1.	(286)
EC1698	pRS316K-BBA. Chimera of Ssa1 and Ssb1.	(286)

Table S.2.4. Antibodies used in this study.

Antigen	Production notes	Type	Dilution	Source
Sup35	Peptide, a.a.s 137-151	Rabbit polyclonal	1:1,500	True lab
Rnq1	Full-length Rnq1	Rabbit polyclonal	1:1,000	True lab
Ssb1/2	C-terminal 80 a.a.s	Rabbit polyclonal	1:2,000	Craig lab (305)
Rpl3	IgG2b, ascites	Mouse monoclonal	1:2,500	Warner lab (306)
Hsp104	Carboxy terminus	Rabbit polyclonal	1:3,000	Glover lab (307)
Sis1	Peptide, a.a.s 339-352	Rabbit polyclonal	1:5,000	Cosmo Bio p89
GFP	N-terminal peptide	Mouse monoclonal	1:1,000	Thermo MA5-15256
Ssa	C-terminal 56 a.a.s	Rabbit polyclonal	1:2,000	Craig lab (305)
Ubiquitin	Full-length bovine Ub	Mouse monoclonal	1:500	Santa Cruz 8017
Rabbit	Rabbit IgG	Goat polyclonal	1:10,000 unless specified	Sigma A0545
Mouse	Mouse IgG	Rabbit polyclonal	1:10,000 unless specified	Sigma A9044

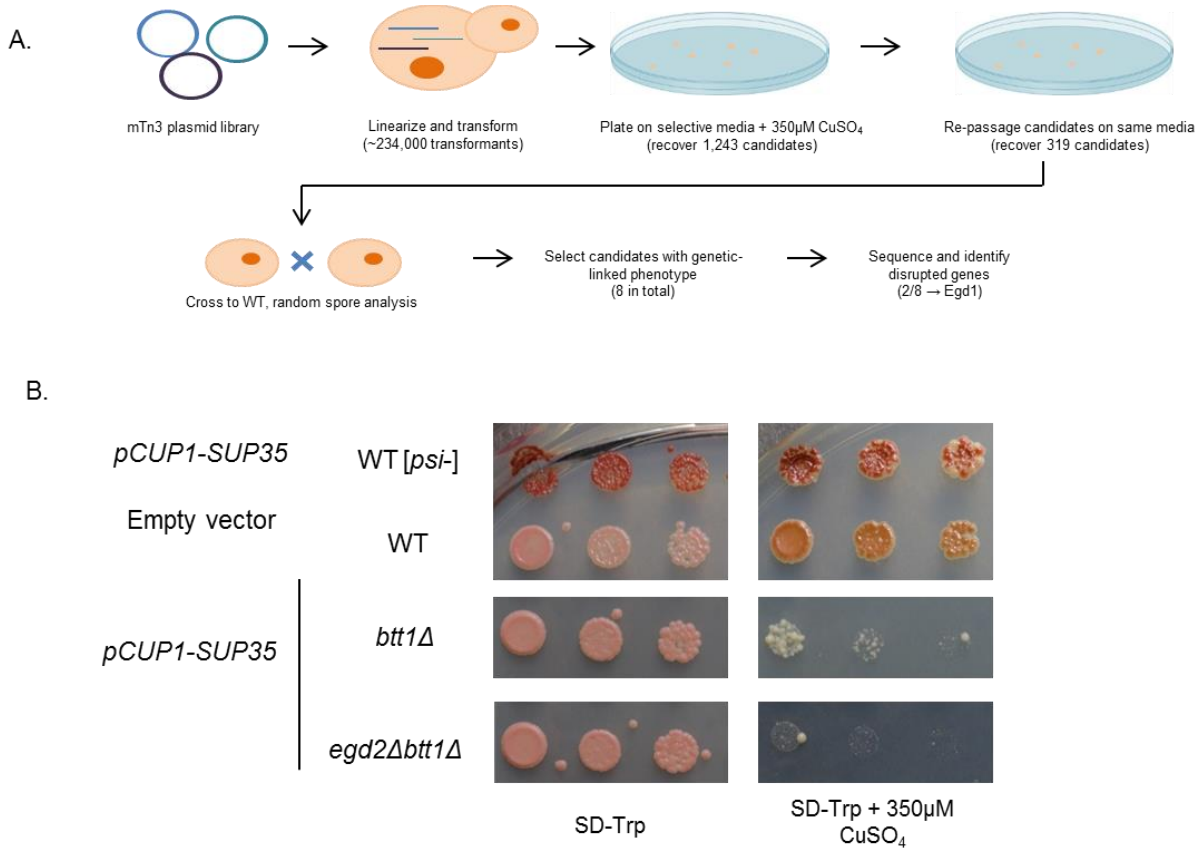

Figure S.2.1. Screen for factors that reduced prion-related toxicity.
(A) We performed a transposon screen with a mini-transposon (3XHA/lacZ URA3 (mTn3)) mutagenized library (308). The library was linearized with NotI and transformed into 74-D694 [*PSI*+] yeast containing pRS315*CUP SUP35* for the copper-inducible expression of Sup35. This strain harbors the strong [*PSI*+] prion variant. Prion variants (also called prion strains) result from particular amyloid structures propagated by the prion-forming protein (309). Transformants were plated onto selective media containing 350μM $CuSO_4$ and 1,243 putative suppressors were recovered. Candidates were picked with inoculating loops and respotted on the same media and 319 true suppressors were confirmed. Remaining candidates were mated to WT 74D-694 strains and sporulated to identify tetrads. Haploid candidates were confirmed by mating type testing. Eight candidates were recovered with phenotypes genetically linked to the transposon insertion. (B) Additional NAC deletion strains do not rescue [*PSI*+]-associated toxicity when Sup35 is overexpressed. The *egd2Δbtt1Δ* and *btt1Δ* strains show poor growth on selective media containing 350μM $CuSO_4$.

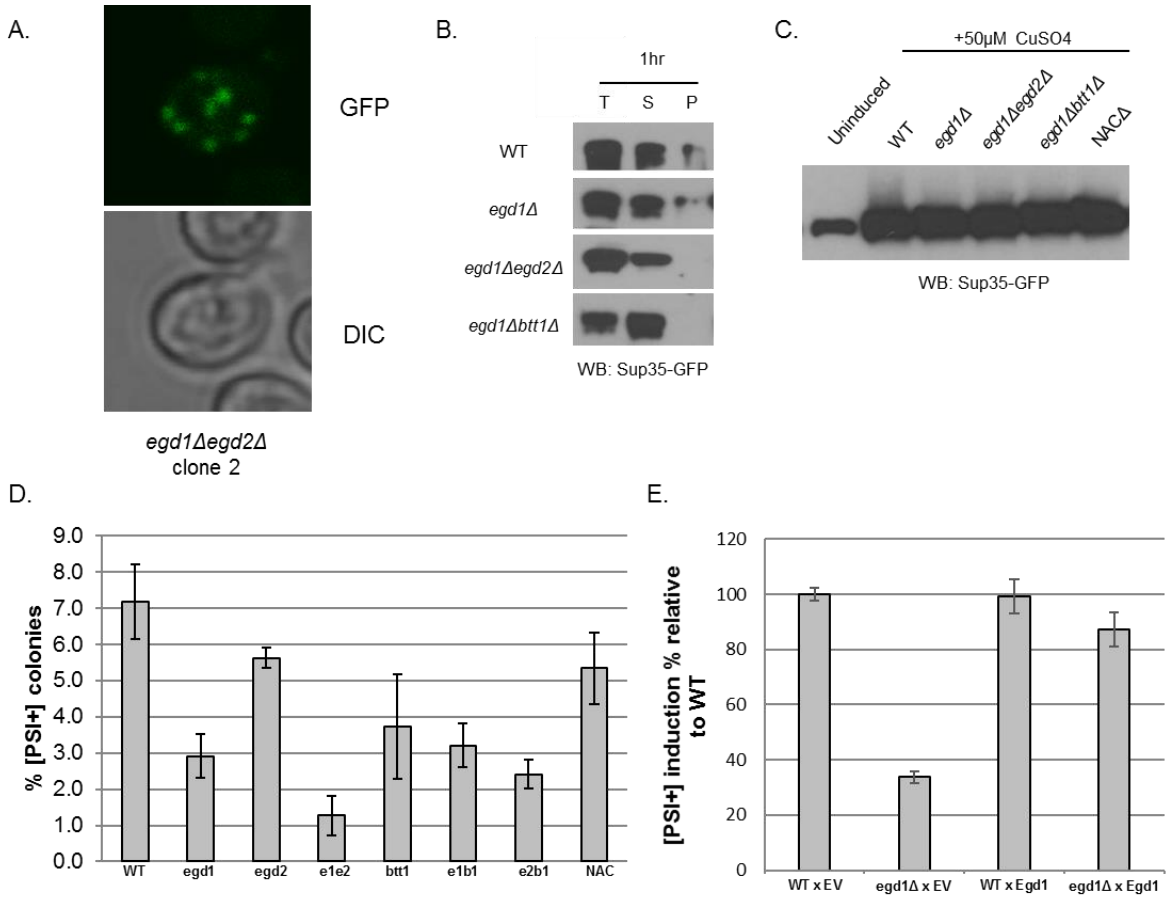

Figure S.2.2. The [*PSI*+] prion is altered in NAC deletion strains.
(A) A second disruption of the *EGD1* and *EGD2* genes ("clone 2") displays a similar pattern of Sup35 aggregation as is shown in Figure 3A. (B) The 1 hour timepoint for the joining assay performed in Figure 3C. (C) The amount of Sup35-GFP induced by addition of $CuSO_4$ to the culture medium was consistent between strains. Note the proportion of Sup35-GFP present in the "uninduced" lane, consistent with leaky expression from the CUP1 promoter (310). (D) WT and NAC deletion strains were cured of all prions by three passages on media containing 5mM GdnHCl. Strains were cytoduced with the "medium" variant of [*RNQ*+] (271) and transformed with pEMBL-SUP35. Induction of [*PSI*+] was performed as previously described (311). At least three independent experiments were performed and a minimum of 600 colonies were counted. Data are represented as mean ± SEM. *= $p<0.07$; **= $p<0.05$. (E) Covering the *egd1Δ* deletion with a plasmid expressing Egd1 gene rescues [*PSI*+] induction to WT levels. Data are represented as mean ± SEM.

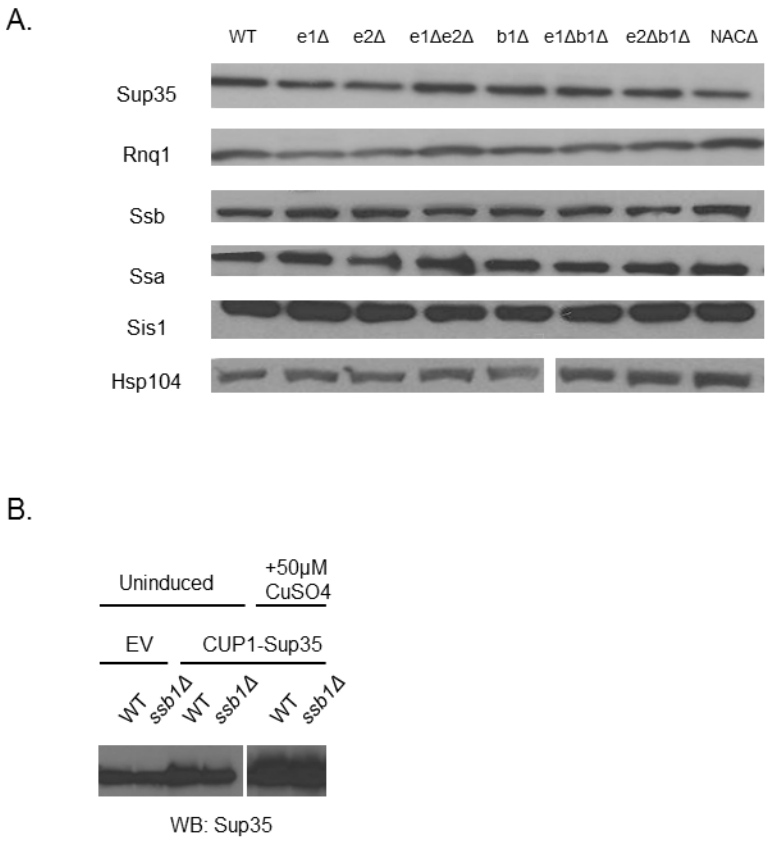

Figure S.2.3. Deletion of NAC subunits does not globally alter protein expression levels. (A) Wild type and NAC deletion strains were grown overnight in YPD before lysis, SDS-PAGE, and Western blotting for the specified proteins. Expression levels of chaperone (Sis1, Ssb1/2, Hsp104) and prion-forming (Sup35, Rnq1) proteins is not changed as a result of NAC deletion. The vertical white bar in the Hsp104 blot indicates non-contiguous lanes of the same blot. (B) Sup35 expression was analyzed by Western blot of lysates of the WT and *ssb1Δ* strains from Figure 4A. The vertical white bar indicates non-contiguous lanes of the same blot.

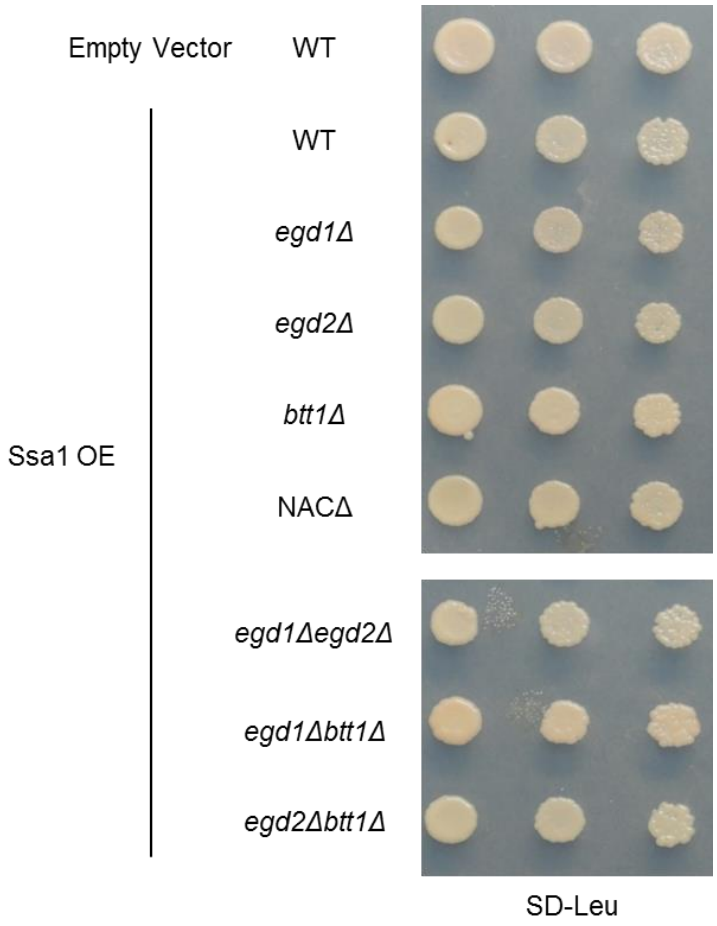

Figure S.2.4. Ssa1 is not toxic at steady-state levels of Sup35 expression
WT and NAC deletion strains were transformed with p415GPD-SSA1 for the overexpression of Ssa1. Overexpression of Ssa1 is not toxic without the concurrent overexpression of Sup35. All strains contain [*RNQ*+] and the strong [*PSI*+] variant; none of the strains are overexpressing Sup35.

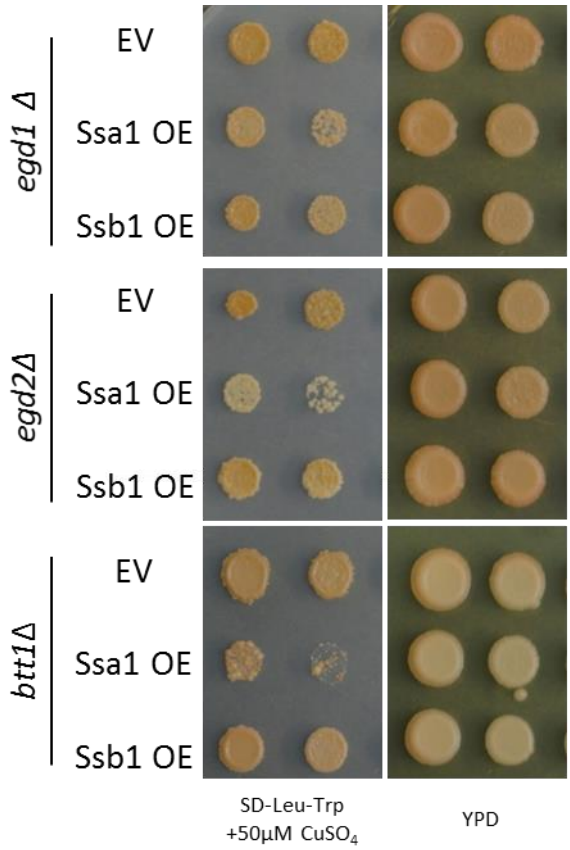

Figure S.2.5. Ssa1 overexpression can be toxic in conjunction with Sup35 overexpression
Spottings performed (as in Figure 4C) demonstrate that the effects of Ssa1 overexpression, in conjunction with Sup35 overexpression, are less toxic in the single NAC deletion strains than in the double deletions. All strains contain [*RNQ+*] and the strong [*PSI+*] variant, and the strains on selective media are overexpressing Sup35.

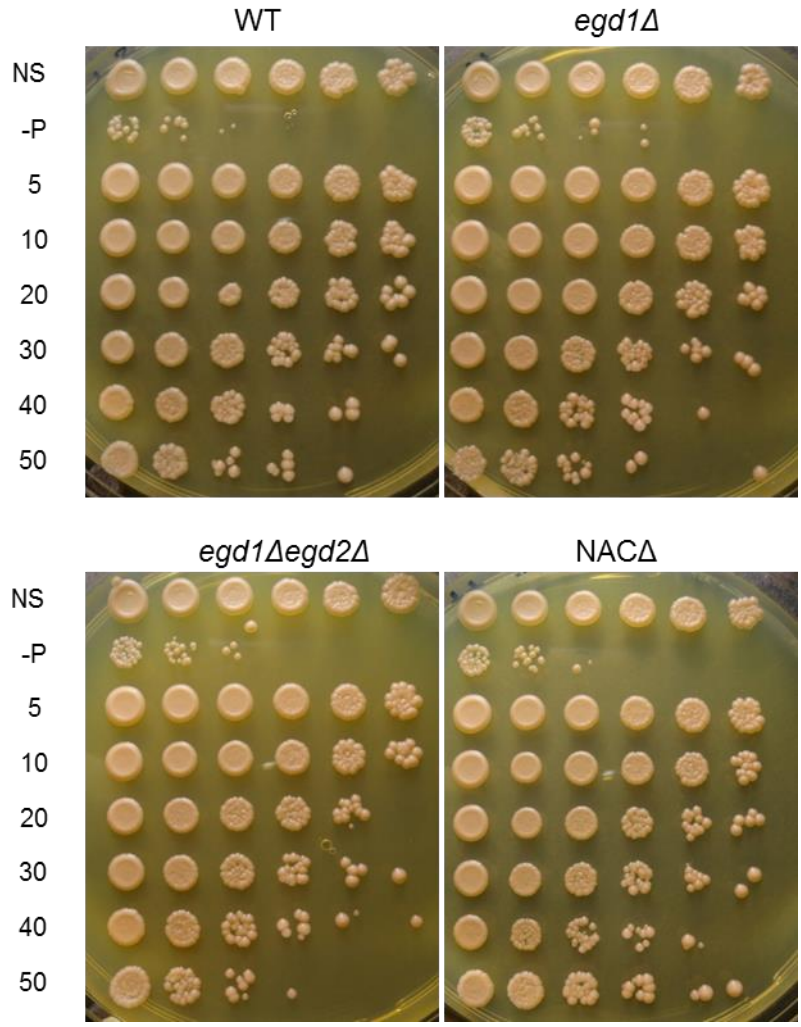

Figure S.2.6. The thermotolerance of NAC deletion strains is unchanged.
Strains (all [*RNQ*+] and strong [*PSI*+]) were grown in YPD at 30C and separated into 500µl fractions in glass culture tubes. Culture tubes were "pretreated" for 30 minutes at 37ºC prior to heatshock to promote the induction of heat-responsive elements. A non-pretreated control (-P) was incubated at 30ºC. Cultures were heat shocked at 50 degrees for the indicated number of minutes. NS = no shock. No differences were observed between the WT and deletion strains.

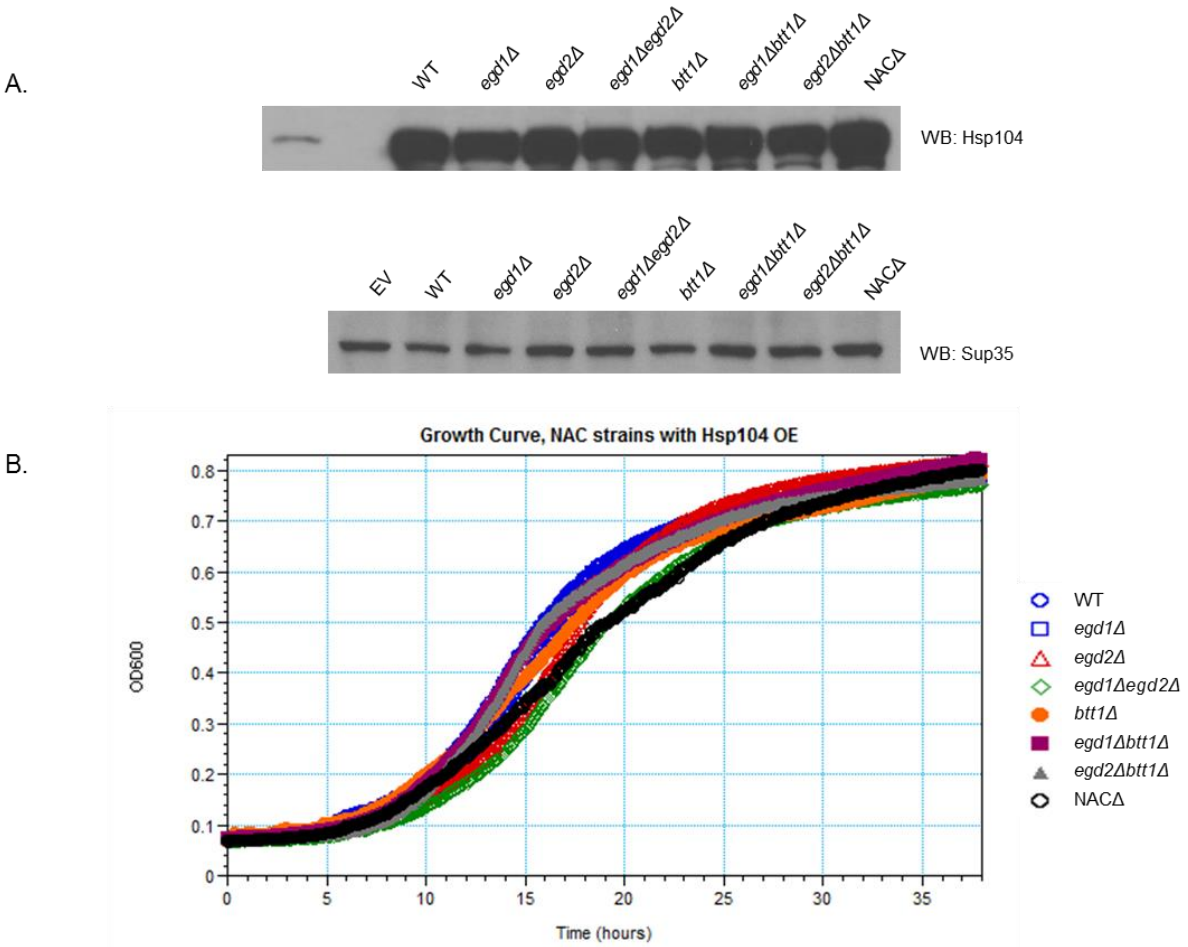

Figure S.2.7. Hsp104 overexpression does not alter Sup35 expression or strain growth
The WT and NAC deletion strains were transformed with a plasmid to overexpress Hsp104, as described in Figure 6. (A) The amount of Hsp104 overexpression was consistent between the transformed strains, and substantially greater than the empty vector control grown in identical media. (B) The levels of expressed Sup35 was unchanged in the Hsp104-overexpressing strains. The empty vector (EV) control does not overexpress Hsp104. (C) Strains overexpressing Hsp104 were grown in selective media in a plate reader to monitor their growth over time. There were no differences between the WT and NAC deletion strains; thus, growth rate does not account for the changes in [PSI+] curing efficiency. Results are the averaged values of three experiments.

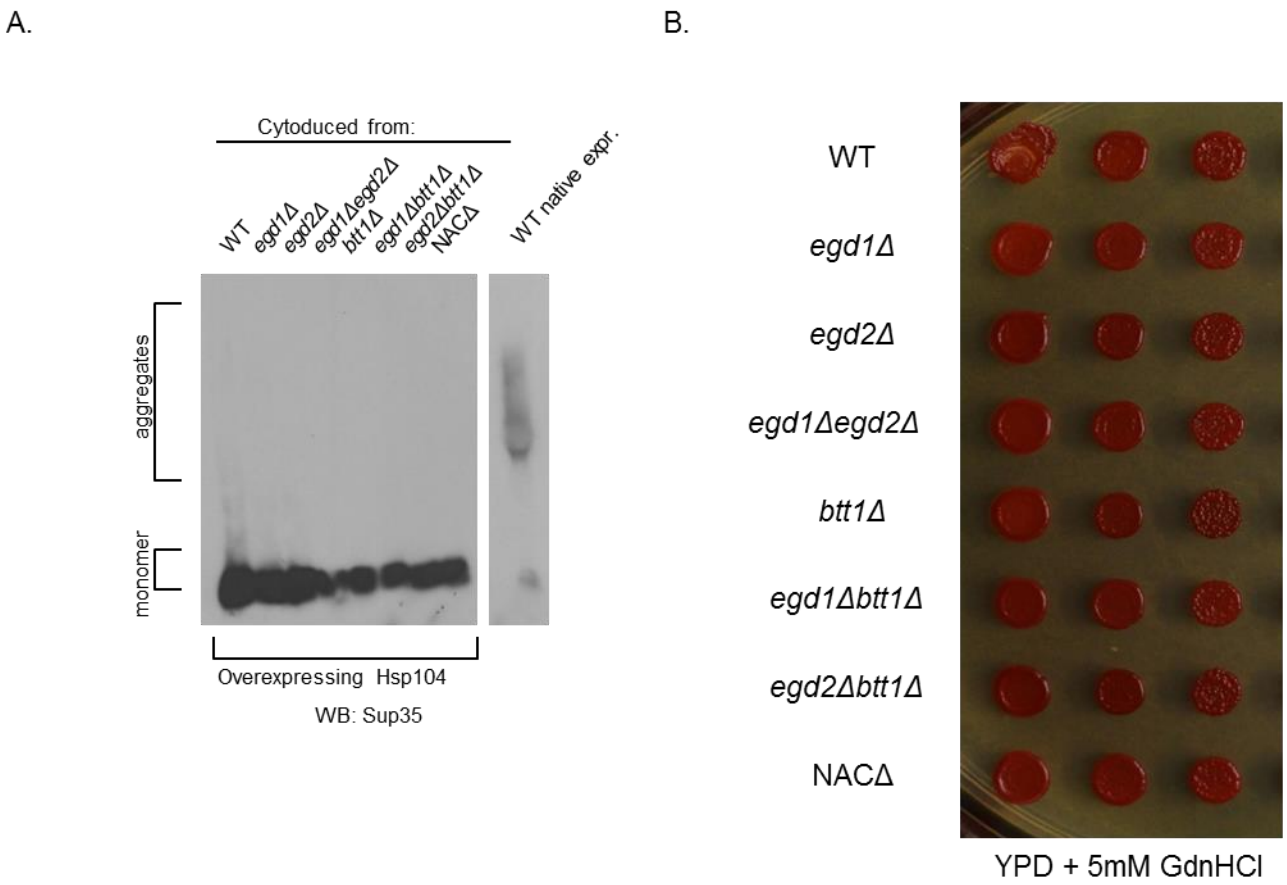

Figure S.2.8. NAC deletion strains are only resistant to [*PSI*+] curing by Hsp104 overexpression.
(A) As in Figure 6D, a WT strain was cytoduced with prion aggregates from WT or NAC deletion strains, and then transformed with a plasmid that overexpresses Hsp104. (B) [*PSI*+] WT and NAC deletion strains were spotted onto plates containing variable levels of GdnHCl (5mM plates are shown), which inactivates Hsp104. All strains demonstrated equal curability, as demonstrated by their red coloration.

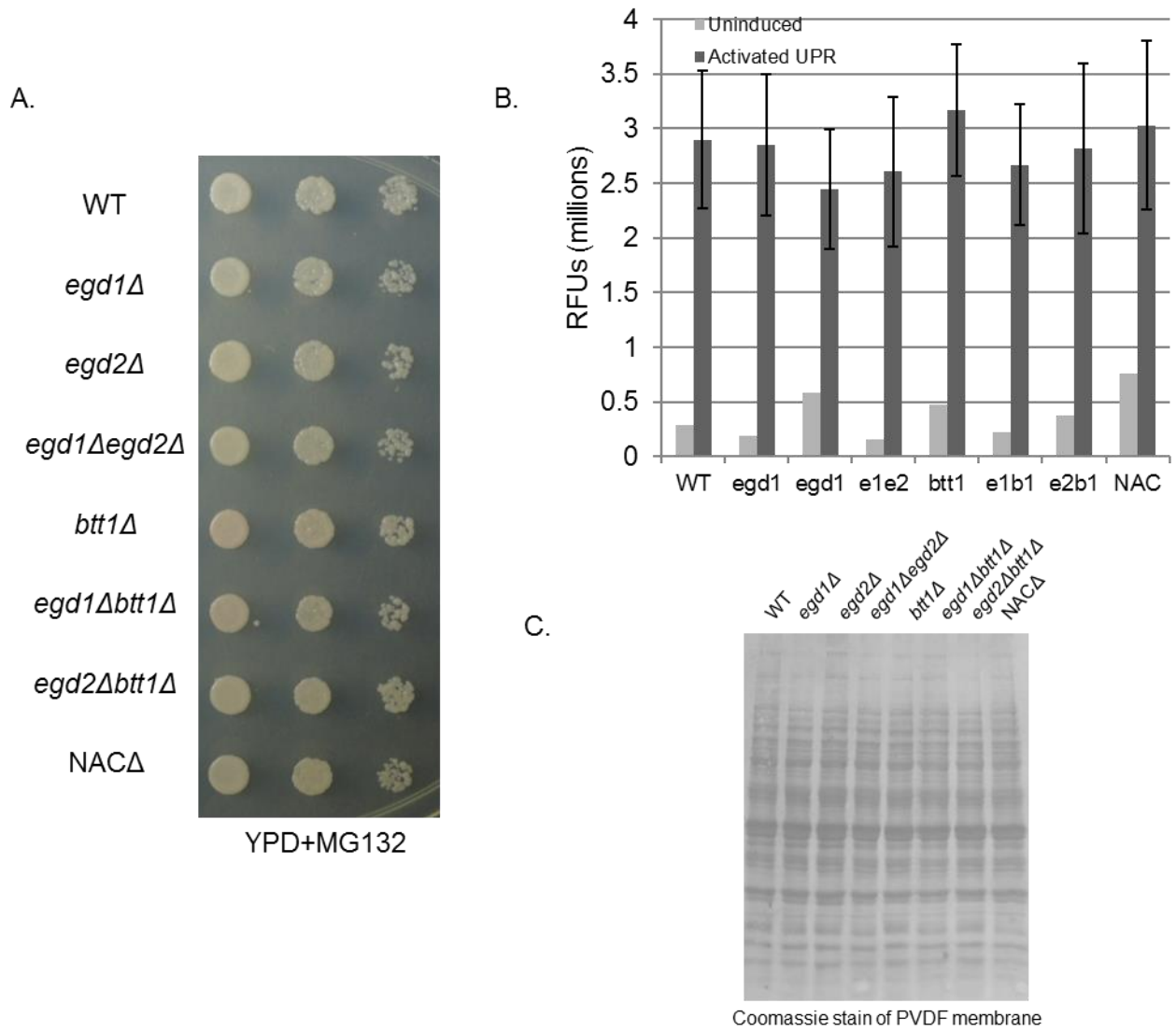

Figure S.2.9. NAC deletion strains do not demonstrate elevated stress responses.
(A) WT and NAC deletion strains (all [*RNQ*+] and strong [*PSI*+]) were spotted onto plates containing the proteasome inhibitor MG132. The strains were not differentially affected by the stressor. (B) The induction of the unfolded protein response (UPR) was measured at baseline (uninduced) and upon addition of tunicamycin to culture medium (activated UPR). The NAC deletion strains did not show a differential ability to induce the UPR in response to misfolding stress. (C) The solubility assay from Figure 7C was repeated with concentrated lysates in order to visualize the insoluble (pellet) fraction. No differences were observed between the WT and NAC deletion strains, indicating that none of these strains show an increased or decreased accumulation of aggregated material.

Chapter 3: A toxic imbalance of Hsp70s in *Saccharomyces cerevisiae* is caused by competition for cofactors

3.1 Abstract

Molecular chaperones are responsible for managing protein folding from translation through degradation. These crucial machines ensure that protein homeostasis is optimally maintained for cell health. However, “too much of a good thing” can be deadly, and the excess of chaperones can be toxic under certain cellular conditions. For example, overexpression of Ssa1, a yeast Hsp70, is toxic to cells in folding-challenged states such as [*PSI*+]. We discovered that overexpression of the nucleotide exchange factor Sse1 can partially alleviate this toxicity. We further argue that the basis of the toxicity is related to the availability of Hsp70 cofactors, such as Hsp40 J-proteins and nucleotide exchange factors. Ultimately, our work informs future studies about functional chaperone balance and cautions against therapeutic chaperone modifications without a thorough examination of cofactor relationships.

3.2 Introduction

Correct protein folding is achieved through a network of chaperones, co-chaperones, and nucleotide exchange factors that collaborate to configure a protein into an ordered state (8). When left unchecked, improper protein folding can lead to disrupted protein homeostasis and cell death, and, in mammalian systems, it can cause diseases such as Alzheimer’s disease and ALS (1). Thus, extensive networks of molecular chaperones have evolved to protect organisms from these adverse events.

Saccharomyces cerevisiae have more than 60 molecular chaperones that act on misfolded proteins, and hundreds of cofactors that assist these activities (9). Hsp70s are one class of chaperones that rely upon other proteins in order to facilitate ATP cycling and binding to clients (154,179). Hsp70s work in concert with other cochaperones to change the conformation of

misfolded proteins to promote proper folding. Hsp40 J-proteins are responsible for both delivering substrates and stimulating the ATPase domain of Hsp70s (312,313). Nucleotide exchange factors remove ADP and allow Hsp70s to return to a "ready" state (314). The repeated binding and release of clients with exposed hydrophobic patches allows the misfolded proteins to regain their correct conformations (154).

Prion aggregation is one consequence of protein misfolding in yeast. Many prions exist in yeast, and they regulate diverse cellular functions including transcription, translation termination, and nitrogen metabolism (88). Prion propagation occurs via specific misfolding of prion proteins into beta sheet-rich structures that promote additional monomers to convert and join the prion template. Yeast prions act as epigenetic mechanisms of inheritance as they are transmitted from mother to daughter cell (88). One well-characterized yeast prion, [*PSI*+], is caused by the misfolding and aggregation of the translation termination factor Sup35 (187). Many chaperones act upon Sup35 aggregates, including members of the Hsp70 and Hsp40 families (88). The activities of these chaperones can either prevent or promote *de novo* prion formation, depending on expression level (211).

Given the thermodynamic and cytosolic pressures that can oppose proper protein folding, one may hypothesize that "more is better" when it comes to intracellular chaperones. It stands to reason that higher levels of chaperone expression could benefit cells by providing more opportunities for misfolded proteins to be captured and refolded. Interestingly, this is not always the case.

We reported previously that the levels of Hsp70s, namely Ssa1 and Ssb1, are at a fine balance in the yeast *Saccharomyces cerevisiae* (315). When more Ssa1 is available relative to Ssb1, [*PSI*+] yeast experience exacerbated toxicity when Sup35 is concurrently overproduced.

This phenomenon did not occur with overexpression of other chaperones, such as Ssb1. We thus wondered what characteristics of Ssa1 influenced its toxic phenotypes. Here, we demonstrate that Hsp70 cofactor availability plays a role in Ssa1-related toxicity, especially when those cofactors are shared between Ssa1 and Ssb1.

3.3 Methods

Yeast cultures and transformation

Yeast were cultured using standard techniques (269) Plasmid transformations were performed by the PEG/LiOAC method (269). All yeast are WT 74D-694 and are strong [*PSI*+] (302). A complete list of plasmids is available in Table S.3.1.

Yeast spotting

Yeast cultures were grown overnight in selective media. Cultures were pelleted, washed, and resuspended in water to an optical density of 1.0. The normalized yeast solutions were pipetted into a 96-well plate, and serial dilutions (1:5) were made using a multichannel pipette. Yeast were spotted onto plates using an ethanol-sterilized 48-pin replicator that was placed in the appropriate wells and then onto an agar plate. Throughout the paper, YPD plates are used as controls to show the total number of cells plated, as even the slight amount of copper in synthetic media is enough to induce toxicity in yeast that contain p314CUP1-Sup35. For all experiments, the amount of $CuSO_4$ in media was titrated to compare growth within each experiment. $CuSO_4$ levels were altered to reveal relative effects of protein overexpression.

3.4 Results

3.4.1 Ssa1 overexpression is toxic to yeast containing aggregated Sup35

Yeast containing the [*PSI*+] prion show toxicity when Sup35, the constituent of [*PSI*+], is overexpressed (101) (Figure 3.1A). When these yeast are subject to a concurrent overexpression

of the chaperone Ssa1, the toxicity phenotype is exacerbated (Figure 3.1B, top row). We previously reported this phenomenon in the context of chaperone balance, and concluded that the relative availability of the Hsp70s is a factor that influences toxicity (315). However, we further demonstrated that imbalances can occur without changes in chaperone expression level. Other factors, such as localization or cofactor availability, can create these functional imbalances. Indeed, Ssa1 overexpression toxicity is not rescued by simultaneous overexpression of Ssb1 from the same promotor (Figure 3.1C). This suggested that chaperone imbalance-related toxicity is related to chaperone cofactors, and not the chaperones exclusively. We hypothesized that Ssa1-dependent toxicity may be due to a change of activity of its cofactors.

We therefore examined the role of Sse1 on Ssa1 activity. Sse1 is a nucleotide exchange factor (NEF) that is specific to the Hsp70 family of chaperones (171,316). We chose Sse1 because it interacts with both the Ssa and Ssb protein families, perhaps exclusively (317). It is known that Hsp70 cofactors, including NEFs, are typically present in sub-stoichiometric amounts in healthy cells (179). Thus, we hypothesized that Ssa1-related toxicity could be due to insufficient NEF activity relative to Ssa1 activity or abundance.

To test this, we overexpressed Ssa1 and Sse1 concurrently in [*PSI*+] cells overexpressing Sup35. We found that the expression of Sse1 strikingly rescued the toxicity associated with Ssa1 overexpression (Figure 3.1B). We tested Sse1 overexpression alone and in conjunction with Ssb1

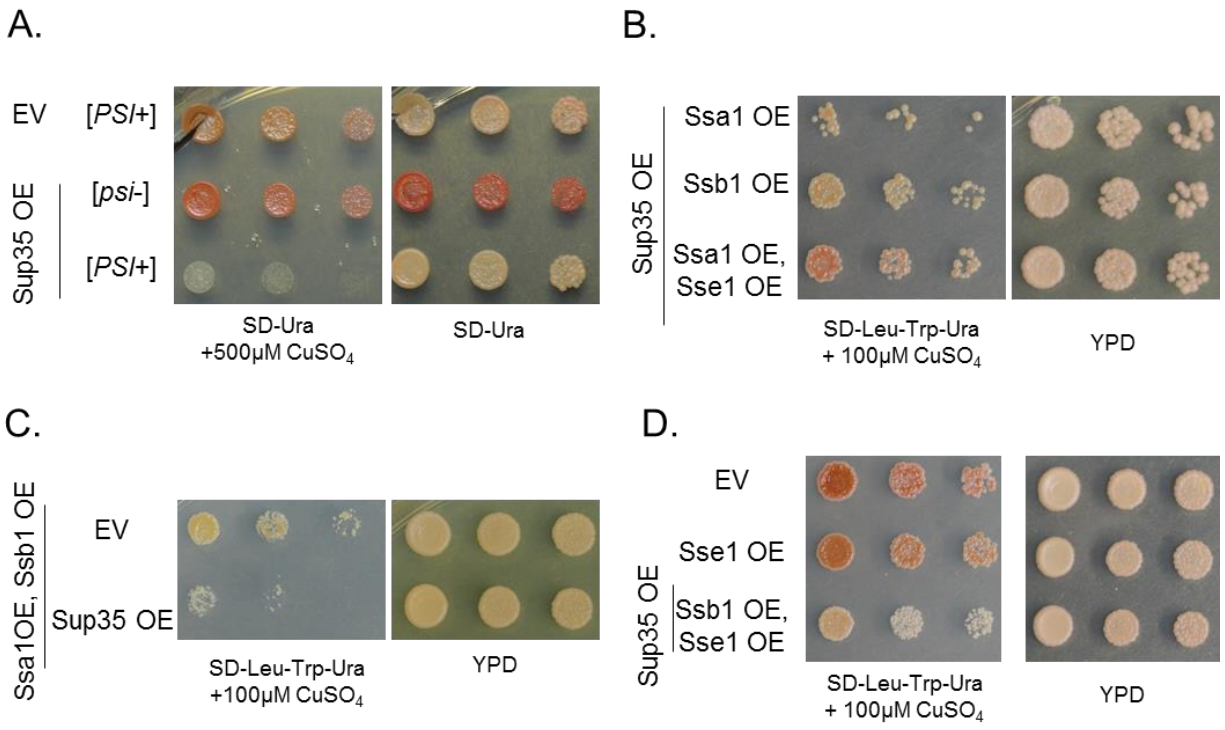

Figure 3.1. Overexpression of Sse1 rescues toxicity associated with excess Ssa1
(A) Sup35 overexpression is toxic to [*PSI*+] yeast. The empty vector (EV) control contains a TRP1-marked vector with no open reading frame (pRS314). (B) Ssa1 overexpression is toxic in [*PSI*+] yeast at low levels of Sup35 overexpression. toxicity is rescued by the overexpression of nucleotide exchange factor Sse1. (C) Sse1 overexpression does not cause enhanced growth of cells relative to empty vector controls. Top panel: the "EV" strain contains LEU2-, TRP1-, and URA3-marked empty vectors (Table S.3.1). Middle panel: the Sse1 OE strain contains LEU2- and TRP1-marked empty vectors.

overexpression (Figure 3.1D), and observed no change in growth relative to empty vector controls.

This indicated that Sse1 overexpression does not globally enhance growth of yeast.

3.4.2 Ssa1 overexpression could trap clients or titrate cofactors

Sse1 is known to interact with both Ssa1 and Ssb1 (171). Thus, we generated two theories about why Sse1 overexpression rescued the toxicity associated with Ssa1 overexpression (Figure 3.2). The first model suggests that the Ssa1 toxicity is due to a "trapping" of substrates caused by an insufficient amount of nucleotide exchange. In other words, overexpression of Ssa1 may overload the cell's nucleotide exchange factors and create a stoichiometric mismatch. After a client protein binds to the substrate-binding domain (SBD), the SBD closes and traps the client until the ADP dissociates and a new ATP binds to open the Hsp70 (317). With too few NEFs available to remove bound ADPs, clients would be sequestered, potentially impacting cell viability. Overexpressing Sse1 would partially relieve the imbalance and allow client proteins to be folded efficiently.

The second model proposes that overexpressing Ssa1 titrates certain nucleotide exchange factors away from other Hsp70s, such as Ssb1. Sse1 is a cofactor for both Ssa1 and Ssb1. An increase in Ssa1 activity could reduce the amount of contact between Sse1 and Ssb1. Overexpressing Sse1 would allow both classes of Hsp70s to resume normal function. The major distinction between the Ssa1 overexpression models lies in which Hsp70 remains trapped in the ADP-bound state: in the "trapping" model, Ssa1 retains substrates, while the "titration" model suggests that Ssa1 cycles substrates while Ssb1 remains ADP-bound.

To distinguish between these models, we first decided to examine the Hsp70 domains. Wild type Hsp70s contain three domains: a 40kDa N-terminal nucleotide binding domain, a 20kDa substrate binding domain, and a 10kDa variable domain (Figure 3.3A) (179,313). We utilized

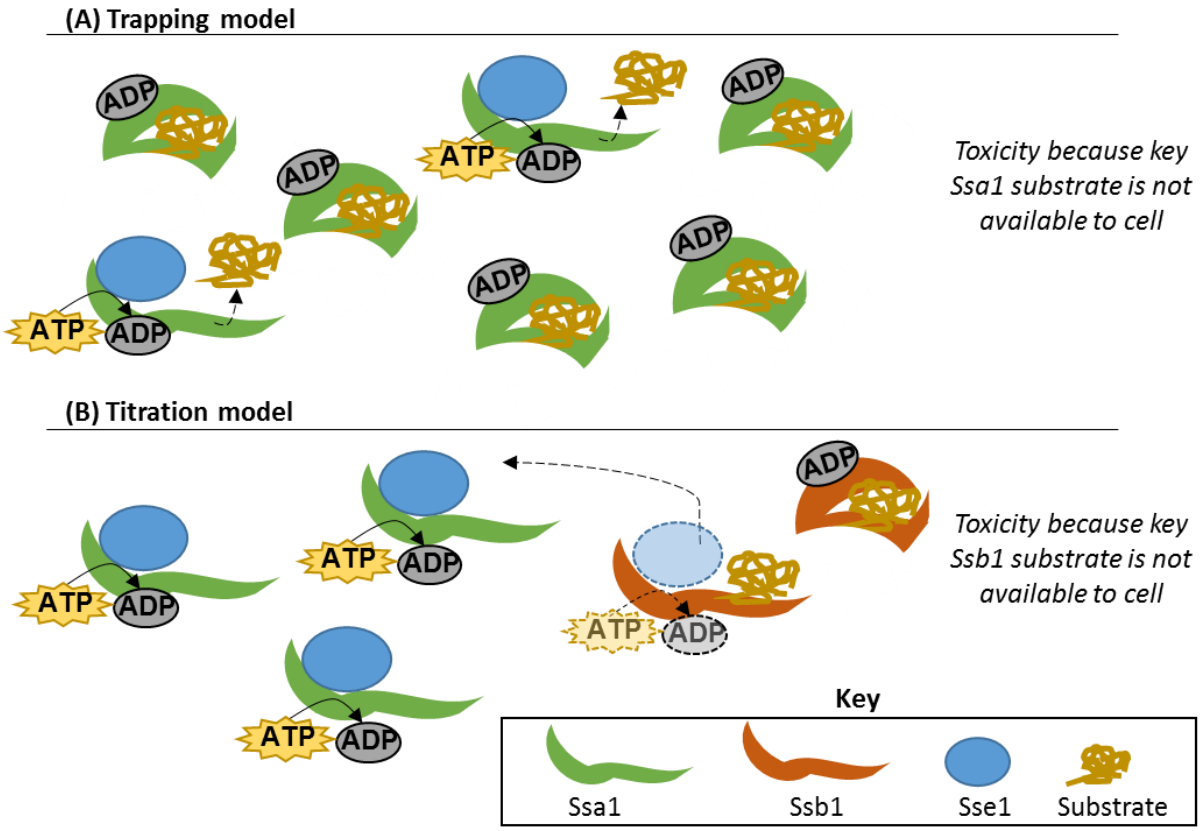

Figure 3.2. Model for cause of Ssa1 toxicity
(A) The "trapping" model suggests that overexpressing Ssa1 is toxic because crucial proteins are not made available to the cell. Ssa1 overexpression leads to a relative lack of available nucleotide exchange factors, so bound substrates are not efficiently cycled through the folding process. Overexpressing Sse1 partially relieves the mismatch between available Ssa1 and available NEFs. (B) The "titration" model suggests that Ssa1 overexpression causes cofactors to interact less frequently with Ssb1 due to stoichiometric imbalances. Titrating cofactors, such as the Sse1, could lead to decreased Ssb1 activity, causing reduced growth. Overexpressing Sse1 would restore the activity of both chaperones by increasing cofactor availability.

chimeric Hsp70 proteins in order to probe the effects of each domain of Ssa1 and Ssb1 (318). In total, we employed six chimeras representing all combinatorial groupings of these domains (Figure 3.3B), along with the wild type proteins in identical vectors. Each construct is referred to by its N-

to C-terminal identity. For example, “ABA” refers to the chimera that contains the Ssa1 nucleotide binding domain, the Ssb1 substrate binding domain, and the Ssa1 variable domain.

We expressed these fusion proteins in conjunction with Sup35 overexpression and observed that the nucleotide binding domain of Ssa1 was responsible for the most toxic phenotypes (Figure 3.3C). Conversely, all chimeras containing the Ssb1 nucleotide binding domain grew strongly when challenged with Sup35 overexpression. Surprisingly, one of the most toxic combinations was ABB, indicating that the Ssa1 nucleotide binding domain alone can be harmful to cell growth. The ABA chimera was also potently toxic, exhibiting almost no growth on selective media. Yeast containing AAB experienced toxicity similar to WT Ssa1. We considered the possibility that a mismatch between nucleotide binding domains and substrate binding domains may be innately toxic; however, the BAB and BAA chimeras both grew robustly.

This result supported the “titration” model; that is, the NBD of Ssa1 draws nucleotide exchange factors away from Ssb1. We arrived at this interpretation by examination of the AAB and ABA chimeras. If excess Ssa1 was retaining key substrates (the “trapping” model), then the AAB chimera would exhibit similar toxicity to Ssa1, but ABB would grow strongly because of its lack of Ssa1 substrate binding domain. However, ABB was even more toxic than Ssa1. We hypothesized that the extreme toxicity of the ABB and ABA chimeras were due to two factors. First, the presence of the Ssa1 nucleotide binding domain titrated NEFs away from Ssb1. Second, the presence of the Ssb1 substrate binding domain attracted client proteins away from the likely more-functional endogenous Ssb1, further harming cellular viability.

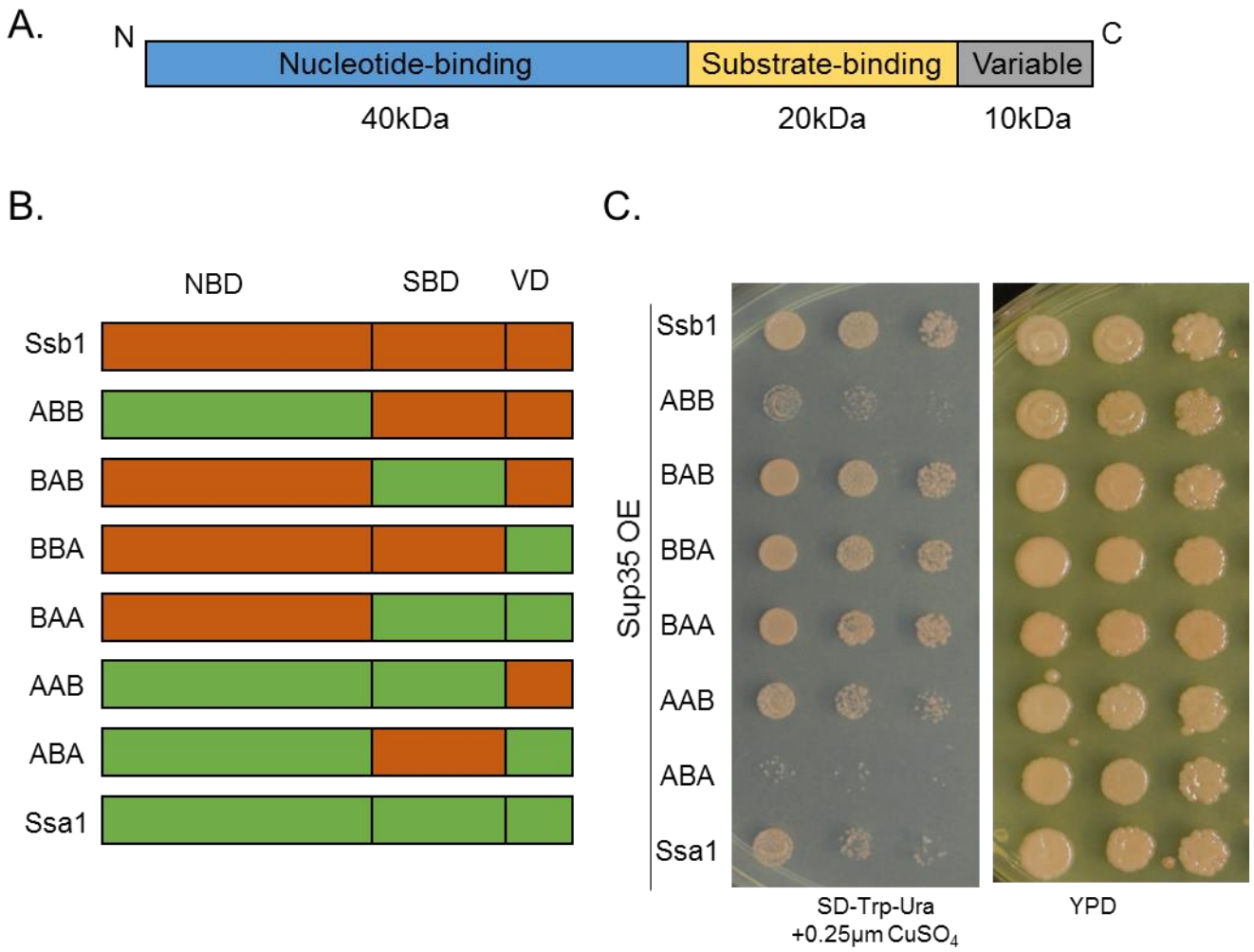

Figure 3.3. The nucleotide binding domain of Ssa1 is responsible for toxicity
(A) The *Saccharomyces cerevisiae* Hsp70s have a common domain architecture consisting of an N-terminal nucleotide binding domain, an intermediate substrate-binding domain, and a C-terminal variable domain. (B) We utilized chimeric proteins to investigate the effect of each domain of Ssa1 and Ssb1. All combinatorial possibilities were tested. Chimeras are named by their domains, e.g. "ABB" contains the Ssa1 nucleotide binding domain, the Ssb1 substrate binding domain, and the Ssb1 variable domain. (C) Expressing the Hsp70 chimeras demonstrates that the ABB and ABA proteins are highly toxic.

3.4.3 Sse1 overexpression confirms the importance of the Ssa1 nucleotide binding domain

To confirm the role of the Ssa1 nucleotide binding domain in toxicity, we again analyzed the effect of Sse1 overexpression. We co-expressed Sse1, Sup35, and each Hsp70 chimera and assessed yeast viability. Again, we found that Sse1 overexpression partially rescued the toxicity associated with ABB, as well as other chimeras containing the Ssa1 nucleotide binding domain. In contrast to the toxicity induced by minimal overexpression of Sup35 without Sse1 overexpression (Figure 3.3C), yeast could withstand higher levels of Sup35 overexpression (induced by 50μM $CuSO_4$) with the co-expression of Sse1 (Figure 3.4, middle panel).

3.4.4 A functional chaperone and cofactor balance is essential to survival

To further validate the titration model, we challenged the Ssa1 nucleotide exchange cycle. We hypothesized that a more active Ssa1 ATPase domain would exacerbate the toxicity associated with Ssa1 overexpression, as more NEFs would be titrated from Ssb1 in order to exchange ADP. Therefore, we examined the effect of Ydj1 on Ssa1-related toxicity. Ydj1 is an Hsp40 J-protein that stimulates Ssa1 ATPase activity, though not Ssb1 ATPase activity, and delivers client proteins to Ssa1 (319,320). We hypothesized that increased levels of Ydj1 could speed the overall nucleotide cycle via enhancing ATPase activity or delivering more substrates to Ssa1 (likely a combination of the two), which would increase the need for NEFs. Indeed, we observed that Ydj1 overexpression was highly toxic, even more than Ssa1 overexpression alone (Figure 3.5, compare to Figure 3.1A). Ydj1 overexpression alone was not detrimental to growth.

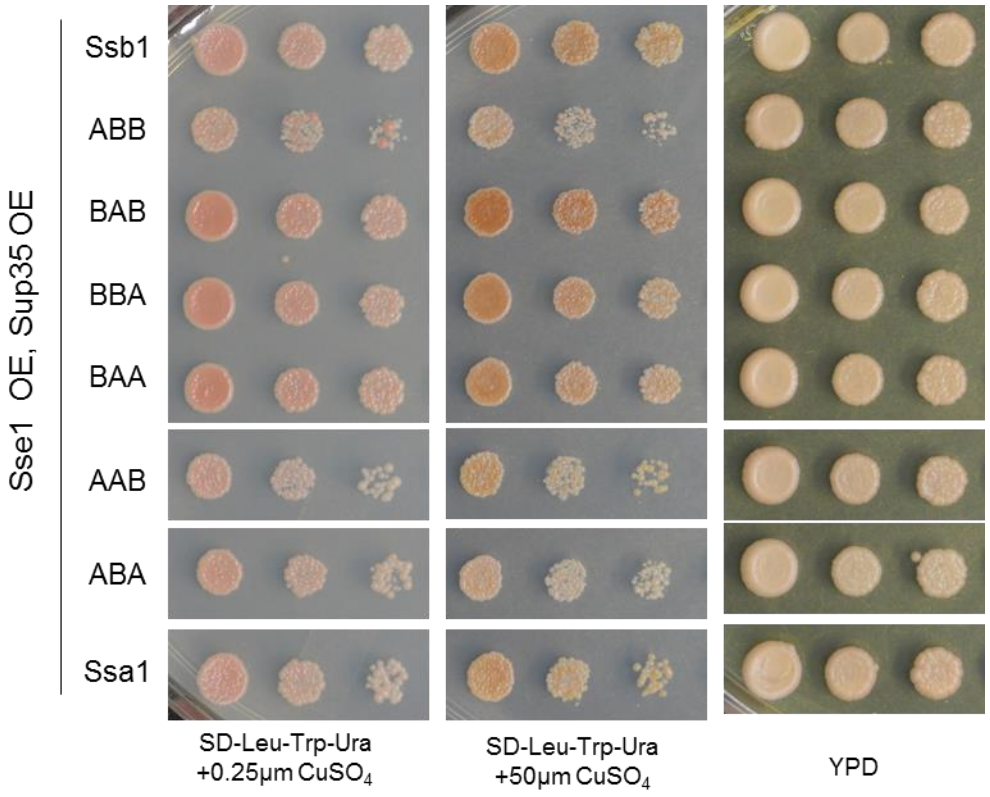

Figure 3.4. Sse1 overexpression rescues Hsp70 chimera toxicity
Introducing excess Sse1 into yeast containing Hsp70 chimeras rescued the toxicity associated with the Ssa1 nucleotide binding domain, even at high levels of Sup35 overexpression (middle panel, induced with 50µM CuSO4). Horizontal white bars separate spottings from the same plate. The original image was rearranged to allow easier comparison with Figures 3B and 3C.

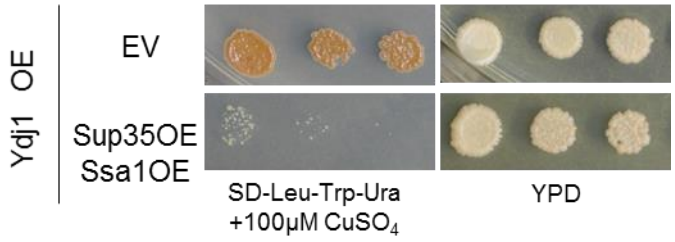

Figure 3.5. Functional chaperone balance is not restored by overexpressing Ydj1 or Ssb1
(A) Ydj1 is an Hsp40 J-protein that enhances Ssa1 ATPase activity. Overexpressing Ydj1 with Sup35 and Ssa1 is more toxic than Sup35 and Ssa1 overexpression alone. Ydj1 overexpression alone is not toxic (upper panel). The EV strain contains LEU2- and TRP1-marked empty vectors. (B) Overexpressing Ssb1 does not ameliorate the toxicity of Ssa1 overexpression. Though excess Ssb1 is generally beneficial to cells, the overabundance of Ssa1 continues to compete with Ssb1 for cofactors. The EV strain contains a TRP1-marked empty vector (pRS314).

3.5 Discussion

Here, we have shown that chaperone-related toxicity is caused in part by stoichiometric imbalances of cofactors. In particular, we demonstrated that the prion-dependent toxicity of Ssa1 overexpression is influenced by changes to the relative availability of the nucleotide exchange factor Sse1. We have provided evidence to support a "titration model," in which Ssa1 overexpression titrates cofactors away from Ssb1, reducing its functionality and its ability to cycle through substrates.

Though we limited this investigation to Ssa1, Ssb1, and Sse1, there are undoubtedly other consequences of chaperone imbalance that are not described herein. Changes in chaperone levels or folding ability can lead to enhanced genetic variation, prion modification, and changes in cytoskeletal organization (321–323). These effects are not limited to yeast, as Hsp70 overproduction in *Drosophila* can be deleterious to growth (324). Future investigation into the downstream effects of chaperone imbalance will shed light on the mechanisms by which they contribute to cells monitoring and reacting to protein folding challenges.

In our lab strains, Ssa1 overexpression was not toxic in [*PSI*+] cells without the concurrent overproduction of the prion-forming protein Sup35 (315). We theorize that this is due to the greater folding burden that is assumed by cells when Sup35 is overexpressed in a [*PSI*+] phenotypic state. Ssa1 overproduction, and subsequent Ssb1 under-function, may be tolerable under endogenous conditions, but becomes toxic when widespread protein misfolding challenges the chaperone network. This is in line with the hypothesis that cells contain excess free chaperones in order to protect against unforeseen folding needs (325). It is reasonable to believe that other methods of inducing protein misfolding could also lead to Ssa1-related toxicity.

In our previous study, we investigated a system that mimicked Ssa1 overexpression, via increased availability of Ssa1 relative to Ssb1, without any change in expression of either Hsp70 (315). Practically, this means that different genetic backgrounds or cellular stressors could make an organism more susceptible to chaperone-related toxicity. Cofactors are typically present in sub-stoichiometric amounts relative to their Hsp70s, a fine balance that is perturbed by either over- or under-expression of J-proteins and NEFs (179). Similar conclusions have been reached for Hsp90s and their cofactors (326). These studies indicate that chaperone networks are finely-tuned and that there are perils associated with altering Hsp availability relative to their cofactors.

To that end, modification of chaperones has been suggested in the treatment of various human diseases, ranging from neurodegenerative conditions to cancer (327–330). Our work informs important considerations for these future research avenues; namely, each chaperone must be considered as part of an interconnected network. Modulating the activity of one chaperone can have unforeseen consequences upon other chaperones, in a manner that may be unpredictable under conditions of cellular stress.

3.6 Acknowledgements

We thank Drs. E. Craig and S. Lindquist for reagents. We are especially grateful to Dr. E. Craig for the use of the Ssa/Ssb chimera constructs. We are appreciative of members of the True lab for helpful discussions and comments on the manuscript.

3.7 Supplementary Information

Table S.3.1. Plasmids used in this study.

Plasmid	Description	Use	Reference
--	pRS314	Empty vector control, TRP1-marked	(331)
--	pRS315	Empty vector control, LEU2-marked	(331)
--	pRS316	Empty vector control, URA3-marked	(331)
6391	p415GPD-SSA1	Overexpress Ssa1 from GPD promotor	(315)
6750	p415GPD-SSB1	Overexpress Ssb1 from GPD promotor	(315)
5162	p314CUP1-SUP35	Express Sup35 from a copper-inducible promotor	(315)
EC1219	p316-SSB1	Express WT Ssb1	(318)
EC1327	p316-SSA1	Express WT Ssa1	(318)
EC1659	p316-ABB	Express Ssa1/Ssb1 chimera	(318)
EC1662	p316-BAA	Express Ssa1/Ssb1 chimera	(318)
EC1695	p316-AAB	Express Ssa1/Ssb1 chimera	(318)
EC1696	p316-ABA	Express Ssa1/Ssb1 chimera	(318)
EC1697	p316-BAB	Express Ssa1/Ssb1 chimera	(318)
EC1698	p316-BBA	Express Ssa1/Ssb1 chimera	(318)
5708	p316-SSE1	Overexpress Sse1 as second copy	This study
5435	p316-YDJ1	Overexpress Ydj1 as second copy	This study
6761	p416GPD-Ssb1	Overexpress Ssb1 from Ura-marked plasmid	This study
6532	p415TEF-Sse1	Overexpress Sse1 from Leu-marked plasmid	This study

Chapter 4: Heterologous prion-forming proteins interact in Saccharomyces cerevisiae

4.1 Abstract

The early stages of protein misfolding remain incompletely understood, as most mammalian proteinopathies are only detected after irreversible protein aggregates have formed. Cross-seeding, where one aggregated protein templates the misfolding of a heterologous protein, is one mechanism proposed to stimulate protein aggregation and facilitate disease pathogenesis. Here, we demonstrate the existence of cross-seeding as a crucial step in the formation of the yeast prion [*PSI+*], formed by the translation termination factor Sup35. We provide evidence for the genetic and physical interaction of the prion protein Rnq1 with Sup35 as a predominant mechanism leading to self-propagating Sup35 aggregation. We identify interacting sites within Rnq1 and Sup35 and probe the effects of breaking and restoring a crucial interaction. Altogether, our results demonstrate that single-residue disruption can drastically reduce the effects of cross-seeding, a finding that has important implications for human protein misfolding disorders.

4.2 Introduction

The aggregation of heterologous proteins is implicated in many human neurodegenerative diseases, including Parkinson's Disease, Alzheimer's Disease, and amyotrophic lateral sclerosis (ALS). These fatal conditions are characterized by progressive neuronal damage and functional decline resulting from the co-aggregation of diverse disease-related proteins. Though the catastrophic effects of protein aggregation have been well-described, less is known about the factors that contribute to the spontaneous formation of heterologous protein inclusions. Recent findings suggest that a cross-seeding mechanism, whereby one protein templates the misfolding of another, may induce the aggregation of heterologous proteins and have a profound impact on disease onset and progression(58,64,332,333). However, while implicated, any instance of direct mechanistic evidence of cross-seeding has yet to be explicated.

Yeast prions, like pathogenic mammalian amyloids, are beta sheet-rich structures that can be transmitted from cell to cell. They are a robust model for studying the aggregation of human proteins, as yeast prions can also form varying structures or "strains" that impart differing cellular phenotypes, in a manner analogous to the distinct structures and pathologies formed by amyloidogenic proteins in humans(120,132,207). Indeed, the study of yeast prions has resulted in significant contributions to elucidating fundamental mechanisms of protein misfolding(116,130). The yeast protein Sup35 is a unique model for probing the nature of heterologous cross-seeding. Sup35 is a translation factor of *Saccharomyces cerevisiae* that aggregates to form the prion known as [*PSI*+]. Interestingly, [*PSI*+] formation is dependent upon the presence in the cell of another yeast prion, [*RNQ*+](116). Yet, like the co-aggregation of mammalian proteins, the nature of the relationship between Sup35 and Rnq1 remains unclear.

There are two predominant models for the dependence of Sup35 on [*RNQ*+] to form [*PSI*+] (Figure 4.1)(114,334,335). The inhibitor titration model posits the existence of an inhibitor molecule that binds to Sup35 and prevents its aggregation in [*rnq*-] cells (Figure 4.1A). Upon formation of [*RNQ*+], this inhibitor is sequestered by the amyloid and titrated away from Sup35, leaving Sup35 free to aggregate to form [*PSI*+]. An extensive screen and other previous work was done to identify the putative inhibitor(114), which has been suggested to be a chaperone or an element of the ubiquitin-proteasome machinery(336), but no candidate molecules have been identified.

In contrast to the titration model, the seeding, or cross-priming, model suggests that Sup35 and Rnq1 physically interact during [*PSI*+] formation (Figure 4.1B). In this manner, the misfolded and aggregated Rnq1 in the [*RNQ*+] state induces Sup35 to misfold via bending the monomer out of its native conformation or templating a spontaneously misfolded monomer into a state

conducive for prion propagation. There is some evidence for the seeding model. Fluorescence microscopy demonstrated that newly-forming Sup35-YFP aggregates co-localized with existing Rnq1-CFP aggregates(118). Promoting the interaction between Rnq1 and Sup35 via a Sup35-Rnq1 fusion protein also enhanced [*PSI*+] formation, whereas fusion of Sup35 to other aggregation-prone molecules did not(337). In addition, preformed aggregates of the Rnq1 prion-forming domain (PFD) have been shown to slightly increase the rate of Sup35 polymerization(117), though only at very high concentrations of Rnq1 seed relative to Sup35.

To gain greater insight into the aggregation of heterologous proteins, we set out to investigate the nature of the Sup35-Rnq1 interaction. Using a variety of techniques *in vivo* and *in vitro*, we have demonstrated a binding interaction that supports the veracity of the seeding model. We probed the functional consequences of disrupting this binding, and for the first time in any system, identified potential sites of interaction between two heterologous amyloidogenic proteins.

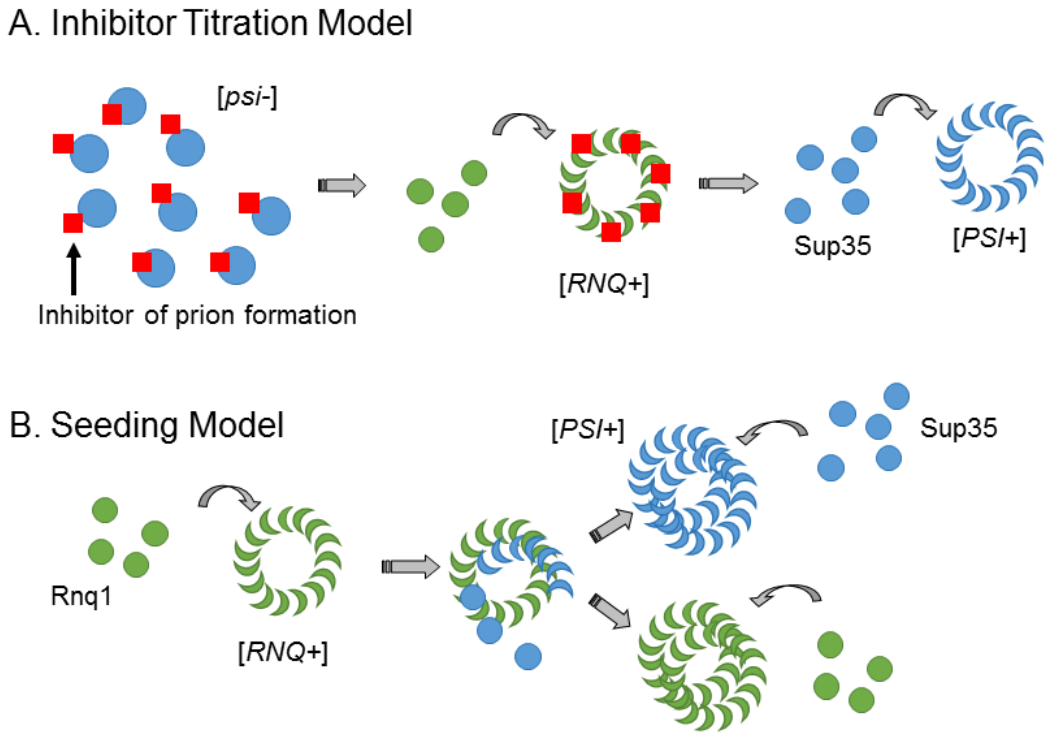

Figure 4.1. Models for the [*RNQ*+]-dependent formation of the [*PSI*+] prion
(A) The inhibitor titration model suggests that an inhibitor molecule (red squares) binds to Sup35 in its soluble state (blue circles). The presence of [*RNQ*+] (green ring) sequesters the inhibitor away from Sup35, thereby allowing the protein to aggregate and form [*PSI*+]. (B) The seeding model suggests that there is a physical interaction between Sup35 and aggregated Rnq1 during the formation of [*PSI*+]. After the interaction, the [*RNQ*+] and [*PSI*+] prions are propagated independently.

4.3 Methods

Yeast strains, plasmids, cultures, and transformations

Yeast strains were cultured using standard techniques(269). Yeast transformation with plasmid DNA was performed by the PEG/LiOAC method(269). Complete lists of strains and plasmids are available in Tables S.4.1 and S.4.2, respectively.

Protein purification

Sup35 and Rnq1 were both tagged with a C-terminal polyhistidine tail and purified on nickel affinity resin. Briefly, BL21 (DE3) bacteria were transformed with the plasmid of interest and grown at 37ºC in LB+Amp media. At OD_{600}=0.6, protein expression was induced with 1mM IPTG and cultures were grown at 25ºC for 6 hours. Cells were pelleted, washed, and frozen at -80ºC until use. Cells were thawed at 4ºC for 2hr, shaken in lysis buffer (Sup35: 20mM Tris, 0.5M NaCl, 5mM imidazole, 2M urea, 0.1% IGEPAL; Rnq1: 20mM Tris, 8M Urea, pH 8) at 4ºC for 30 minutes, and then sonicated 5x10 seconds at high power. Lysates were cleared by centrifugation at 20,000xg for 30 minutes, and the supernatant was incubated with a nickel resin for 30 minutes at 4ºC. Resin columns and bound proteins were washed with washing buffer (Sup35: 20mM Tris-HCl, 0.5M NaCl, 20mM imidazole, 2M urea; Rnq1: 20mM Tris, 8M Urea, pH 6.3-5.9) and eluted with wash buffer + 400mM imidazole for Sup35 or wash buffer at pH 4.5 for Rnq1. Elution fractions were pooled, concentrated, and methanol-precipitated prior to use. Rnq1 purification protocol adapted from(338).

Rnq1-Trap

His-tagged Sup35 was expressed in BL21 (DE3) cells and partially purified as described above, stopping after binding to the nickel resin but before protein elution. Yeast cultures were grown to

mid-log phase and mechanically lysed with acid-washed glass beads (Sigma) in Sup35 binding buffer + protease inhibitors (20mM Tris, 0.5M NaCl, 5mM imidazole, 2M urea, 0.1% IGEPAL, 50mM NEM, 3mM PMSF, 1 tablet Roche Protease Inhibitor Cocktail #4693159001). Cleared lysates were incubated for 30 minutes with the Sup35-bound nickel resin prior to washing with 150mL washing buffer (20mM Tris-HCl, 0.5M NaCl, 20mM imidazole, 2M urea) and elution with 100mL elution buffer (20mM Tris-HCl, 0.5M NaCl, 400mM imidazole, 2M urea). Fraction collection was followed by standard SDS-PAGE (10% polyacrylamide) and western blotting.

Thioflavin T kinetics

Purified Sup35 and Rnq1 were resuspended to 300µM in 7M guanidine hydrochloride. Fiber formation and kinetics assays were performed as previously described(339), with minor alterations to buffers (Sup35: 5mM KPO_4, 150mM NaCl, pH 7.4; Rnq1: 50mM KPO_4, 2M Urea, 150mM NaCl, pH 6).

Boiled gels

Yeast strains of interest were cultured overnight in selective media. Cells were lysed in buffer (25mM Tris-HCl pH 7.5, 50mM KCl, 10mM $MgCl_2$, 1mM EDTA, 10% glycerol, protease inhibitors) by mechanical disruption with acid-washed glass beads (Sigma). Lysates were normalized to total protein and mixed with SDS-PAGE sample buffer (200mM Tris-HCl pH 6.8, 4% SDS, 0.4% bromophenol blue, 40% glycerol). Unboiled samples were loaded into the wells of a 12% polyacrylamide gel and run under 140V of current until the dye front migrated halfway through the resolving gel. The current was stopped and the gel and glass plates were sealed in plastic sheets prior to boiling upright for 15 minutes in a 95ºC water bath. The gels were removed from the plastic and reinserted into the PAGE apparatus, where voltage was re-applied (140V)

until the dye front migrated to the bottom of the gel. This procedure was followed by standard western blotting with Sup35 and Rnq1 antibodies (Table S.4.3).

Prion manipulation and protein biochemistry

[*PSI*+] induction and SDD-AGE experiments were performed as previously described (120,340). Cytoduction was performed as previously described(134,315).

Screen for Sup35 mutations

The screen for suppressor mutations was performed using SP5, a chimeric Sup35 protein that contains 5 repeat domains from the prion protein PrP in place of the endogenous repeat domains of Sup35(341,342). As *SUP35* is an essential gene, SP5 was utilized in the screen because it allowed us to monitor prion formation in the absence of the potentially confounding effects of WT Sup35 expression in conjunction with mutant Sup35 overexpression. To introduce mutations, six error-prone PCR reactions were performed in the presence of 25uM MnCl2 using Taq polymerase and 35 cycles to amplify the NM domains of SP5. PCR reactions were combined to create three separate libraries, followed by SpeI/BclI digestion and ligation into p415TEF-SP5. Yeast cells propagating m.d. high [*RNQ*+] and harboring episomal copies of *SUP35* and *rnq1-Q298R* were transformed with each library, with selection on SD-His-Leu. Transformation plates were replica plated onto SD-His-Leu + 5-FOA to select for cells having replacement of the *URA3*-marked *SUP35* plasmid. These colonies were replica plated onto YPD and YPD+3mM GdnHCl to identify white [*PSI*+] colonies that were also curable. More than ~3000 colonies were assessed, of which 193 were pink (putative [*PSI*+]) and 38 were curable (validating the prion). After plasmid recovery and sequencing, we identified 13 mutant *SP5* alleles.

Crosslinking

PCR was performed on pAED4-*SCNM-his7* to introduce the G7C mutation, using forward primer 5'GCGCATATGATGTCGGATTCAAACCAATGTAACAATCAGCAAAAC (mutated bases underlined) and reverse primer 5'CATCGATGAATTCTTAATGGTGG. The PCR product and pAED4 vector were digested with NdeI and EcoRI restriction enzymes, ligated, and transformed into BL21 (DE3) cells for protein expression and purification as described above. Following methanol precipitation, Sup35NM-G7C and Rnq1 were dissolved to 0.1mM in conjugation buffer (PBS, 2mM EDTA, pH 7.4). Rnq1 was attached to the heterobifunctional crosslinker SMPB (Thermo #22416) by incubating 1.3mg protein with a final SMPB concentration of 1mM for 30 minutes at room temperature. Disulfide bonds in Sup35NM-G7C were reduced with TCEP (Sigma). Excess SMPB and TCEP were removed by passing proteins through Zeba desalting columns (Thermo #89890). Equimolar amounts of Sup35-G7C and Rnq1-SMPB were combined and incubated at room temperature for 30 minutes, followed by SDD-AGE and western blotting.

4.4 Results

4.4.1 Sup35 stably binds to ex vivo Rnq1

We began by assessing the interaction between Rnq1 and Sup35 *ex vivo*. Since the previously demonstrated in vitro cross-seeding was weak(117), we hypothesized that the conformation of Rnq1 in [*RNQ*+] lysates differed from that readily obtained in the in vitro amyloid formation reaction. Therefore, we sought to test the binding of Sup35 to biologically relevant aggregates of Rnq1 isolated from [*RNQ*+] yeast cell lysates. To do so, we bound recombinant, tagged Sup35 prion-forming domain (Sup35NM-7xHis) to nickel affinity resin. We then prepared

cell lysates from [*RNQ+*][*psi-*] yeast and incubated the lysate with the nickel resin to allow for binding between Rnq1 aggregates and immobilized Sup35. We hypothesized that the bound Sup35 would "trap" untagged Rnq1 that would ordinarily flow through the column. We washed the column with increasing amounts of imidazole to displace the bound proteins, and collected unbound, wash, and elution (bound) fractions (Figure 4.2A). We found that there was a strong interaction between Rnq1 and Sup35 when the Sup35NM-7xHis protein was used as bait, as a large proportion of Rnq1 appeared in the bound fractions. Rnq1 was still present in the unbound fraction, yet not all Rnq1 is expected to be aggregated or Sup35-binding-competent in [*RNQ+*] cells. Importantly, when no Sup35NM-7xHis was present on the beads, all Rnq1 protein was present in the unbound fraction, indicating the lack of non-specific binding of Rnq1 to the column.

To control for non-specific interactions between Rnq1 and Sup35, we repeated the experiment with a Sup35 C-terminal domain fragment (Sup35C-7xHis) that lacks the crucial prion-forming region that is believed to interact with Rnq1. In this instance, most of the Rnq1 protein was present in the unbound fraction, with none detected in the elution fractions. Some Rnq1 appeared during an intermediate wash fraction, indicating weak or non-specific binding to the Sup35 C-terminal domain. Thus, the strong binding between *ex vivo* Rnq1 to the Sup35 prion-forming domain appears to be specific and stable.

Interestingly, incubating lysates from [*rnq-*][*psi-*] cells also showed binding between Rnq1 and Sup35 (not shown). This suggests that there is a Sup35-Rnq1 interaction in [*rnq-*] cells, but that the intermolecular binding is not prion-forming. Rather, the [*PSI+*]-inducing properties of Rnq1 in [*RNQ+*] strains may be due to the specific conformation of Rnq1, as previously suggested, and not simply the interaction itself(120,132).

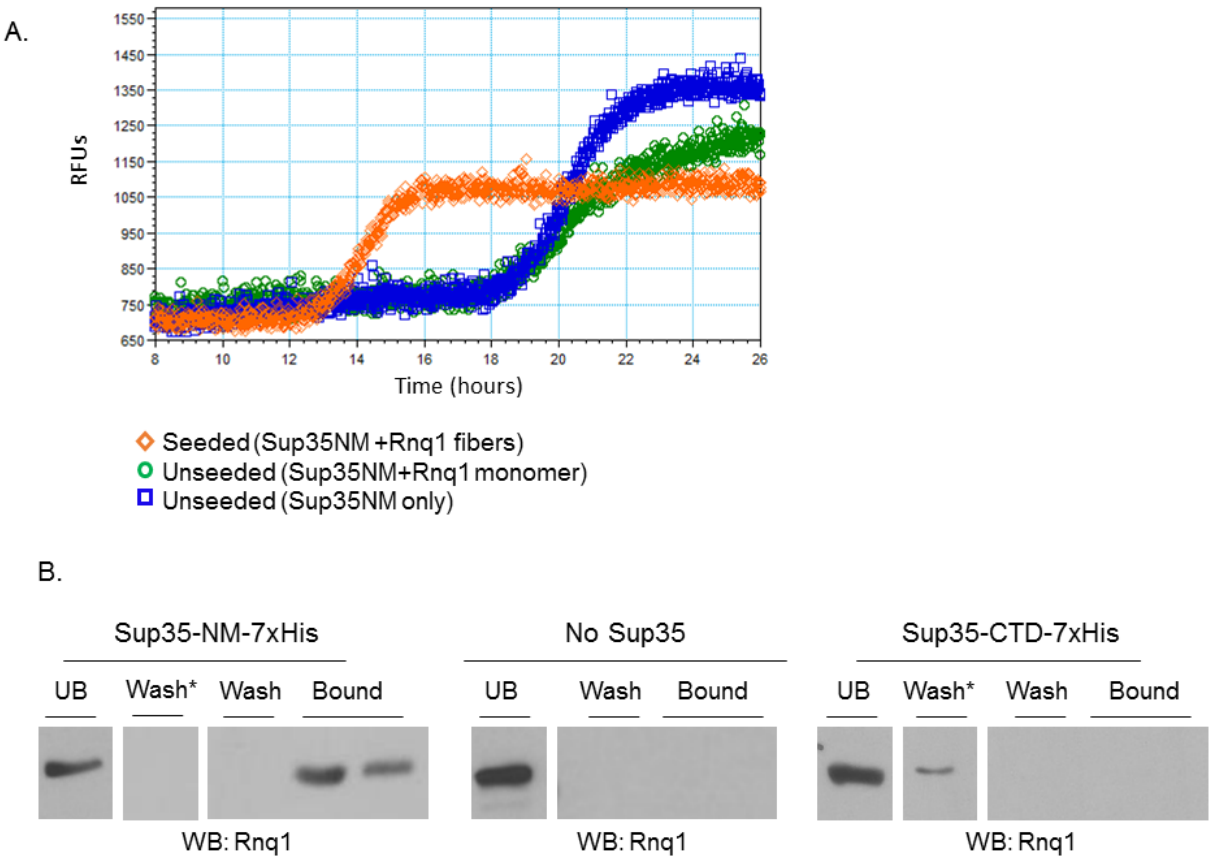

Figure 4.2. Rnq1 and Sup35 physically interact
(A) ThT kinetic experiments monitor the polymerization of amyloid via enhanced fluorescent emission. Unseeded Sup35 (blue line) polymerizes and aggregates after approximately 17 hours, as does Sup35 incubated with Rnq1 monomer alone (green line). The addition of Rnq1 fibers (orange line) reduces the lag time for Sup35 polymerization to approximately 12.5 hours. Curves represent data from three experiments. (B) Sup35 was immobilized on resin and utilized as bait for a [*RNQ*+] trap assay. Cell lysates were incubated with the resin, washed with buffer, and eluted. The presence of trapped, untagged Rnq1 was detected via western blot with anti-Rnq1 antibody. Lanes shown are the unbound (UB) fraction, the final wash fraction and the first two elution fractions. "Wash*" indicates an intermediate wash fraction. Blots are representative images from three independent experiments.

4.4.2 Rnq1 aggregates seed the polymerization of Sup35

To understand whether the physical interaction between Rnq1 conformers and Sup35NM might facilitate the aggregation of Sup35, we assessed the kinetics of *in vitro* aggregation using Thioflavin T (ThT)(343). ThT binds specifically to amyloid fibers and an increase in the fluorescent emission signal indicates formation of amyloid. When incubated with agitation at room temperature, Sup35 will form amyloid after a reproducible lag phase(338,342). This lag phase can be reduced or eliminated if Sup35 aggregation is "seeded" by preformed Sup35 fibers that provide a template for amyloid formation. We hypothesized that including preformed Rnq1 fibers in Sup35 polymerization reactions would also decrease the lag phase of Sup35 aggregation, albeit to a lesser extent, as observed in vivo: cross-seeding ([*PSI*+] induction in [*RNQ*+] cells) is not as efficient as self-seeding ([*PSI*+] propagation in [*PSI*+] cells). Though previous work has demonstrated that very high molar concentrations of the Rnq1 prion-forming domain (PFD) can slightly increase Sup35 polymerization(117), we now know that regions outside of the PFD are important for [*RNQ*+] prion status(344–346). Thus, we utilized full-length Rnq1 at a lower molar ratio. We further hypothesized that cross-seeding would be dependent on the conformation of the Rnq1 aggregates formed in vitro, as [*RNQ*+] variants, also called prion strains, have a significant effect on [*PSI*+] induction levels in vivo(132). Thus, we aimed to create a mixed population of seeds that could mimic the aggregation states that may be present in vivo.

In light of these considerations, we purified recombinant Sup35 and Rnq1, and formed Rnq1 fibers *in vitro* to serve as "seeds" for the polymerization reaction. As temperature can affect the conformation of Rnq1 aggregates(339), we formed Rnq1 fibers at a range of temperatures and combined them to create a broad pool of potential seed structures. We then performed ThT aggregation assays with monomeric Sup35NM in both unseeded and seeded conditions (Figure 4.2B). We found that the presence of pooled Rnq1 seeds at a 12μM final concentration reduced

the lag phase of Sup35 aggregation as predicted (Figure 4.2B, orange curve). The addition of equimolar levels of monomeric Rnq1 did not have this effect relative to the Sup35-only control (Figure 2B, green and blue curves). Thus, the initiation of Sup35 aggregation *in vitro* is enhanced by the presence of Rnq1 amyloid. As this experiment used pure, recombinant protein, no inhibitor cofactors (Figure 4.1A) are necessary to enhance Sup35 polymerization. Therefore, the facilitation of Sup35 aggregation relies on direct binding of Rnq1 and Sup35.

4.4.3 The rnq1-Q298R mutation causes a [PSI+] induction defect

Upon demonstrating the physical interaction between Sup35 and Rnq1, we sought to identify the specific residues in each protein that were important to binding. To do so, we utilized a mutation in Rnq1, Q298R, that had been previously identified by our lab and demonstrated to impart a [*PSI*+] induction defect (Figure 4.3A)(347). This mutant was previously shown to be capable of propagating [*RNQ*+], and our additional tests of thermal stability (Figure 4.3B, Figure S.2.1A) and mitotic stability (Figure 4.3C) showed that the Q298R mutant maintains Rnq1 aggregates that are biochemically indistinguishable from WT Rnq1(347). However, cells harboring *rnq1-Q298R* have a [*PSI*+] induction defect, in that they become [*PSI*+] at a much lower frequency than *RNQ1* cells(347).

We first verified this defect with [*PSI*+] induction experiments. [*PSI*+] induction utilizes a colorimetric assay to visualize the frequency of Sup35 aggregation *in vivo*. The colorimetric readout relies upon a well-described phenotypic [*PSI*+] reporter, *ade1-14*, which impacts adenine production depending on nonsense suppression. The *ade1-14* allele contains a premature stop codon in the *ade1* gene (348). Yeast containing *ade1-14* cannot make adenine and colonies grown

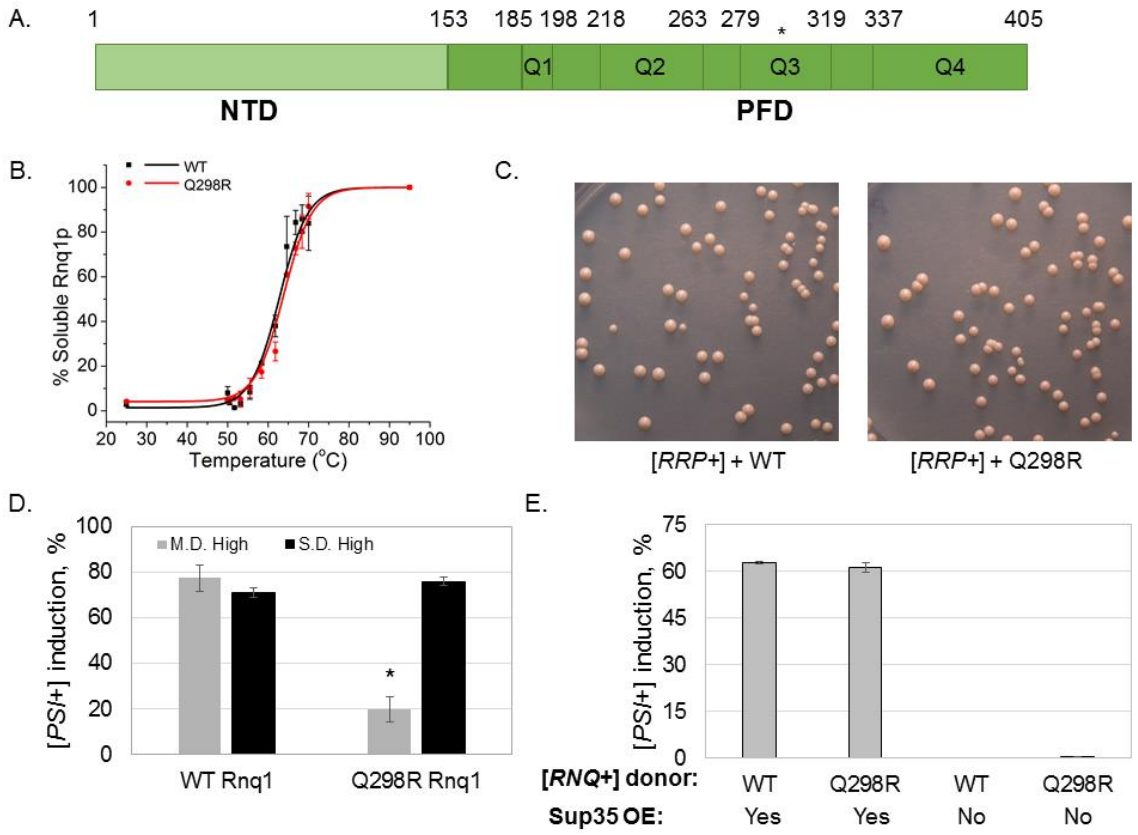

Figure 4.3. Rnq1-Q298R causes a [*PSI*+] induction defect

(A) The Rnq1 protein contains an N-terminal domain (NTD) and a glutamine/asparagine-rich prion-forming domain (PFD). The PFD contains four glutamine-dense regions, Q1-4 (113). The Q298R mutation occurs in region Q3 of the PFD. (B) Rnq1 aggregates were treated at a gradient of temperatures in SDS to determine the melting point of the Rnq1-Q298R aggregates versus the WT. There were no significant differences in the thermostable properties of either protein aggregate. Western blot signal from multiple experiments was quantified using ImageJ, normalized by the 95C band, and plotted using Origin 9.0. Error bars represent standard error of the mean (s.e.m). (C) There are no detectable differences in mitotic stability of Rnq1-Q298R aggregates as compared to WT Rnq1 aggregates. [*RNQ*+] strains containing the [*RNQ*+] Reporter Protein (RRP), a phenotypic readout for the [*RNQ*+] prion(347), were transformed with plasmids harboring either WT *RNQ1* or *rnq1-Q298R*. We assessed the mitotic stability, or spontaneous prion loss, of resulting strains and found that [*RNQ*+] formed from WT or Rnq1-Q298R was similarly maintained. (D) The *rnq1-Q298R* mutant shows a strong defect in [*PSI*+] induction relative to WT cells of the m.d. high variant of [*RNQ*+]. [*PSI*+] was induced by overexpression of Sup35 in [*psi*-][*RNQ*+] cells of either a *RNQ1* or *rnq1-Q298R* genetic background. Colonies were assessed by color, with white or pink colonies or sectored colonies scored as [*PSI*+]. Error bars represent mean ± s.e.m. The "*" symbol represents a significant difference between [*PSI*+] induction in *RNQ1* versus *rnq1-Q298R* backgrounds, $p<0.001$. (E) Results from [*PSI*+] induction following cytoplasmic transfer of either WT Rnq1 or Rnq1-Q298R protein aggregates into a [*rnq*-] *RNQ1* strain. The propagated [*RNQ*+] would be templated from the WT or mutant aggregate, but be comprised of only WT protein. Error bars represent mean ± s.e.m.

on media containing adenine appear red due to the buildup of a pigmented metabolic byproduct. Since Sup35 is a translation termination factor, its aggregation to form [*PSI*+] increases nonsense suppression. Thus, [*PSI*+] allows cells to read through the *ade1-14* premature stop codon and synthesize adenine. As such, [*PSI*+] cells can grow on synthetic media lacking adenine (SD-Ade) and appear white or pink on rich media plates (YPD).

Utilizing this colorimetric test to monitor [*PSI*+] induction, we overexpressed Sup35 in [*RNQ*+][*psi*-] yeast expressing either Rnq1 or Rnq1-Q298R. Cells were spread on rich media plates to allow for development of red or white colonies. The presence of productive Rnq1-Sup35 interactions would induce the formation of [*PSI*+]. In agreement with our previous results, strains with WT Rnq1 aggregates induced [*PSI*+] at a high level, whereas yeast with Rnq1-Q298R aggregates exhibited a significant decrease in [*PSI*+] formation (Figure 4.3D). This suggests that Q298 is an important site of interaction between Rnq1 and Sup35, and that mutating the glutamine residue leads to decreased or non-productive interactions with Sup35.

We then sought additional confirmation that the [*PSI*+] induction defect of *rnq1-Q298R* was indeed related to the genetic mutation and not a heritable change in the [*RNQ*+] prion conformation. We utilized cytoduction to transfer aggregates from a [*RNQ*+]^{Q298R} donor cell to a [*rnq*-]^{WT} recipient cell expressing *RNQ1*. Thus, the recipient yeast would become [*RNQ*+] and propagate the prion conformation from the donor strain, but with WT Rnq1 protein. Following cytoduction from either [*RNQ*+]^{WT} or [*RNQ*+]^{Q298R} donors, we monitored [*PSI*+] induction and found that the *RNQ1* [*rnq*-] recipient strains receiving WT Rnq1 and Rnq1-Q298R aggregates both induced [*PSI*+] to equivalent levels (Figure 3E). Thus, the *rnq1-Q298R* [*PSI*+] induction defect is a consequence of the genetic mutation as opposed to a templating defect that is transmitted to WT Rnq1.

4.4.4 Suppressor mutations rescue the [PSI+]-induction defect

After confirming the role of *rnq1-Q298R* in [*PSI*+] induction, we sought to identify putative binding sites in Sup35. We performed a second site suppressor screen to identify mutations within the Sup35 prion forming domain that could restore the interaction with Rnq1-Q298R and rescue the [*PSI*+] induction defect. Briefly, we transformed strains containing *rnq1-Q298R* with a pool of mutagenized *SP5,* a chimeric *SUP35* construct that allowed us to assess screen candidates without confounding effects of mutating endogenous *SUP35*. We then assessed the ability of yeast cells to form [*PSI*+] (see *Methods* for screen details). Our secondary tests verified that bona fide [*PSI*+] was formed by showing that the nonsense suppresion phenotypes were reversible on plates containing 3mM GdnHCl, which cures yeast prions (not shown). To assess [*PSI*+] formation, we spotted the screen candidates onto SD-Ade to test their growth (Figure 4.4A, Figure S.4.2). The most promising mutants were those that grew strongly on SD-Ade relative to WT *SP5* in a *rnq1-Q298R* genetic background. In all, we isolated 12 *sup35* mutants containing a total of sixteen mutations within the "NM" prion-forming domain (Figure 4.4B).

4.4.5 Sup35-N5Y robustly rescues the [PSI+]-induction defect

After cloning the candidate mutations into Sup35, we then tested the ability of these Sup35 mutants to suppress the [*PSI*+] induction defect of *rnq1-Q298R*. We again utilized [*PSI*+] induction experiments to evaluate the individual *sup35* screen candidates (Figure 4.5A). We overexpressed either WT or mutant Sup35 in [*RNQ*+] cells expressing either Rnq1 or Rnq1-Q298R. Importantly, [*PSI*+] formation was never observed in the [*rnq*-] control strains, and a high degree of induction occurred in WT [*RNQ*+] cells. Moreover, the [*PSI*+] induction defect was evident in [*RNQ*+] *rnq1-Q298R SUP35* cells. However, three Sup35 mutants rescued the defect and induced [*PSI*+] to near-WT levels: N5Y, Q6R, and G116V (Figure 4.5A). Interestingly,

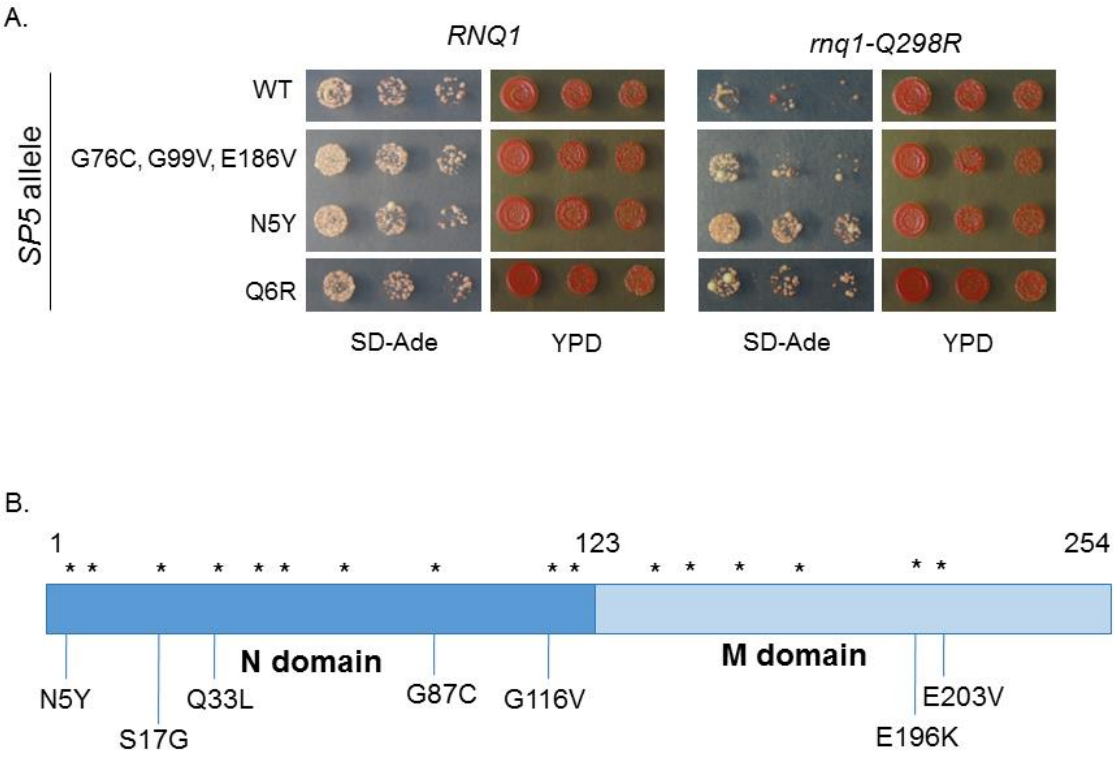

Figure 4.4. Sup35 mutations can restore interaction with Rnq1-Q298R
(A) Candidates from a suppressor screen to identify Sup35 mutants that can rescue the [*PSI*+] induction defect associated with *rnq1-Q298R*. These mutants enhanced [*PSI*+] formation in the *rnq1-Q298R* genetic background relative to WT *SP5*. Horizontal white bars separate non-adjacent spottings from the same plate. Complete spottings of screen candidates appear in Supplementary Figure S.4.2. (B) The indicated mutations were cloned into *SUP35* for further testing.

despite M domain mutations also being identified and tested, the three rescuing mutations all fall within the N-terminal region of Sup35, which is thought to be the most crucial domain for prion formation(92,335).

The *sup35-N5Y* candidate was isolated as a single mutant during our screen, whereas many other *sup35* alleles emerged as double- or triple-mutants. We decided to individually examine this mutant's potential binding to Rnq1-Q298R. To assess this, we examined Sup35 aggregation biochemically via "boiled gel" assays. In these experiments, room temperature cell lysates are loaded on SDS-PAGE gels. Native (non-denatured) aggregated material is too large to enter the resolving gel and becomes trapped in the wells and the stacking gel. Upon boiling the gel midway through electrophoresis, aggregated material breaks down and enters the resolving gel. Following western blots, two bands are visible per lane: a lower band of soluble material, and a higher band of insoluble material that was delayed in entering the gel (see *Methods*). We performed boiled gel experiments with cell lysates from [*RNQ*+] strains containing WT or *rnq1-Q298R* and WT or *sup35-N5Y* (Figure 4.5B). We also examined a [*rnq*-] control with WT *RNQ1* and *SUP35*. As expected, the [*rnq*-] control showed no Sup35 aggregation, since [*PSI*+] rarely forms without [*RNQ*+] present. In WT cells, nearly all of the Sup35 was visualized in the aggregated band, indicating prolific [*PSI*+] formation. Conversely, the *rnq1-Q298R* in conjunction with WT *SUP35* exhibited the [*PSI*+] induction defect, and little aggregated Sup35 was detected. Finally, in *rnq1-Q298R* cells harboring the *sup35-N5Y* screen candidate, abundant Sup35 aggregation was restored. The lack of complete restoration of Sup35 aggregation may be due to the shorter yeast culture period for this protocol (16 hours) versus [*PSI*+] induction experiments (4 days), potentially indicating that Rnq1-Q298R is a sufficient, yet non-optimal template for seeding [*PSI*+] formation

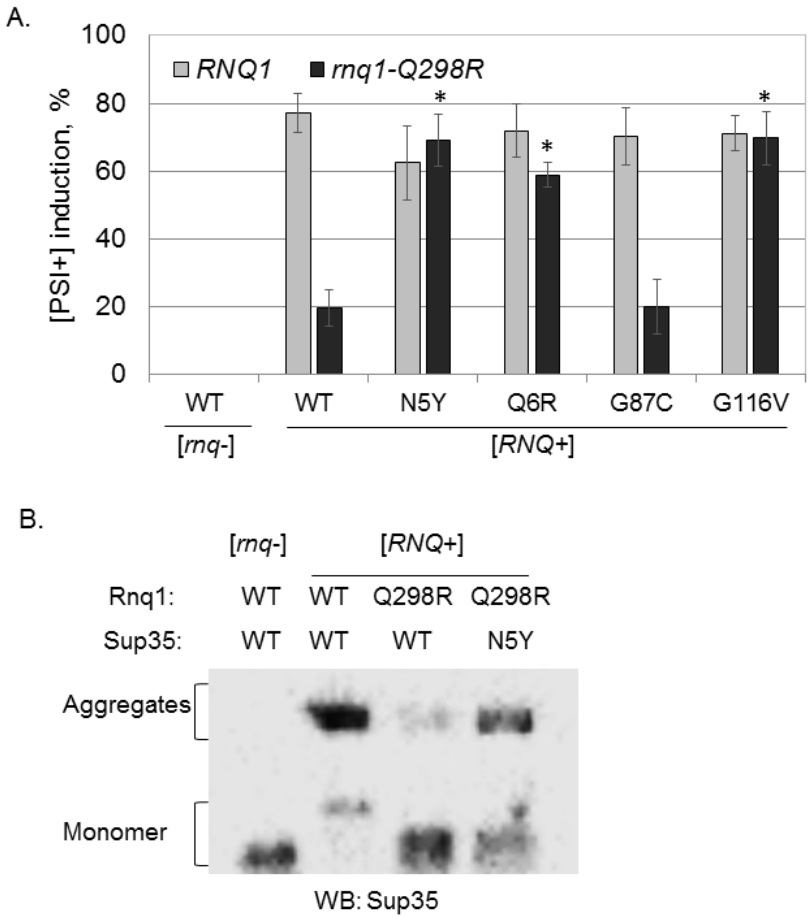

Figure 4.5. Sup35-N5Y strongly rescues the [*PSI*+] induction defect
(A) [*PSI*+] induction experiments demonstrate that three Sup35 mutants restore [*PSI*+] formation to nearly WT levels in *rnq1-Q298R* cells. These mutations do not increase [*PSI*+] formation in a *RNQ1* genetic background. Horizontal axis labels denote *SUP35* genetic status. The [*rnq*-] control cells express *RNQ1* and *SUP35*. More than 13,000 colonies were assessed over five biological replicates. Error bars represent mean ± s.e.m. The "*" symbols represent a significant difference between [*PSI*+] induction with WT Sup35 in *rnq1-Q298R* versus induction with the indicated *sup35* mutants, $p<0.005$. (B) Boiled gel assays allow separate migration of monomeric and aggregated materials, confirming that Sup35 aggregation is reduced in the *SUP35 rnq1-Q298R* background relative to *SUP35 RNQ1* cells. Sup35 aggregation is restored in *sup35-N5Y rnq1-Q298R* cells. We attribute the slightly aberrant monomer bands as an artifact of the experimental procedure, as samples were unboiled (and likely non-denatured) as per the protocol, and Sup35 may shed unevenly from aggregates in addition to the soluble pool. Western blot is a representative image from three independent experiments.

relative to WT Rnq1. These results demonstrate that the Sup35 N5Y mutation affects Sup35 aggregation and [*PSI*+] formation in the presence of Rnq1-Q298R.

4.4.6 The Sup35 N-terminus binds to Rnq1 in vitro

After demonstrating that Sup35 and Rnq1 physically interact and that Rnq1-Q298 and Sup35-N5 may be an important site of contact, we sought to verify the interaction by crosslinking *in vitro*. We decided to use a sulfhydryl-reactive crosslinker to take advantage of the lack of cysteine residues in Sup35. We chose to introduce a cysteine mutation close to the putative binding site so as not to disturb the residue identified as being important in the interaction. We mutated the Sup35 G7 residue to cysteine to direct crosslinking to the N-terminal region of the protein. The G7C mutation of Sup35 has previously been shown to form and propagate the [*PSI*+] state in a manner identical to WT Sup35(110). After treating recombinant Rnq1 with a heterobifunctional crosslinker, SMPB, the two proteins were combined and analyzed via semi-denaturing detergent agarose gel electrophoresis (SDD-AGE), a protocol that allows for the visualization of large SDS-resistant aggregated species (Figure 4.6).

In all crosslinked reactions, a very high molecular-weight product was visible in the wells of the gel. This product reacted with both Sup35 and Rnq1 antibodies (Figure 4.6 and Figure S.4.3), and was not present in control lanes containing Rnq1 alone, Sup35NM-G7C alone, or the two proteins combined without SMPB. Based on the spacer arm length of SMPB (11.5Å), this indicates that Rnq1 and Sup35 physically bind within the first 15 amino acids of Sup35, and agrees with the genetic interaction found in our second site suppressor screen.

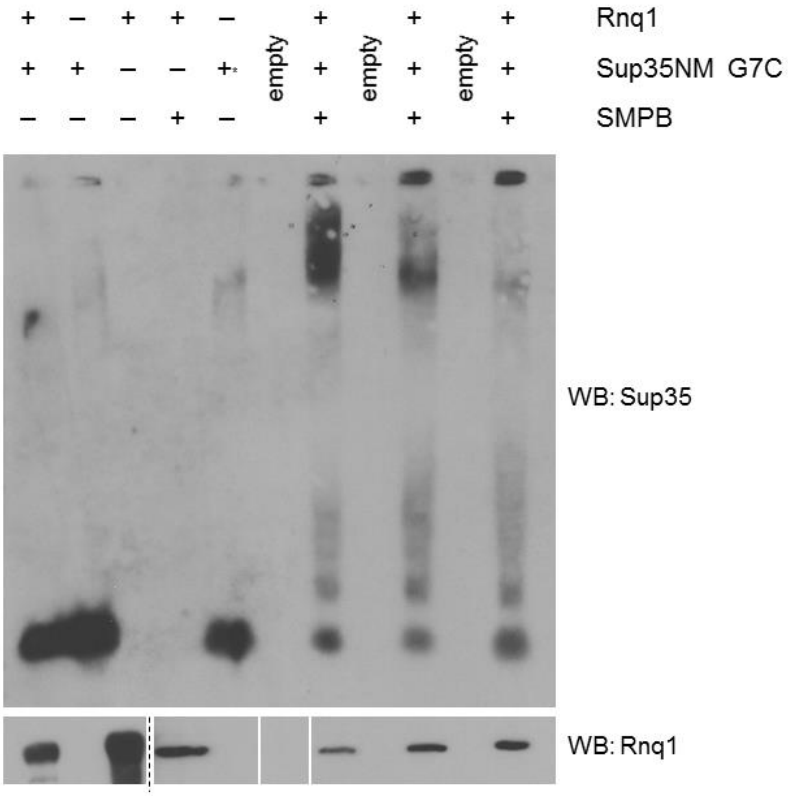

Figure 4.6. The N terminal region of Sup35 crosslinks to Rnq1
Site-directed crosslinking of Sup35-G7C to Rnq1 created high-molecular weight aggregates as visualized by SDD-AGE. Rnq1 alone, Sup35-G7C alone, and both proteins together without SMPB did not create large aggregates. The "+*" notation in the fifth lane indicates Sup35 monomer following treatment with TCEP. Western blot is a representative image from three independent experiments. In the lower blot, Rnq1 loading was confirmed by SDS-PAGE. Vertical white bars separate non-adjacent lanes of the same blot. The dashed line separates adjacent lanes of the same blot under differing film exposures for image clarity (full blots in Supplementary Figure S.4.3). There is excess Rnq1 in lanes 1 and 3, samples prepared without crosslinker, to adjust for protein that is lost during sample desalting following attachment of the crosslinker (see *Methods*). Three trials of crosslinking were included in each experiment and the crosslinking experiment was repeated with different batches of purified proteins three times.

4.5 Discussion

Rnq1 seeds [PSI+] formation by Sup35

To our knowledge we have demonstrated, for the first time in any system, the physical interaction of heterologous prion-forming proteins *in vitro* and *in vivo*. We demonstrated the functional outcomes of this interaction via ThT kinetic assays and [*PSI+*] induction. We utilized genetic techniques and crosslinking to identify specific amino acids that are important to binding between Sup35 and Rnq1; namely, the N5 residue of Sup35 and the Q298 residue of Rnq1.

Importantly, though our work strongly supports the "seeding" model of Rnq1-Sup35 interaction, it does not disprove the inhibitor titration model (Figure 4.1). It may be that a combination of both models contribute to [*PSI+*] formation in vivo. It is possible that an inhibitor molecule is titrated away from Sup35 but a physical interaction between Sup35 andRnq1 is still necessary for [*PSI+*] to form. The inhibitor itself, having affinity for both Sup35 and Rnq1, may even facilitate the binding. Previous work, by our lab and others, has demonstrated that several classes of chaperones can have opposing effects upon prion formation and propagation, sometimes in a conformation-dependent manner(204,280,349). It is even possible that the Rnq1 monomer itself may have an inhibitory effect upon Sup35 aggregation, a concept that is supported by the binding between Sup35 and Rnq1 from [*rnq-*] cell lysate. Future research may implicate one or more of these proteins as an inhibitor of [*PSI+*] formation. However, the seeding model is sufficient for Sup35 polymerization *in vitro* and is clearly a factor in [*PSI+*] formation *in vivo*.

Many points of contact may exist between Rnq1 and Sup35

Our research demonstrates that the Sup35 N-terminal region, specifically N5, is important in the Rnq1-Sup35 interaction. However, we uncovered several other mutations that could partially rescue the [*PSI+*] induction defect associated with Rnq1-Q298R (Figure 4.4). This suggests that

there are multiple residues where Sup35 and Rnq1 may interact *en route* to Sup35 aggregation. Though each Sup35 mutation was alone sufficient to restore interaction with Rnq1-Q298R, there may be multiple points of contact necessary before Sup35 assumes its prion conformation. The total number of necessary interactions and their order of occurrence (if any) remain avenues of further research.

Sup35-Rnq1 interactions may vary by prion strain

Different prion strains, or variants, adopt different tertiary protein conformations(109). These differences may be related to both the adoption of beta sheets within the protein conformer and the size of the amyloid core(109,350). As the beta sheet locations within Sup35 and Rnq1 may differ between variants, so might their intermolecular contacts. Indeed, our work with the "multi-dot high" variant of [*RNQ*+] identified Q298 as an important site of interaction with Sup35, but Q298R had no apparent effect on Sup35-Rnq1 binding in the "very high" prion strain (not shown). There may be a cohort of interacting sites that remain consistent between prions strains, or each variant of [*PSI*+] and [*RNQ*+] may have entirely distinct residues of importance.

Further, it is known that certain strains of [*RNQ*+] are more likely to stimulate the formation of certain strains of [*PSI*+](351).This phenomenon may be explained by the existence of different interaction sites between the two prion-forming proteins. In our experiments, we observed our Sup35 mutants forming both the strong and weak strains of [*PSI*+] under both WT and *rnq1-Q298R* genetic backgrounds (not shown). Thus, this suggests that the Sup35-N5 and Rnq1-Q298 residues are a key binding site that supports general [*PSI*+] formation with multi-dot high [*RNQ*+]. Other sites of interaction may be strain-specific.

Interactions between aggregating proteins can impact human health

Many human pathologies involve the aggregation of misfolded, beta sheet-rich proteins(2). These diseases include Alzheimer's Disease, Parkinson's Disease, and amyotrophic lateral sclerosis (ALS). Though these incurable diseases have profound effects upon patients, and a multi-billion dollar impact on the healthcare system, little is known about the factors that cause the *de novo* protein misfolding. It is possible that a seeding or templating mechanism is responsible for the misfolding and subsequent aggregation of human proteins. In support of this concept, polymerization of amyloid-beta (Aβ) was recently shown to be promoted by the presence of misfolded islet amyloid polypeptide (IAPP), which aggregates in the islet cells of patients with type 2 diabetes(64). Our work demonstrates that multiple binding sites may be involved in cross-seeding (Figure 4.4), but that blocking one crucial site may be sufficient to alter the outcomes of the interaction. Further work in yeast will help to inform additional translatable principles of protein misfolding.

4.6 Acknowledgements

We thank Dr. Patrick Bardill for his work to identify Rnq1 mutations, and the True Lab for helpful comments on the manuscript. We gratefully acknowledge Drs. J. Glover, S. Lindquist, M. Tuite, and J. Weissman for reagents.

4.7 Supplementary Information

Table S.4.1. Strains used in this study.

Strain	Description	Reference
2261	74D-694; [*psi*-], high [*RNQ*+], *MATα, ade1-14 his3□-200 trp1-289 ura3-52 leu2-3,112, sup35□::HygBMX4, RNQ1*	(346)
2160	74D-694; [psi-], high [RNQ+], *MATα, ade1-14 his3□-200 trp1-289 ura3-52 leu2-3,112, sup35□::HygBMX4, RNQ1-Q298R*	This study
1890	74D-694; [*psi*-], [*rnq*-], *MATA, ade1-14 his3□-200 trp1-289 ura3-52 leu2-3,112, sup35□::HygBMX4, RNQ1*	(346)
1951	74D-694; [*psi*-], [*rnq*-], *MATA, ade1-14 his3□-200 trp1-289 ura3-52 leu2-3,112, sup35□::HygBMX4, RNQ1-Q298R*	This study
2040	74D-694; [*psi*-], [*rnq*-], *MATα, ade1-14 his3□-200 trp1-289 ura3-52 leu2-3,112, sup35□::HygBMX4, kar1-□15*, ρ0	This study
2047	74D-694; [*psi*-], high [*RRP*+], *MATA, ade1-14 his3□-200 trp1-289 ura3-52 leu2-3,112, sup35□::RMC, rnq1□::KANMX4*	(346)
1282	74D-694; [*psi*-], high [*RNQ*+], *MATA, ade1-14 his3□-200 trp1-289 ura3-52 leu2-3,112, sup35□::KANMX4, rnq1□::KANMX4*	This study

Table S.4.2. Plasmids used in this study.

Plasmid	Description	Use	Reference
5049	pYK810	Cover *SUP35* deletion with *SUP35*	(93)
5281	p416*TEF-SP5*	Template for screen	This study
5787	p415*TEF-SP5*	Backbone for screen candidate expression	This study
6244	pEMBL-*SUP35*	[*PSI*+] induction – WT	(346)
6257	pRS315-*sup35-N5Y*	Cover *SUP35* deletion with *sup35-N5Y*	This study
6342	pEMBL-*sup35-N5Y*	[*PSI*+] induction – N5Y	This study
6473	pRS315-*sup35-Q6R*	Cover *SUP35* deletion with *sup35-Q6R*	This study
6483	pEMBL- *sup35-Q6R*	[*PSI*+] induction – Q6R	This study
6474	pRS315-*sup35-G116V*	Cover *SUP35* deletion with *sup35-G116V*	This study
6484	pEMBL- *sup35-G116V*	[*PSI*+] induction – G116V	This study
5074	pPROEX-Htb-*RNQ1*	WT Rnq1 purification	This study
SL7111	pAED4-*SCNM-his7*	WT Sup35 bait for Rnq1-trap on resin	(335)
6771	pAED4-*SCNM-G7C-his7*	Purification for crosslinking reagent	This study
6772	pAED4-*SCTD-his7*	Control bait for Rnq1-trap on resin	This study
5719	pRS313-*rnq1-Q298R*	Mitotic stability testing of Rnq1-Q298R	This study
6312	pRS313-*RNQ1*	Mitotic stability testing of WT Rnq1	(346)

Table S.4.3. Antibodies used in this study.

Antigen	Production notes	Type	Dilution	Source
Sup35	Peptide, a.a.s 137-151	Rabbit polyclonal	1:1,500	Lindquist lab
Rnq1	Full-length Rnq1	Rabbit polyclonal	1:1,000	True lab
Rnq1	Full-length Rnq1	Rat polyclonal	1:2,000	True lab
Rabbit	Rabbit IgG	Goat polyclonal	1:10,000	Sigma A0545
Rat	Rat IgG	Rabbit polyclonal	1:10,000	Sigma A5795

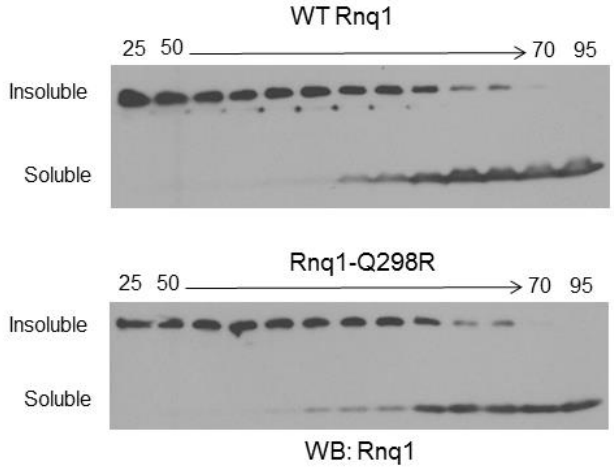

Figure S.4.1. Rnq1-Q298R aggregates have similar properties to WT Rnq1 aggregates
Representative western blots from thermal stability experiments quantified in Figure 3B. Cell lysates were subjected to a temperature gradient before SDS-PAGE and western blotting. Insoluble material, such as prion aggregates, requires treatment at high temperatures in order to enter the resolving gel. There were no observable differences between WT and Rnq1-Q298R aggregates.

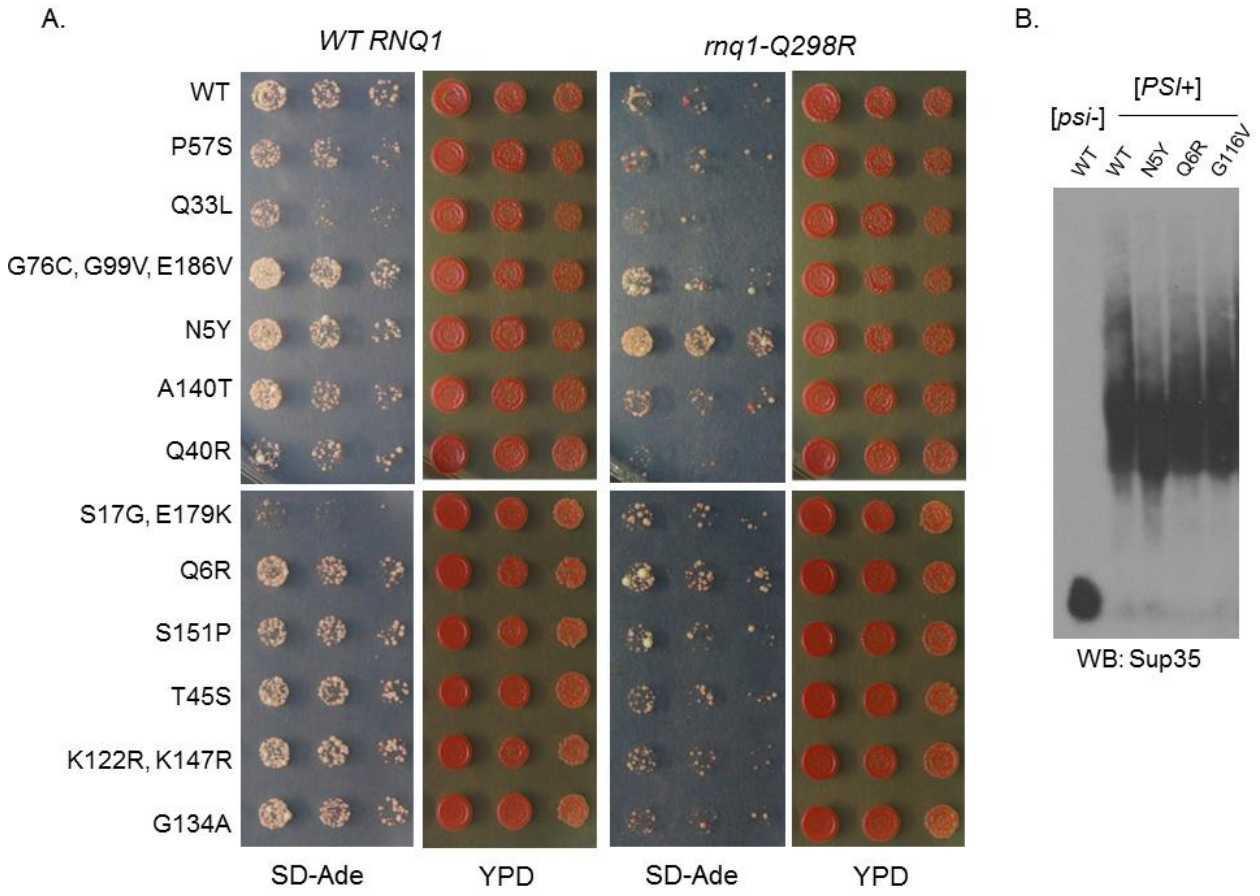

Figure S.4.2. Mutants isolated from *SP5* suppressor screen
(A) Full spottings of screen candidates from Figure 4A. (B) SDD-AGE analysis demonstrates that the rescuing mutants Sup35-N5Y, Sup35-Q6R, and Sup35-G116V can all propagate [*PSI+*].

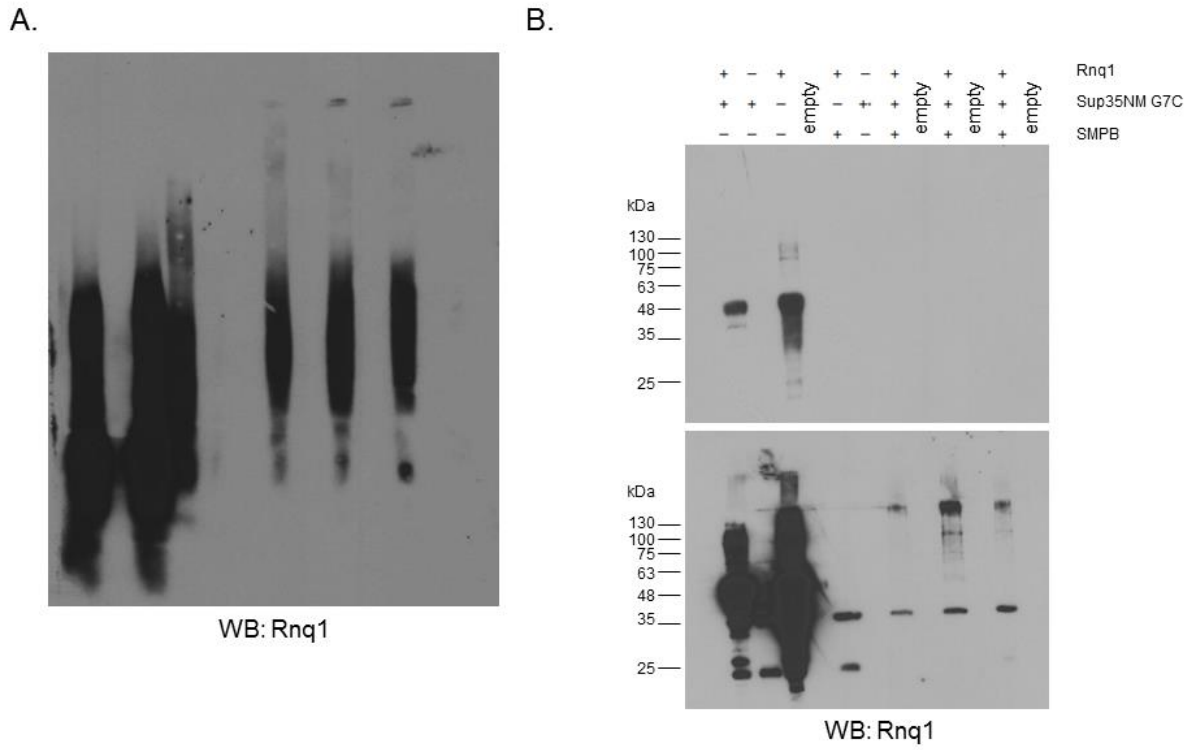

Figure S.4.3. Full crosslinking blots
(A) SDD-AGE from Figure 6, probed with rat anti-Rnq1 primary and rabbit anti-rat secondary antibodies. (B) Complete SDS-PAGE blot from Figure 6. Two exposures are shown to allow for clear viewing of the recombinant Rnq1 in lanes 1 and 3.

Chapter 5: Conclusions and Future Directions

This thesis has laid groundwork for future studies of chaperone balance and interactions between heterologous aggregation-prone proteins. This chapter describes the experiments that could continue to advance these two concepts.

5.1 Effect of chaperone balance on other prions and misfolded proteins

In Chapters 2 and 3, it was demonstrated that shifting the balance of available Hsp70s was sufficient to alter [*PSI+*]-associated toxicity in a manner that was beneficial to cells. The beneficial effects of this balance were sufficient to improve folding outcomes related to more general proteotoxic stress, such as the induction of global protein misfolding with canavanine. This suggests that perturbing the chaperone balance might be broadly advantageous in certain environments, which is an intriguing concept in the context of human disease. Examining the breadth of the chaperone imbalance effect would help inform studies that aim to utilize the principles of chaperone balance to prevent or treat human proteinopathies.

In the context of translational research, it would be ideal to assess the changes in toxicity of human disease proteins, such as TDP-43 and Huntington's-associated polyQ, in response to a shift in chaperone balance. However, the effects of these aggregates in yeast are difficult to reproduce and rely upon the presence of other aggregated species. This may be due, at least in part, to the chaperone machinery – yeast chaperones might not be adapted to recognize or act on these human proteins. It has been demonstrated that yeast and human chaperones have differential interactions with aggregates (204), and TDP-43 aggregates do not require Hsp104 to propagate in yeast (352). Thus, in order to assess the breadth of the effects of chaperone imbalance, other yeast prions could be investigated as models for the diversity of misfolding that can occur in other systems.

Chaperones can have different effects on different yeast prions. For example, overexpression of the Hsp70 Ssa1 promotes [*PSI*+] formation, but inhibits the generation of [URE3] (131,185). Further, prions display different requirements for Hsp40s (191,208). Chaperone imbalance might have a similarly inconsistent effect upon yeast prions. Deletion of the highly-conserved NAC subunits creates an imbalance of Hsp70s. Thus, to assess how NAC deletion affects the folding of other prion or prion-like proteins, we must first understand how the Hsp70s affect other yeast prion proteins. Overexpression and deletion of the Ssa and Ssb prions in [*PRION*+] and [*prion*-] cells would provide this information. The "pro-[*PSI*+]" Ssa1 and "anti-[*PSI*+]" Ssb1 (185,199) may similarly promote and repress the formation of other prions, they may have opposing effects, or they may not differentially act on these prions. This can be assessed by overexpressing each Hsp70 and monitoring yeast for increased or decreased levels of prion curing and formation. In particular, the [*SWI*+] and [*MOT3*+] prions would be my chosen models for investigating the ubiquity of chaperone imbalance.

Both [*SWI*+] and [*MOT3*+] have a regulatory role within *S. cerevisiae* and both have phenotypic readouts (126,353). Further, they are better characterized than other prions in yeast and preliminary research about their interactions with other chaperones has already been performed. Previous data indicate that Ssa1 targets Hsp104 to Mot3 fibrils and suggests that this affect is generalizable to all prions (193). [*SWI*+] propagation is dependent upon canonical Ssa1 cofactors, such as Sis1 and Sse1 (208). Thus, it is possible that Ssa1 overexpression will have similar affects upon [*SWI*+] and [*MOT3*+] as it does on [*PSI*+]; namely, it will promote prion propagation and reduce curing. Due to the opposing roles of Ssa and Ssb on [*PSI*+], I would further hypothesize that Ssb overexpression will enhance the curing of [*SWI*+] and [*MOT3*+]. However, the relatively

high prevalence of [*MOT3*+] in nature may indicate that this prion is generally cured at a low baseline frequency; thus, the Ssb effect may be less potent than with [*PSI*+].

There are several phenotypic readouts that could be utilized to assess both [*MOT3*+] and [*SWI*+] formation and loss, as both prions have affects upon yeast multicellularity (126,353). For [*MOT3*+], altered multicellularity is a readout of prion formation: upon [*MOT3*+] formation, cells exhibit an invasive growth phenotype, altered colony morphology, increased biofilm formation, and reduced flocculation (126). If Ssa overexpression does promote the formation and propagation of [*MOT3*+], then [*mot3*-] cells overexpressing Ssa1 should become [*MOT3*+] at a higher frequency relative to an empty vector control. This could be monitored phenotypically by assessing invasive growth on plates containing proline. A higher number of invasive colonies would be present in Ssa1-overexpressing strains if Ssa is "pro-[*MOT3*+]." Conversely, if Ssb1 overexpression promotes curing of [*MOT3*+], then liquid cultures of Ssb1-overexpressing strains would become increasingly flocculent over time. These experiments would be performed in a Mot3-reporter strain (126) that is more flocculation-prone than most lab strains. Any phenotypes resulting from chaperone perturbation in [*MOT3*+] cells should be verified as specifically prion-related by testing in isogenic [*mot3*-] cells. For example, if reduced flocculation was observed in [*MOT3*+] cells when *SSB1* is deleted, a [*mot3*-] *ssb1Δ* strain should be assessed for its growth to determine the prion dependence of the phenotype.

The [*SWI*+] prion reduces yeast flocculation (similar to [*MOT3*+]), but it also eliminates the invasive growth phenotype (in opposition to [*MOT3*+]) (353). This decoupling of multicellular phenotypes is advantageous, as it would demonstrate that any chaperone overexpression effects are a result of prion formation and not simply chaperone activity on other factors that might alter

multicellularity. A table of predicted experimental outcomes for Hsp70 overexpression in regards to [*MOT3+*] and [*SWI+*] is available in Table 5.1.

Interestingly, I have found that deletion of Btt1 changes the invasive growth characteristics of the 74-D694 laboratory yeast strain (Figure 5.1). Deletion of NAC components alters the Hsp70 balance and decreases the availability of Ssb. Thus, the *btt1Δ* strain may be mimicking an Ssa overexpression phenotype and promoting the formation of other prions. Testing these strains for [*MOT3+*] would support this hypothesis, though I predict that the yeast are [*swi-*] due to their invasive growth. Thus, I hypothesize that the change in the ability of this strain to adhere to agar plates is related to a prion-associated characteristic that is perturbed by altered chaperone balance brought about by Btt1 deletion.

Though I predict that the Hsp70s will have similar affects upon all yeast prions, I do not assume that the Hsp40s would follow this pattern. Hsp40 interactions are known to vary between prions (208), and thus I would elect to investigate the Hsp70 balance directly (as opposed to perturbing Hsp40s). If the Hsp70s are demonstrated to have similar directional affects upon different types of yeast prions, then I would extend my analysis to disease-related proteins and their associated human chaperones. This concept is further discussed in section 5.3.1.

Table 5.1. Predicted phenotypes for overexpression of the Hsp70s Ssa and Ssb in [*MOT3*+] and [*SWI*+] reporter strains, with the hypothesis that Ssa is generally "pro-[*PRION*+]" and Ssb is generally "anti-[*PRION*+]." N/A = phenotype not described in literature. The predicted phenotypes are relative to isogenic controls that are not overexpressing an Hsp70.

	[MOT3+] reporter		**[SWI+] reporter**	
Phenotype	Ssa OE	Ssb OE	Ssa OE	Ssb OE
Invasive growth	Increased	Decreased	Decreased	Increased
Flocculation	Decreased	Increased	Decreased	Increased
Biofilm formation	Increased	Decreased	N/A	N/A
Alt. morphology	Increased	Decreased	N/A	N/A
Growth on gal, raf	N/A	N/A	Decreased	Increased

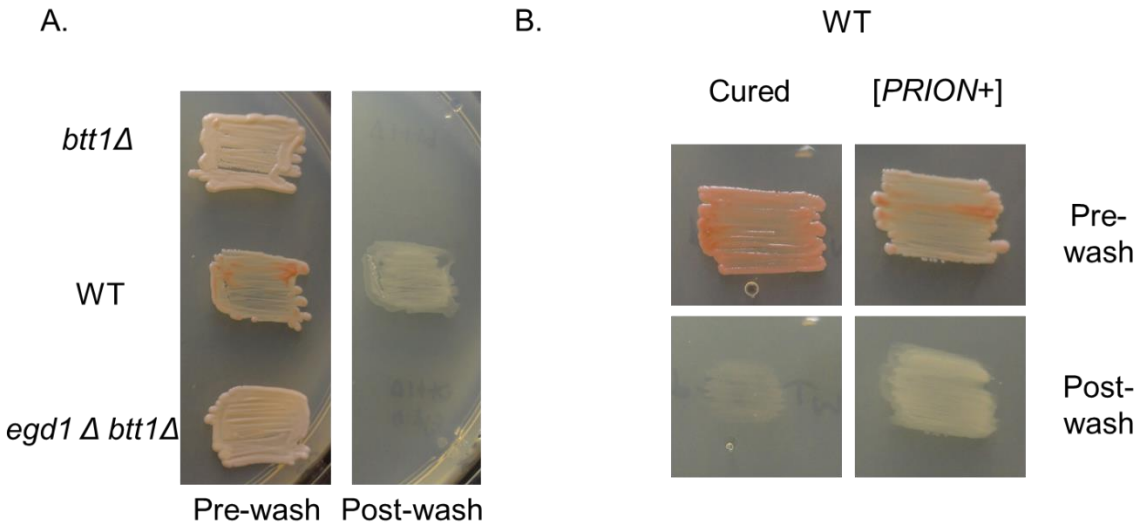

Figure 5.1. Invasive growth of yeast in response to NAC subunit deletion and prion curing. (A) [*PSI*+][*RNQ*+] strains were patched onto synthetic media plates + 0.5%proline, grown for 5 days at 30ºC, and then washed vigorously with flowing water. The *btt1Δ* and *egd1Δbtt1Δ* strains exhibited less adherence than the WT strain (middle patch) or the whole-NAC deletion (not shown). (B) Curing the WT strain of prions via growth on 5µM GdHCl reduced the invasive growth phenotype, suggesting an epigenetic component of adhesion in these strains.

5.2 Further investigation of Sup35-Rnq1 interactions

5.2.1 Are there regions of Rnq1 that are always required for [*PSI+*] *formation?*

In Chapter 4, the binding interaction between Sup35 and Rnq1 was demonstrated to be important for the formation of [*PSI+*]. Two residues in particular, Q298 of Rnq1 and N5 of Sup35, were identified as important sites of interaction. It is known that interactions with Rnq1 aggregates are crucial to the misfolding of Sup35 (114,117,337). Further, the phenotype of the resulting [*PSI+*] variant depends upon the misfolded conformation of Sup35 (109,350). Thus, it seems plausible that certain polymorphisms of Rnq1 and/or Sup35 could bias the interaction so that only certain prion variants result.

Preliminary evidence supports this concept, as [*RNQ+*] isolated from wild yeast strains predominantly induce strong strains of [*PSI+*] (134). The canonical [*RNQ+*] variants in lab strains – low, medium, single-dot high, multi-dot high, and very high – induce a spectrum of [*PSI+*] variants. When Rnq1 aggregates from wild strains were cytoduced into lab strains to be propagated in an isogenic background, the high frequency of strong [*PSI+*] induction persisted (134), suggesting that as-yet undescribed conformational differences are responsible for the bias towards stronger strains of [*PSI+*].

We know that [*RNQ+*] variants are dependent upon different amyloidogenic regions within the protein, and that perturbing these regions can affect Sup35 by increasing or decreasing the frequency of [*PSI+*] formation (346). However, the impact of these Rnq1 amyloidogenic regions on [*PSI+*] strains is unknown. It may be that interactions with a subset of these Rnq1 regions make [*PSI+*] more or less likely to form a stronger prion strain. As discussed in Chapter 1, the strength of the [*PSI+*] phenotype is at least partly dependent upon the size of the amyloid core: a smaller core is associated with a stronger phenotype, and vice versa (110). It is possible that interactions of Sup35 with adjacent amyloid-forming regions of Rnq1 are sufficient to induce small-core

misfolding, while interactions with non-adjacent disordered regions creates a larger core and a weaker [*PSI*+] phenotype. Further, these putative interactions may be Rnq1 region-specific, or the proximity of the regions may be more important than the regions themselves.

To test this, I could utilize a set of previously generated Rnq1 alanine mutants (346). These mutant constructs replace each of 11 putative amyloidogenic regions of Rnq1 with a polyalanine tract. However, in contrast to previous work, I would mutate multiple Rnq1 regions at a time, verify that the resultant proteins could propagate [*RNQ*+], and then assess the [*PSI*+] prion variants that were induced by these proteins. Specifically, I would create Rnq1 constructs without adjacent amyloidogenic regions, as well as constructs with pairs or triplets of adjacent amyloidogenic regions. I hypothesize that the Rnq1 without adjacent disordered domains will form weaker [*PSI*+] variants, because the intermolecular contacts between Rnq1 and Sup35 would be spread over a longer distance in the Sup35 molecule.

An important caveat to this hypothesis is the lack of information about Rnq1 tertiary structure. As Rnq1 adopts a prion fold, non-adjacent amyloidogenic regions may be brought into closer proximity, thus generating a strong [*PSI*+] strain from far-spaced regions of Rnq1. To address this, the Rnq1-Sup35 complex could be crosslinked, trypsinated, and analyzed via mass spectrometry to identify the specific interacting regions.

It is possible that the Rnq1 amyloidogenic regions have amino acid-specific effects on [*PSI*+] formation. Certain residues may be more important in converting Sup35 into weak or strong strains. To investigate this, I would examine the A1 (a.a. 45-53), A3 (a.a. 92-102), and A11 (a.a. 386-394) regions of Rnq1, which exhibit hindered propagation of all five characterized [*RNQ*+] variants, though to differing extents (346). Within these regions, I would systematically mutate each residue to alanine and assess the propagation of [*RNQ*+] and the formation of [*PSI*+]. One

interesting potential result would be the identification of an alanine mutant that does not detectably impact the strain of [*RNQ*+], but that changes the strength of the resulting [*PSI*+] strains without necessarily impacting the levels of [*PSI*+] induction. This would indicate that conformational changes in a small region of an inducing protein are sufficient to modulate the phenotype of a heterologous aggregate.

5.2.2 Could Rnq1 also be an inhibitor of [PSI+] formation?

Chapter 4 investigated two paradigms for Sup35-Rnq1 interaction, the cross-seeding model and the inhibitor titration model. The cross-seeding model was supported, but this does not preclude the existence of an inhibitor molecule that prevents Sup35 aggregation until [*RNQ*+] has formed. As discussed, it is possible that the same molecule could both inhibit Sup35 aggregation when alone, but also facilitate Sup35-Rnq1 binding due to affinity for both proteins. Alternatively, soluble Rnq1 may itself be an inhibitor molecule, binding to Sup35 and blocking [*PSI*+] formation in [*rnq*-] cells.

Preliminary data demonstrates that Rnq1 from [*rnq*-] cell lysates binds to Sup35 stably *in vitro* (not shown). The *in vivo* consequences of this binding have yet to be determined. If the Rnq1 monomer is an inhibitor of [*PSI*+] formation, then [*PSI*+] would theoretically form at a higher frequency in *rnq1Δ* cells relative to [*rnq*-] *RNQ1* cells. However, *rnq1Δ* cells cannot form [*RNQ*+] and thus cannot template Sup35 misfolding; therefore, the spontaneous formation of [*PSI*+] would be extremely low. Further, [*rnq*-] strains can spontaneously convert to [*RNQ*+], which would increase templated [*PSI*+] induction and confound the experimental results.

One way to overcome this challenge would be to assess [*PSI*+] formation in the context of a Rnq1 mutant that can bind to Sup35 but not propagate the [*RNQ*+] prion. Though no such mutant has yet been verified, previous work done by our lab (347) has identified *rnq1* mutants that

destabilize the [*RNQ*+] prion. Further, some His-tagged Rnq1 constructs may not propagate [*RNQ*+], yet they can still bind to Sup35 *in vitro* (238). Consequently, it is possible that a non-prion-forming Rnq1 mutant could be generated by combining destabilizing mutants and tags. For the purpose of experimental description, this theoretical allele shall be called *rnq1-NP* for "non-prion."

To assess [*PSI*+] formation, Sup35 could be overexpressed in both *rnq1Δ* and *rnq1-NP* genetic backgrounds in conjunction with another [*PIN*+] element, such as [URE3]. However, the binding of any [*PIN*+] element to Sup35 may be inhibitory, so it would be less confounding to assess the spontaneous (untemplated) formation of [*PSI*+], however rare. The *ade1-14* colorimetric assay that is commonly used in [*PSI*+] studies would be too low-throughput to efficiently identify a statistically significant change in spontaneous [*PSI*+] formation frequency. Thus, any experiment to assess Sup35 aggregation should be able to rapidly detect interaction between homologous proteins.

Coupling Forsters resonance energy transfer (FRET) with fluorescence activated cell sorting (FACS) could address these points. Such a scheme has previously been utilized to study protein-protein interactions (354). FRET involves tagging different proteins with different fluorophores and then exciting the "donor" with a laser. The "receptor" signal is generated when two tagged proteins are in close proximity and energy is transferred from the donor to the receptor fluorophore. Though often applied to heterologous proteins, FRET has been utilized to study the intermolecular aggregation of homologous amyloid-forming proteins (355). For yeast prion experiments, two tagged copies of Sup35 could be expressed in a *rnq1Δ* or a *rnq1-NP* strain: Sup35-CFP (donor) and Sup35-YFP (receptor). Expressing two copies of Sup35 is advantageous, as Sup35 overexpression enhances the spontaneous formation of [*PSI*+]. After growing large

cultures of cells, yeast could be sorted via FACS. If Sup35 has aggregated to form [*PSI*+], excitation of the cells with a 405nm laser should result in a YFP signal as energy is transferred from the CFP donor within Sup35 aggregates. The [*psi*-] cells would emit only CFP signal, as Sup35 would remain soluble. Retaining the putative [*PSI*+] cells for validation of the phenotype would be important to control for false positives. If the Rnq1 monomer is a *bona fide* inhibitor of [*PSI*+] formation, then the *rnq1Δ* strain should exhibit higher levels of spontaneous [*PSI*+] formation than the *RNQ1* strain.

The conclusions from this research would inform studies related to the prevention of disease-related protein aggregation in humans. A phenotypically-silent protein converting from an aggregation inhibitor to an aggregation promoter is a concept that has yet to be explored in mammalian systems. Demonstrating that aggregation can be prevented by modifying this dual inhibitor/promoter could have significant effects on pathologies where cross-seeding is thought to be a contributing factor.

5.3 Develop yeast as a model for human pathologies

The translatable relevance of protein misfolding has been discussed throughout this work. Human proteinopathies involve heterologous aggregating proteins, and animal models are not sufficient for the study of complex interactions. *S. cerevisiae* is a valuable system by which to elucidate basic mechanisms of such aggregation. However, more can be done to develop yeast into a powerful model for the further investigation of human disease. This could be achieved by recapitulating a mock human chaperone system in yeast or by utilizing yeast biochemical assays to assess the interaction and cross-seeding between human proteins.

5.3.1 Develop a human chaperone model in yeast

Yeast have been utilized to study disease-related human proteins such as the glutamine-expanded Huntingtin protein (polyQ). However, the toxicity of polyQ in yeast is dependent upon the presence of [*RNQ*+] (356). One potential reason for this [*RNQ*+]-dependent effect is the differential interaction of yeast chaperones with different amyloids. For instance, deletion of Hsp104 renders polyQ non-toxic in yeast, and deletions or loss-of-function mutants of Ssa1, Ssa2, Sis1, and Ydj1 all have varying affects upon the aggregation and toxicity of polyQ (356). Studying this type of aggregation in a yeast system makes it difficult to predict which human chaperones may play a role in promoting or ameliorating disease-related toxicity. Thus, I propose to model a human system by systematically replacing yeast chaperones with their nearest human homologs. As humans do not contain a hexameric disaggregase akin to Hsp104, this model strain should be *hsp104Δ*. It is already known that the essential yeast chaperone Sis1 can be replaced by human Hdj1 (357), and other human Hsp70s, J-proteins, and nucleotide exchange factors can be tested for their ability to support yeast viability. To validate this strain's utility as a model for human protein aggregation, its sensitivity to polyQ aggregation should be tested. If the depletion and replacement of yeast chaperones does provide a better mimic to a human system, then the aggregation of expanded polyQ-103 should be toxic in [*rnq*-] cells.

5.3.2 Investigate heterologous cross-seeding of human proteins

As demonstrated in chapter 4, cross-seeding is an important mechanism by which aggregation is templated between heterologous proteins. Studies of cross-seeding of mammalian proteins have identified potential interactors, but not specific binding sites. Again, there is an opportunity for the development of a yeast system for assessing human disease-related proteins. Previous yeast models of human disease have focused on single proteins, such as TDP-43 (358), polyA (359), and α-synuclein (360). However, emerging evidence shows that heterologous

amyloidogenic proteins may interact *en route* to disease onset (58,60). By examining these cross-seeded proteins in yeast, it may be possible to identify and block interacting sites to reduce the disease-associated aggregation.

The relationship between type-2 diabetes (T2D) and various neurological diseases could be probed with the yeast system. Islet amyloid polypeptide (IAPP) has been shown to promote the aggregation of the Aβ peptide *in vitro* (64), may interact with α-synuclein (61), and can seed Tau (58). Further, T2D is a risk factor for Alzheimer's and Parkinson's Diseases (62,63), in a way that may be analogous to [*RNQ*+] serving as a "risk factor" for [*PSI*+] formation. By identifying how and where IAPP cross-seeds other proteins, it may be possible to develop techniques to prevent the spread of amyloid to the nervous system.

Performing this research in a yeast system would involve utilizing well-described methods of genetics and protein biochemistry. First, each candidate amyloid should be shown to be propagable in yeast. Then, the ability of one protein to cross-seed another would be verified by evaluating *de novo* aggregate formation with and without the presence of other amyloids. Finally, mutagenesis could identify residues of importance for the interaction, and protein biochemistry could evaluate the degree to which disrupting these residues destabilizes the resulting amyloid. If combined with the human chaperone model as suggested above, the interactions between heterologous amyloids and molecular chaperones could also be investigated. Ultimately, performing these experiments in yeast allows for rapid and tractable *in vivo* results while avoiding the confounding effects of other (potentially unknown) mammalian chaperones and protein interactors.

Previously, studies with yeast models have led to the discovery of novel Parkinson's disease-related phenotypes (361), and other work has suggested the utility of yeast in screening

for drug compounds to treat neurodegenerative disorders (362). A “humanized” yeast model would lend even more translational power to this system.

5.4 Conclusion

This work has examined multiple facets of protein misfolding and aggregation, including factors that contribute to templated prion formation, chaperone interactions with prions, and chaperone balance itself. Together, these chapters demonstrate that the biology of protein aggregation is complex. Each prion protein is acted upon – directly or indirectly – by a network of molecular chaperones (Chapter 2), cofactors (Chapter 3), and heterologous amyloids (Chapter 4) in a system that strives to maintain protein homeostasis. Perturbing the balance of that system can have unpredictable and sometimes non-intuitive consequences for cells. For example, the deletion of cotranslational chaperones can improve cell viability in the face of prion-associated toxicity, a result that would not make sense without considering the broad web of proteins involved in homeostasis. Further research in the field of protein aggregation, in yeast or in mammalian systems, should continue to consider the implications of system-wide changes on experimental results.

References

1. Labbadia J, Morimoto RI. The Biology of Proteostasis in Aging and Disease. Annu Rev Biochem. 2015;84:435–64.

2. Knowles TPJ, Vendruscolo M, Dobson CM. The amyloid state and its association with protein misfolding diseases. Nat Rev Mol Cell Biol. 2014 Jun;15(6):384–96.

3. Wang F, Durfee LA, Huibregtse JM. A cotranslational ubiquitination pathway for quality control of misfolded proteins. Mol Cell. 2013 May 9;50(3):368–78.

4. Cabrita LD, Dobson CM, Christodoulou J. Protein folding on the ribosome. Curr Opin Struct Biol. 2010 Feb;20(1):33–45.

5. Frydman J. Folding of newly translated proteins in vivo: the role of molecular chaperones. Annu Rev Biochem. 2001;70:603–47.

6. Hipp MS, Park S-H, Hartl FU. Proteostasis impairment in protein-misfolding and -aggregation diseases. Trends Cell Biol. 2014 Sep 1;24(9):506–14.

7. Molecular Chaperone Functions in Protein Folding and Proteostasis. Annu Rev Biochem. 2013;82(1):323–55.

8. Hartl FU, Bracher A, Hayer-Hartl M. Molecular chaperones in protein folding and proteostasis. Nature. 2011 Jul 21;475(7356):324–32.

9. Gong Y, Kakihara Y, Krogan N, Greenblatt J, Emili A, Zhang Z, et al. An atlas of chaperone–protein interactions in Saccharomyces cerevisiae: implications to protein folding pathways in the cell. Mol Syst Biol. 2009 Jun 16;5:275.

10. Kaganovich D, Kopito R, Frydman J. Misfolded proteins partition between two distinct quality control compartments. Nature. 2008 Aug 28;454(7208):1088–95.

11. Miller SBM, Mogk A, Bukau B. Spatially organized aggregation of misfolded proteins as cellular stress defense strategy. J Mol Biol. 2015 Apr 10;427(7):1564–74.

12. Tyedmers J, Mogk A, Bukau B. Cellular strategies for controlling protein aggregation. Nat Rev Mol Cell Biol. 2010 Nov;11(11):777–88.

13. Hershko A, Ciechanover A. The ubiquitin system. Annu Rev Biochem. 1998;67:425–79.

14. Hochstrasser M. Ubiquitin-dependent protein degradation. Annu Rev Genet. 1996;30:405–39.

15. Murata S, Yashiroda H, Tanaka K. Molecular mechanisms of proteasome assembly. Nat Rev Mol Cell Biol. 2009 Feb;10(2):104–15.

16. Vilchez D, Saez I, Dillin A. The role of protein clearance mechanisms in organismal ageing and age-related diseases. Nat Commun. 2014 Dec 8;5:5659.

17. Levine B, Klionsky DJ. Development by Self-Digestion: Molecular Mechanisms and Biological Functions of Autophagy. Dev Cell. 2004 Apr;6(4):463–77.

18. Mizushima N. Autophagy: process and function. Genes Dev. 2007 Nov 15;21(22):2861–73.

19. Takeshige K, Baba M, Tsuboi S, Noda T, Ohsumi Y. Autophagy in yeast demonstrated with proteinase-deficient mutants and conditions for its induction. J Cell Biol. 1992 Oct 15;119(2):301–11.

20. Moriyasu Y, Ohsumi Y. Autophagy in Tobacco Suspension-Cultured Cells in Response to Sucrose Starvation. Plant Physiol. 1996 Aug 1;111(4):1233–41.

21. Suriapranata I, Epple UD, Bernreuther D, Bredschneider M, Sovarasteanu K, Thumm M. The breakdown of autophagic vesicles inside the vacuole depends on Aut4p. J Cell Sci. 2000 Nov 15;113(22):4025–33.

22. Yang Z, Huang J, Geng J, Nair U, Klionsky DJ. Atg22 Recycles Amino Acids to Link the Degradative and Recycling Functions of Autophagy. Mol Biol Cell. 2006 Dec 1;17(12):5094–104.

23. Toyama BH, Weissman JS. Amyloid structure: conformational diversity and consequences. Annu Rev Biochem. 2011;80:557–85.

24. Eanes ED, Glenner GG. X-Ray Diffraction Studies on Amyloid Filaments. J Histochem Cytochem. 1968 Nov 1;16(11):673–7.

25. Astbury WT, Dickinson S, Bailey K. The X-ray interpretation of denaturation and the structure of the seed globulins. Biochem J. 1935 Oct;29(10):2351–2360.1.

26. Biology and Genetics of Prions Causing Neurodegeneration. Annu Rev Genet. 2013;47(1):601–23.

27. Peralta OA, Eyestone WH. Quantitative and qualitative analysis of cellular prion protein (PrPC) expression in bovine somatic tissues. Prion. 2009;3(3):161–70.

28. Ford MJ, Burton LJ, Morris RJ, Hall SM. Selective expression of prion protein in peripheral tissues of the adult mouse. Neuroscience. 2002;113(1):177–92.

29. Bendheim PE, Brown HR, Rudelli RD, Scala LJ, Goller NL, Wen GY, et al. Nearly ubiquitous tissue distribution of the scrapie agent precursor protein. Neurology. 1992 Jan;42(1):149–56.

30. Westergard L, Christensen HM, Harris DA. The cellular prion protein (PrP(C)): its physiological function and role in disease. Biochim Biophys Acta. 2007 Jun;1772(6):629–44.

31. Collinge J. Prion diseases of humans and animals: their causes and molecular basis. Annu Rev Neurosci. 2001;24:519–50.

32. Prusiner SB. Novel proteinaceous infectious particles cause scrapie. Science. 1982 Apr 9;216(4542):136–44.

33. Prusiner SB. Prion encephalopathies of animals and humans. Dev Biol Stand. 1993;80:31–44.

34. Chesebro B. Introduction to the transmissible spongiform encephalopathies or prion diseases. Br Med Bull. 2003 Jun 1;66(1):1–20.

35. Safar J, Wille H, Itri V, Groth D, Serban H, Torchia M, et al. Eight prion strains have PrP(Sc) molecules with different conformations. Nat Med. 1998 Oct;4(10):1157–65.

36. Collinge J, Sidle KC, Meads J, Ironside J, Hill AF. Molecular analysis of prion strain variation and the aetiology of "new variant" CJD. Nature. 1996 Oct 24;383(6602):685–90.

37. Kascsak RJ, Rubenstein R, Merz PA, Carp RI, Wisniewski HM, Diringer H. Biochemical differences among scrapie-associated fibrils support the biological diversity of scrapie agents. J Gen Virol. 1985 Aug;66 (Pt 8):1715–22.

38. Bartz JC, Bessen RA, McKenzie D, Marsh RF, Aiken JM. Adaptation and selection of prion protein strain conformations following interspecies transmission of transmissible mink encephalopathy. J Virol. 2000 Jun;74(12):5542–7.

39. Peretz D, Scott MR, Groth D, Williamson RA, Burton DR, Cohen FE, et al. Strain-specified relative conformational stability of the scrapie prion protein. Protein Sci Publ Protein Soc. 2001 Apr;10(4):854–63.

40. Morales R, Abid K, Soto C. The prion strain phenomenon: Molecular basis and unprecedented features. Biochim Biophys Acta. 2007 Jun;1772(6):681–91.

41. Bessen RA, Marsh RF. Identification of two biologically distinct strains of transmissible mink encephalopathy in hamsters. J Gen Virol. 1992 Feb;73 (Pt 2):329–34.

42. Bessen RA, Marsh RF. Distinct PrP properties suggest the molecular basis of strain variation in transmissible mink encephalopathy. J Virol. 1994 Dec;68(12):7859–68.

43. Brundin P, Melki R, Kopito R. Prion-like transmission of protein aggregates in neurodegenerative diseases. Nat Rev Mol Cell Biol. 2010 Apr;11(4):301–7.

44. Cushman M, Johnson BS, King OD, Gitler AD, Shorter J. Prion-like disorders: blurring the divide between transmissibility and infectivity. J Cell Sci. 2010 Apr 15;123(Pt 8):1191–201.

45. Frost B, Diamond MI. Prion-like mechanisms in neurodegenerative diseases. Nat Rev Neurosci. 2010 Mar;11(3):155–9.

46. Lugaresi E, Tobler I, Gambetti P, Montagna P. The Pathophysiology of Fatal Familial Insomnia. Brain Pathol. 1998 Jul 1;8(3):521–6.

47. Gambetti P, Kong Q, Zou W, Parchi P, Chen SG. Sporadic and familial CJD: classification and characterisation. Br Med Bull. 2003 Jun 1;66(1):213–39.

48. Kuru: A Neurological Disorder [Internet]. Pharma Research Library. [cited 2017 Mar 6]. Available from: http://www.pharmaresearchlibrary.com/kuru-a-neurological-disorder/

49. Bruce ME, Will RG, Ironside JW, McConnell I, Drummond D, Suttie A, et al. Transmissions to mice indicate that "new variant" CJD is caused by the BSE agent. Nature. 1997 Oct 2;389(6650):498–501.

50. Will RG, Ironside JW, Zeidler M, Cousens SN, Estibeiro K, Alperovitch A, et al. A new variant of Creutzfeldt-Jakob disease in the UK. Lancet Lond Engl. 1996 Apr 6;347(9006):921–5.

51. Williams ES. Chronic wasting disease. Vet Pathol. 2005 Sep;42(5):530–49.

52. Moore RA, Vorberg I, Priola SA. Species barriers in prion diseases--brief review. Arch Virol Suppl. 2005;(19):187–202.

53. Roberson ED, Scearce-Levie K, Palop JJ, Yan F, Cheng IH, Wu T, et al. Reducing endogenous tau ameliorates amyloid beta-induced deficits in an Alzheimer's disease mouse model. Science. 2007 May 4;316(5825):750–4.

54. Lewis J, Dickson DW, Lin WL, Chisholm L, Corral A, Jones G, et al. Enhanced neurofibrillary degeneration in transgenic mice expressing mutant tau and APP. Science. 2001 Aug 24;293(5534):1487–91.

55. Leroy K, Ando K, Laporte V, Dedecker R, Suain V, Authelet M, et al. Lack of tau proteins rescues neuronal cell death and decreases amyloidogenic processing of APP in APP/PS1 mice. Am J Pathol. 2012 Dec;181(6):1928–40.

56. Bloom GS. Amyloid-β and Tau: The Trigger and Bullet in Alzheimer Disease Pathogenesis. JAMA Neurol. 2014 Apr 1;71(4):505–8.

57. Stancu I-C, Vasconcelos B, Terwel D, Dewachter I. Models of β-amyloid induced Tau-pathology: the long and "folded" road to understand the mechanism. Mol Neurodegener. 2014;9:51.

58. Guo JL, Covell DJ, Daniels JP, Iba M, Stieber A, Zhang B, et al. Distinct α-synuclein strains differentially promote tau inclusions in neurons. Cell. 2013 Jul 3;154(1):103–17.

59. Sanders DW, Kaufman SK, DeVos SL, Sharma AM, Mirbaha H, Li A, et al. Distinct tau prion strains propagate in cells and mice and define different tauopathies. Neuron. 2014 Jun 18;82(6):1271–88.

60. Brender JR, Salamekh S, Ramamoorthy A. Membrane disruption and early events in the aggregation of the diabetes related peptide IAPP from a molecular prospective. Acc Chem Res. 2012 Mar 20;45(3):454–62.

61. Geng X, Lou H, Wang J, Li L, Swanson AL, Sun M, et al. α-Synuclein binds the K(ATP) channel at insulin-secretory granules and inhibits insulin secretion. Am J Physiol Endocrinol Metab. 2011 Feb;300(2):E276-286.

62. Xu Q, Park Y, Huang X, Hollenbeck A, Blair A, Schatzkin A, et al. Diabetes and risk of Parkinson's disease. Diabetes Care. 2011 Apr;34(4):910–5.

63. Biessels GJ, Staekenborg S, Brunner E, Brayne C, Scheltens P. Risk of dementia in diabetes mellitus: a systematic review. Lancet Neurol. 2006 Jan;5(1):64–74.

64. Moreno-Gonzalez I, Edwards Iii G, Salvadores N, Shahnawaz M, Diaz-Espinoza R, Soto C. Molecular interaction between type 2 diabetes and Alzheimer's disease through cross-seeding of protein misfolding. Mol Psychiatry. 2017 Jan 3;

65. Hammar M, Arnqvist A, Bian Z, Olsén A, Normark S. Expression of two csg operons is required for production of fibronectin- and congo red-binding curli polymers in Escherichia coli K-12. Mol Microbiol. 1995 Nov;18(4):661–70.

66. Hammar M, Bian Z, Normark S. Nucleator-dependent intercellular assembly of adhesive curli organelles in Escherichia coli. Proc Natl Acad Sci U S A. 1996 Jun 25;93(13):6562–6.

67. Cherny I, Rockah L, Levy-Nissenbaum O, Gophna U, Ron EZ, Gazit E. The formation of Escherichia coli curli amyloid fibrils is mediated by prion-like peptide repeats. J Mol Biol. 2005 Sep 16;352(2):245–52.

68. Austin JW, Sanders G, Kay WW, Collinson SK. Thin aggregative fimbriae enhance Salmonella enteritidis biofilm formation. FEMS Microbiol Lett. 1998 May 15;162(2):295–301.

69. Barnhart MM, Chapman MR. Curli Biogenesis and Function. Annu Rev Microbiol. 2006;60:131–47.

70. Sjöbring U, Pohl G, Olsén A. Plasminogen, absorbed by Escherichia coli expressing curli or by Salmonella enteritidis expressing thin aggregative fimbriae, can be activated by simultaneously captured tissue-type plasminogen activator (t-PA). Mol Microbiol. 1994 Nov;14(3):443–52.

71. Coustou V, Deleu C, Saupe S, Begueret J. The protein product of the het-s heterokaryon incompatibility gene of the fungus Podospora anserina behaves as a prion analog. Proc Natl Acad Sci U S A. 1997 Sep 2;94(18):9773–8.

72. Saupe SJ. The [Het-s] prion of Podospora anserina and its role in heterokaryon incompatibility. Semin Cell Dev Biol. 2011 Jul;22(5):460–8.

73. Balguerie A, Reis SD, Ritter C, Chaignepain S, Coulary-Salin B, Forge V, et al. Domain organization and structure–function relationship of the HET-s prion protein of Podospora anserina. EMBO J. 2003 May 1;22(9):2071–81.

74. Tompa P. Intrinsically unstructured proteins. Trends Biochem Sci. 2002;27(10):527–33.

75. Si K, Giustetto M, Etkin A, Hsu R, Janisiewicz AM, Miniaci MC, et al. A Neuronal Isoform of CPEB Regulates Local Protein Synthesis and Stabilizes Synapse-Specific Long-Term Facilitation in Aplysia. Cell. 2003 Dec 26;115(7):893–904.

76. Majumdar A, Cesario WC, White-Grindley E, Jiang H, Ren F, Khan M "Repon," et al. Critical Role of Amyloid-like Oligomers of Drosophila Orb2 in the Persistence of Memory. Cell. 2012 Feb 3;148(3):515–29.

77. Stephan JS, Fioriti L, Lamba N, Colnaghi L, Karl K, Derkatch IL, et al. The CPEB3 Protein Is a Functional Prion that Interacts with the Actin Cytoskeleton. Cell Rep. 2015 Jun 23;11(11):1772–85.

78. Fioriti L, Myers C, Huang Y-Y, Li X, Stephan JS, Trifilieff P, et al. The Persistence of Hippocampal-Based Memory Requires Protein Synthesis Mediated by the Prion-like Protein CPEB3. Neuron. 2015 Jun 17;86(6):1433–48.

79. Pavlopoulos E, Trifilieff P, Chevaleyre V, Fioriti L, Zairis S, Pagano A, et al. Neuralized1 Activates CPEB3: A Function for Nonproteolytic Ubiquitin in Synaptic Plasticity and Memory Storage. Cell. 2011 Dec 9;147(6):1369–83.

80. Huang Y-S, Kan M-C, Lin C-L, Richter JD. CPEB3 and CPEB4 in neurons: analysis of RNA-binding specificity and translational control of AMPA receptor GluR2 mRNA. EMBO J. 2006 Oct 18;25(20):4865–76.

81. Drisaldi B, Colnaghi L, Fioriti L, Rao N, Myers C, Snyder AM, et al. SUMOylation Is an Inhibitory Constraint that Regulates the Prion-like Aggregation and Activity of CPEB3. Cell Rep. 2015 Jun 23;11(11):1694–702.

82. Darnell RB. Memory, Synaptic Translation, and…Prions? Cell. 2003 Dec 26;115(7):767–8.

83. Heinrich SU, Lindquist S. Protein-only mechanism induces self-perpetuating changes in the activity of neuronal Aplysia cytoplasmic polyadenylation element binding protein (CPEB). Proc Natl Acad Sci. 2011 Feb 15;108(7):2999–3004.

84. Saborio GP, Permanne B, Soto C. Sensitive detection of pathological prion protein by cyclic amplification of protein misfolding. Nature. 2001 Jun 14;411(6839):810–3.

85. Colby DW, Zhang Q, Wang S, Groth D, Legname G, Riesner D, et al. Prion detection by an amyloid seeding assay. Proc Natl Acad Sci. 2007 Dec 26;104(52):20914–9.

86. Gonzalez-Montalban N, Makarava N, Ostapchenko VG, Savtchenk R, Alexeeva I, Rohwer RG, et al. Highly efficient protein misfolding cyclic amplification. PLoS Pathog. 2011 Feb 10;7(2):e1001277.

87. Watts JC, Prusiner SB. Mouse Models for Studying the Formation and Propagation of Prions. J Biol Chem. 2014 Jul 18;289(29):19841–9.

88. Liebman SW, Chernoff YO. Prions in Yeast. Genetics. 2012 Aug;191(4):1041–72.

89. Halfmann R, Jarosz DF, Jones SK, Chang A, Lancaster AK, Lindquist S. Prions are a common mechanism for phenotypic inheritance in wild yeasts. Nature. 2012 Feb 16;482(7385):363–8.

90. True HL, Lindquist SL. A yeast prion provides a mechanism for genetic variation and phenotypic diversity. Nature. 2000 Sep 28;407(6803):477–83.

91. Tuite MF, Cox BS. Propagation of yeast prions. Nat Rev Mol Cell Biol. 2003 Nov;4(11):878–90.

92. Shkundina IS, Kushnirov VV, Tuite MF, Ter-Avanesyan MD. The Role of the N-Terminal Oligopeptide Repeats of the Yeast Sup35 Prion Protein in Propagation and Transmission of Prion Variants. Genetics. 2006 Feb;172(2):827–35.

93. Parham SN, Resende CG, Tuite MF. Oligopeptide repeats in the yeast protein Sup35p stabilize intermolecular prion interactions. EMBO J. 2001 May 1;20(9):2111–9.

94. Helsen CW, Glover JR. A new perspective on Hsp104-mediated propagation and curing of the yeast prion [PSI (+)]. Prion. 2012 Jul 1;6(3):234–9.

95. Liu J-J, Sondheimer N, Lindquist SL. Changes in the middle region of Sup35 profoundly alter the nature of epigenetic inheritance for the yeast prion [PSI+]. Proc Natl Acad Sci U S A. 2002 Dec 10;99 Suppl 4:16446–53.

96. Ter-Avanesyan MD, Kushnirov VV, Dagkesamanskaya AR, Didichenko SA, Chernoff YO, Inge-Vechtomov SG, et al. Deletion analysis of the SUP35 gene of the yeast Saccharomyces cerevisiae reveals two non-overlapping functional regions in the encoded protein. Mol Microbiol. 1993 Mar;7(5):683–92.

97. Cox BS. PSI, a cytoplasmic suppressor of super-suppressor in yeast. Heredity. 1965;20.

98. Liebman SW, Derkatch IL. The Yeast [PSI +] Prion: Making Sense of Nonsense. J Biol Chem. 1999 Jan 15;274(3):1181–4.

99. Pezza JA, Langseth SX, Raupp Yamamoto R, Doris SM, Ulin SP, Salomon AR, et al. The NatA Acetyltransferase Couples Sup35 Prion Complexes to the [PSI+] Phenotype. Mol Biol Cell. 2009 Feb 1;20(3):1068–80.

100. Salnikova AB, Kryndushkin DS, Smirnov VN, Kushnirov VV, Ter-Avanesyan MD. Nonsense Suppression in Yeast Cells Overproducing Sup35 (eRF3) Is Caused by Its Non-heritable Amyloids. J Biol Chem. 2005 Mar 11;280(10):8808–12.

101. Vishveshwara N, Bradley ME, Liebman SW. Sequestration of essential proteins causes prion associated toxicity in yeast. Mol Microbiol. 2009 Sep;73(6):1101–14.

102. Nakayashiki T, Ebihara K, Bannai H, Nakamura Y. Yeast [PSI+] "prions" that are crosstransmissible and susceptible beyond a species barrier through a quasi-prion state. Mol Cell. 2001 Jun;7(6):1121–30.

103. Schweingruber C, Rufener SC, Zünd D, Yamashita A, Mühlemann O. Nonsense-mediated mRNA decay — Mechanisms of substrate mRNA recognition and degradation in mammalian cells. Biochim Biophys Acta BBA - Gene Regul Mech. 2013 Jun;1829(6–7):612–23.

104. Derkatch IL, Chernoff YO, Kushnirov VV, Inge-Vechtomov SG, Liebman SW. Genesis and variability of [PSI] prion factors in Saccharomyces cerevisiae. Genetics. 1996 Dec;144(4):1375–86.

105. Huang Y-W, Chang Y-C, Diaz-Avalos R, King C-Y. W8, a new Sup35 prion strain, transmits distinctive information with a conserved assembly scheme. Prion. 2015;9(3):207–27.

106. King CY. Supporting the structural basis of prion strains: induction and identification of [PSI] variants. J Mol Biol. 2001 Apr 13;307(5):1247–60.

107. Uptain SM, Sawicki GJ, Caughey B, Lindquist S. Strains of [PSI+] are distinguished by their efficiencies of prion-mediated conformational conversion. EMBO J. 2001 Nov 15;20(22):6236–45.

108. Tanaka M, Chien P, Naber N, Cooke R, Weissman JS. Conformational variations in an infectious protein determine prion strain differences. Nature. 2004 Mar 18;428(6980):323–8.

109. Tanaka M, Collins SR, Toyama BH, Weissman JS. The physical basis of how prion conformations determine strain phenotypes. Nature. 2006 Aug 3;442(7102):585–9.

110. Krishnan R, Lindquist SL. Structural insights into a yeast prion illuminate nucleation and strain diversity. Nature. 2005 Jun 9;435(7043):765–72.

111. Stein KC, True HL. The [RNQ+] prion: a model of both functional and pathological amyloid. Prion. 2011 Dec;5(4):291–8.

112. Sondheimer N, Lindquist S. Rnq1: an epigenetic modifier of protein function in yeast. Mol Cell. 2000 Jan;5(1):163–72.

113. Kadnar ML, Articov G, Derkatch IL. Distinct Type of Transmission Barrier Revealed by Study of Multiple Prion Determinants of Rnq1. PLOS Genet. 2010 Jan 22;6(1):e1000824.

114. Derkatch IL, Bradley ME, Hong JY, Liebman SW. Prions affect the appearance of other prions: the story of [PIN(+)]. Cell. 2001 Jul 27;106(2):171–82.

115. Derkatch IL, Bradley ME, Zhou P, Chernoff YO, Liebman SW. Genetic and environmental factors affecting the de novo appearance of the [PSI+] prion in Saccharomyces cerevisiae. Genetics. 1997 Oct;147(2):507–19.

116. Derkatch IL, Bradley ME, Masse SVL, Zadorsky SP, Polozkov GV, Inge-Vechtomov SG, et al. Dependence and independence of [PSI+] and [PIN+]: A two-prion system in yeast? EMBO J. 2000;19(9):1942–52.

117. Vitrenko YA, Gracheva EO, Richmond JE, Liebman SW. Visualization of Aggregation of the Rnq1 Prion Domain and Cross-seeding Interactions with Sup35NM. J Biol Chem. 2007 Jan 19;282(3):1779–87.

118. Derkatch IL, Uptain SM, Outeiro TF, Krishnan R, Lindquist SL, Liebman SW. Effects of Q/N-rich, polyQ, and non-polyQ amyloids on the de novo formation of the [PSI+] prion in yeast and aggregation of Sup35 in vitro. Proc Natl Acad Sci U S A. 2004 Aug 31;101(35):12934–9.

119. Bradley ME, Liebman SW. Destabilizing Interactions Among [PSI +] and [PIN +] Yeast Prion Variants. Genetics. 2003 Dec 1;165(4):1675–85.

120. Huang VJ, Stein KC, True HL. Spontaneous variants of the [RNQ+] prion in yeast demonstrate the extensive conformational diversity possible with prion proteins. PloS One. 2013;8(10):e79582.

121. Lacroute F. Non-Mendelian mutation allowing ureidosuccinic acid uptake in yeast. J Bacteriol. 1971 May;106(2):519–22.

122. Wickner RB. [URE3] as an altered URE2 protein: evidence for a prion analog in Saccharomyces cerevisiae. Science. 1994 Apr 22;264(5158):566–9.

123. Du Z, Park K-W, Yu H, Fan Q, Li L. Newly identified prion linked to the chromatin-remodeling factor Swi1 in Saccharomyces cerevisiae. Nat Genet. 2008 Apr;40(4):460–5.

124. Patel BK, Gavin-Smyth J, Liebman SW. The yeast global transcriptional co-repressor protein Cyc8 can propagate as a prion. Nat Cell Biol. 2009 Mar;11(3):344–9.

125. Grishin AV, Rothenberg M, Downs MA, Blumer KJ. Mot3, a Zn finger transcription factor that modulates gene expression and attenuates mating pheromone signaling in Saccharomyces cerevisiae. Genetics. 1998 Jun;149(2):879–92.

126. Holmes DL, Lancaster AK, Lindquist S, Halfmann R. Heritable Remodeling of Yeast Multicellularity by an Environmentally Responsive Prion. Cell. 2013 Mar 28;153(1):153–65.

127. Rogoza T, Goginashvili A, Rodionova S, Ivanov M, Viktorovskaya O, Rubel A, et al. Non-Mendelian determinant [ISP+] in yeast is a nuclear-residing prion form of the global transcriptional regulator Sfp1. Proc Natl Acad Sci U S A. 2010 Jun 8;107(23):10573–7.

128. Brown JCS, Lindquist S. A heritable switch in carbon source utilization driven by an unusual yeast prion. Genes Dev. 2009 Oct 1;23(19):2320–32.

129. Suzuki G, Shimazu N, Tanaka M. A Yeast Prion, Mod5, Promotes Acquired Drug Resistance and Cell Survival Under Environmental Stress. Science. 2012 Apr 20;336(6079):355–9.

130. Du Z, Li L. Investigating the Interactions of Yeast Prions: [SWI+], [PSI+], and [PIN+]. Genetics. 2014 Jun 1;197(2):685–700.

131. Schwimmer C, Masison DC. Antagonistic Interactions between Yeast [PSI+] and [URE3] Prions and Curing of [URE3] by Hsp70 Protein Chaperone Ssa1p but Not by Ssa2p. Mol Cell Biol. 2002 Jun 1;22(11):3590–8.

132. Bradley ME, Edskes HK, Hong JY, Wickner RB, Liebman SW. Interactions among prions and prion "strains" in yeast. Proc Natl Acad Sci U S A. 2002 Dec 10;99(Suppl 4):16392–9.

133. Nakayashiki T, Kurtzman CP, Edskes HK, Wickner RB. Yeast prions [URE3] and [PSI+] are diseases. Proc Natl Acad Sci U S A. 2005 Jul 26;102(30):10575–80.

134. Westergard L, True HL. Wild yeast harbor a variety of distinct amyloid structures with strong prion-inducing capabilities. Mol Microbiol. 2014 Apr;92(1):183–93.

135. Halfmann R, Alberti S, Lindquist S. Prions, protein homeostasis, and phenotypic diversity. Trends Cell Biol. 2010 Mar;20(3):125–33.

136. Chernova TA, Wilkinson KD, Chernoff YO. Physiological and environmental control of yeast prions. FEMS Microbiol Rev. 2014 Mar;38(2):326–44.

137. Alberti S, Halfmann R, King O, Kapila A, Lindquist S. A systematic survey identifies prions and illuminates sequence features of prionogenic proteins. Cell. 2009 Apr 3;137(1):146–58.

138. Lancaster AK, Bardill JP, True HL, Masel J. The Spontaneous Appearance Rate of the Yeast Prion [PSI+] and Its Implications for the Evolution of the Evolvability Properties of the [PSI+] System. Genetics. 2010 Feb 1;184(2):393–400.

139. Neuwald AF, Aravind L, Spouge JL, Koonin EV. AAA+: A class of chaperone-like ATPases associated with the assembly, operation, and disassembly of protein complexes. Genome Res. 1999 Jan;9(1):27–43.

140. Grimminger-Marquardt V, Lashuel HA. Structure and function of the molecular chaperone Hsp104 from yeast. Biopolymers. 2010 Mar;93(3):252–76.

141. Sanchez Y, Taulien J, Borkovich KA, Lindquist S. Hsp104 is required for tolerance to many forms of stress. EMBO J. 1992 Jun;11(6):2357–64.

142. Ferreira PC, Ness F, Edwards SR, Cox BS, Tuite MF. The elimination of the yeast [PSI+] prion by guanidine hydrochloride is the result of Hsp104 inactivation. Mol Microbiol. 2001 Jun;40(6):1357–69.

143. Kummer E, Oguchi Y, Seyffer F, Bukau B, Mogk A. Mechanism of Hsp104/ClpB inhibition by prion curing Guanidinium hydrochloride. FEBS Lett. 2013 Mar 18;587(6):810–7.

144. Wendler P, Shorter J, Plisson C, Cashikar AG, Lindquist S, Saibil HR. Atypical AAA+ subunit packing creates an expanded cavity for disaggregation by the protein-remodeling factor Hsp104. Cell. 2007 Dec 28;131(7):1366–77.

145. Wendler P, Shorter J, Snead D, Plisson C, Clare DK, Lindquist S, et al. Motor mechanism for protein threading through Hsp104. Mol Cell. 2009 Apr 10;34(1):81–92.

146. Oguchi Y, Kummer E, Seyffer F, Berynskyy M, Anstett B, Zahn R, et al. A tightly regulated molecular toggle controls AAA+ disaggregase. Nat Struct Mol Biol. 2012 Dec;19(12):1338–46.

147. Dulle JE, Stein KC, True HL. Regulation of the Hsp104 Middle Domain Activity Is Critical for Yeast Prion Propagation. PLoS ONE [Internet]. 2014 [cited 2017 Feb 9];9(1). Available from: https://www-ncbi-nlm-nih-gov.beckerproxy.wustl.edu/pmc/articles/PMC3900729/

148. DeSantis ME, Shorter J. The elusive middle domain of Hsp104 and ClpB: Location and function. Biochim Biophys Acta BBA - Mol Cell Res. 2012 Jan;1823(1):29–39.

149. Tessarz P, Mogk A, Bukau B. Substrate threading through the central pore of the Hsp104 chaperone as a common mechanism for protein disaggregation and prion propagation. Mol Microbiol. 2008 Apr;68(1):87–97.

150. Schaupp A, Marcinowski M, Grimminger V, Bösl B, Walter S. Processing of proteins by the molecular chaperone Hsp104. J Mol Biol. 2007 Jul 20;370(4):674–86.

151. Yokom AL, Gates SN, Jackrel ME, Mack KL, Su M, Shorter J, et al. Spiral architecture of the Hsp104 disaggregase reveals the basis for polypeptide translocation. Nat Struct Mol Biol. 2016 Sep;23(9):830–7.

152. Jackrel ME, DeSantis ME, Martinez BA, Castellano LM, Stewart RM, Caldwell KA, et al. Potentiated Hsp104 Variants Antagonize Diverse Proteotoxic Misfolding Events. Cell. 2014 Jan 16;156(1):170–82.

153. Winkler J, Tyedmers J, Bukau B, Mogk A. Chaperone networks in protein disaggregation and prion propagation. J Struct Biol. 2012 Aug;179(2):152–60.

154. Mayer MP. Hsp70 chaperone dynamics and molecular mechanism. Trends Biochem Sci. 2013 Oct 1;38(10):507–14.

155. Werner-Washburne M, Stone DE, Craig EA. Complex interactions among members of an essential subfamily of hsp70 genes in Saccharomyces cerevisiae. Mol Cell Biol. 1987 Jul 1;7(7):2568–77.

156. Peisker K, Chiabudini M, Rospert S. The ribosome-bound Hsp70 homolog Ssb of Saccharomyces cerevisiae. Biochim Biophys Acta BBA - Mol Cell Res. 2010 Jun;1803(6):662–72.

157. Takuno S, Innan H. Selection to Maintain Paralogous Amino Acid Differences Under the Pressure of Gene Conversion in the Heat-Shock Protein Genes in Yeast. Mol Biol Evol. 2009 Dec 1;26(12):2655–9.

158. Heinen RC, Diniz-Mendes L, Silva JT, Paschoalin VMF. Identification of the divergent calmodulin-binding motif in yeast Ssb1/Hsp75 protein and in other HSP70 family members. Braz J Med Biol Res. 2006;39(11):1399–408.

159. Dunn CD, Jensen RE. Suppression of a defect in mitochondrial protein import identifies cytosolic proteins required for viability of yeast cells lacking mitochondrial DNA. Genetics. 2003;165(1):35–45.

160. Flaherty KM, DeLuca-Flaherty C, McKay DB. Three-dimensional structure of the ATPase fragment of a 70K heat-shock cognate protein. Nature. 1990 Aug 16;346(6285):623–8.

161. Vogel M, Mayer MP, Bukau B. Allosteric regulation of Hsp70 chaperones involves a conserved interdomain linker. J Biol Chem. 2006 Dec 15;281(50):38705–11.

162. Schmid D, Baici A, Gehring H, Christen P. Kinetics of molecular chaperone action. Science. 1994 Feb 18;263(5149):971–3.

163. Buchberger A, Theyssen H, Schröder H, McCarty JS, Virgallita G, Milkereit P, et al. Nucleotide-induced conformational changes in the ATPase and substrate binding domains of the DnaK chaperone provide evidence for interdomain communication. J Biol Chem. 1995 Jul 14;270(28):16903–10.

164. Bracher A, Verghese J. The nucleotide exchange factors of Hsp70 molecular chaperones. Front Mol Biosci [Internet]. 2015 Apr 7 [cited 2017 Feb 2];2. Available from: http://www.ncbi.nlm.nih.gov/pmc/articles/PMC4753570/

165. McKay D, Wilbanks S, Flaherty K, Ha J-H, O'Brien M, Shirvanee L. Stress-70 Proteins and Their Interaction with Nucleotides. In: The Biology of Heat Shock Proteins & Molecular Chaperones. Plainview, NY: Cold Spring Harbor Lab. Press; 1994. p. 153–178.

166. Mayer MP, Schröder H, Rüdiger S, Paal K, Laufen T, Bukau B. Multistep mechanism of substrate binding determines chaperone activity of Hsp70. Nat Struct Biol. 2000 Jul;7(7):586–93.

167. Mukai H, Kuno T, Tanaka H, Hirata D, Miyakawa T, Tanaka C. Isolation and characterization of SSE1 and SSE2, new members of the yeast HSP70 multigene family. Gene. 1993 Sep 30;132(1):57–66.

168. Ghaemmaghami S, Huh W-K, Bower K, Howson RW, Belle A, Dephoure N, et al. Global analysis of protein expression in yeast. Nature. 2003 Oct 16;425(6959):737–41.

169. Kulak NA, Pichler G, Paron I, Nagaraj N, Mann M. Minimal, encapsulated proteomic-sample processing applied to copy-number estimation in eukaryotic cells. Nat Methods. 2014 Mar;11(3):319–24.

170. Liu XD, Morano KA, Thiele DJ. The yeast Hsp110 family member, Sse1, is an Hsp90 cochaperone. J Biol Chem. 1999 Sep 17;274(38):26654–60.

171. Shaner L, Wegele H, Buchner J, Morano KA. The yeast Hsp110 Sse1 functionally interacts with the Hsp70 chaperones Ssa and Ssb. J Biol Chem. 2005 Dec 16;280(50):41262–9.

172. Yam AY-W, Albanèse V, Lin H-TJ, Frydman J. Hsp110 cooperates with different cytosolic HSP70 systems in a pathway for de novo folding. J Biol Chem. 2005 Dec 16;280(50):41252–61.

173. Trott A, Shaner L, Morano KA. The molecular chaperone Sse1 and the growth control protein kinase Sch9 collaborate to regulate protein kinase A activity in Saccharomyces cerevisiae. Genetics. 2005 Jul;170(3):1009–21.

174. Abrams JL, Verghese J, Gibney PA, Morano KA. Hierarchical functional specificity of cytosolic heat shock protein 70 (Hsp70) nucleotide exchange factors in yeast. J Biol Chem. 2014 May 9;289(19):13155–67.

175. Dragovic Z, Shomura Y, Tzvetkov N, Hartl FU, Bracher A. Fes1p acts as a nucleotide exchange factor for the ribosome-associated molecular chaperone Ssb1p. Biol Chem. 2006 Dec;387(12):1593–600.

176. Gowda NKC, Kandasamy G, Froehlich MS, Dohmen RJ, Andréasson C. Hsp70 nucleotide exchange factor Fes1 is essential for ubiquitin-dependent degradation of misfolded cytosolic proteins. Proc Natl Acad Sci U S A. 2013 Apr 9;110(15):5975–80.

177. Verghese J, Morano KA. A Lysine-Rich Region within Fungal BAG Domain-Containing Proteins Mediates a Novel Association with Ribosomes. Eukaryot Cell. 2012 Aug;11(8):1003–11.

178. Sondermann H, Ho AK, Listenberger LL, Siegers K, Moarefi I, Wente SR, et al. Prediction of novel Bag-1 homologs based on structure/function analysis identifies Snl1p as an Hsp70 co-chaperone in Saccharomyces cerevisiae. J Biol Chem. 2002 Sep 6;277(36):33220–7.

179. Kampinga HH, Craig EA. The HSP70 chaperone machinery: J proteins as drivers of functional specificity. Nat Rev Mol Cell Biol. 2010 Aug;11(8):579–92.

180. Sahi C, Craig EA. Network of general and specialty J protein chaperones of the yeast cytosol. Proc Natl Acad Sci U S A. 2007 Apr 24;104(17):7163–8.

181. Caplan AJ, Douglas MG. Characterization of YDJ1: a yeast homologue of the bacterial dnaJ protein. J Cell Biol. 1991 Aug;114(4):609–21.

182. Greene MK, Maskos K, Landry SJ. Role of the J-domain in the cooperation of Hsp40 with Hsp70. Proc Natl Acad Sci U S A. 1998 May 26;95(11):6108–13.

183. Peisker K, Braun D, Wölfle T, Hentschel J, Fünfschilling U, Fischer G, et al. Ribosome-associated Complex Binds to Ribosomes in Close Proximity of Rpl31 at the Exit of the Polypeptide Tunnel in Yeast. Mol Biol Cell. 2008 Dec;19(12):5279–88.

184. Sahi C, Lee T, Inada M, Pleiss JA, Craig EA. Cwc23, an essential J protein critical for pre-mRNA splicing with a dispensable J domain. Mol Cell Biol. 2010 Jan;30(1):33–42.

185. Allen KD, Wegrzyn RD, Chernova TA, Müller S, Newnam GP, Winslett PA, et al. Hsp70 chaperones as modulators of prion life cycle: novel effects of Ssa and Ssb on the Saccharomyces cerevisiae prion [PSI+]. Genetics. 2005 Mar;169(3):1227–42.

186. Wegrzyn RD, Bapat K, Newnam GP, Zink AD, Chernoff YO. Mechanism of prion loss after Hsp104 inactivation in yeast. Mol Cell Biol. 2001 Jul;21(14):4656–69.

187. Paushkin SV, Kushnirov VV, Smirnov VN, Ter-Avanesyan MD. Propagation of the yeast prion-like [psi+] determinant is mediated by oligomerization of the SUP35-encoded polypeptide chain release factor. EMBO J. 1996 Jun 17;15(12):3127–34.

188. Cox B, Ness F, Tuite M. Analysis of the generation and segregation of propagons: entities that propagate the [PSI+] prion in yeast. Genetics. 2003 Sep;165(1):23–33.

189. Ness F, Cox BS, Wongwigkarn J, Naeimi WR, Tuite MF. Over-expression of the molecular chaperone Hsp104 in Saccharomyces cerevisiae results in the malpartition of [PSI+] propagons. Mol Microbiol. 2017 Feb 1;n/a-n/a.

190. Chernoff YO, Lindquist SL, Ono B, Inge-Vechtomov SG, Liebman SW. Role of the chaperone protein Hsp104 in propagation of the yeast prion-like factor [psi+]. Science. 1995 May 12;268(5212):880–4.

191. Moriyama H, Edskes HK, Wickner RB. [URE3] Prion Propagation in Saccharomyces cerevisiae: Requirement for Chaperone Hsp104 and Curing by Overexpressed Chaperone Ydj1p. Mol Cell Biol. 2000 Dec 1;20(23):8916–22.

192. Helsen CW, Glover JR. Insight into Molecular Basis of Curing of [PSI+] Prion by Overexpression of 104-kDa Heat Shock Protein (Hsp104). J Biol Chem. 2012 Jan 2;287(1):542–56.

193. Winkler J, Tyedmers J, Bukau B, Mogk A. Hsp70 targets Hsp100 chaperones to substrates for protein disaggregation and prion fragmentation. J Cell Biol. 2012 Aug 6;198(3):387–404.

194. Newnam GP, Birchmore JL, Chernoff YO. Destabilization and recovery of a yeast prion after mild heat shock. J Mol Biol. 2011 May 6;408(3):432–48.

195. Park Y-N, Zhao X, Yim Y-I, Todor H, Ellerbrock R, Reidy M, et al. Hsp104 Overexpression Cures Saccharomyces cerevisiae [PSI+] by Causing Dissolution of the Prion Seeds. Eukaryot Cell. 2014 May;13(5):635–47.

196. Kryndushkin DS, Engel A, Edskes H, Wickner RB. Molecular Chaperone Hsp104 Can Promote Yeast Prion Generation. Genetics. 2011 Jun 1;188(2):339–48.

197. Newnam GP, Wegrzyn RD, Lindquist SL, Chernoff YO. Antagonistic interactions between yeast chaperones Hsp104 and Hsp70 in prion curing. Mol Cell Biol. 1999 Feb;19(2):1325–33.

198. Jung G, Jones G, Wegrzyn RD, Masison DC. A role for cytosolic hsp70 in yeast [PSI(+)] prion propagation and [PSI(+)] as a cellular stress. Genetics. 2000 Oct;156(2):559–70.

199. Chernoff YO, Newnam GP, Kumar J, Allen K, Zink AD. Evidence for a protein mutator in yeast: role of the Hsp70-related chaperone ssb in formation, stability, and toxicity of the [PSI] prion. Mol Cell Biol. 1999 Dec;19(12):8103–12.

200. Chacinska A, Szczesniak B, Kochneva-Pervukhova NV, Kushnirov VV, Ter-Avanesyan MD, Boguta M. Ssb1 chaperone is a [PSI+] prion-curing factor. Curr Genet. 2001 Apr;39(2):62–7.

201. Fan Q, Park K-W, Du Z, Morano KA, Li L. The role of Sse1 in the de novo formation and variant determination of the [PSI+] prion. Genetics. 2007 Nov;177(3):1583–93.

202. Moran C, Kinsella GK, Zhang Z-R, Perrett S, Jones GW. Mutational Analysis of Sse1 (Hsp110) Suggests an Integral Role for this Chaperone in Yeast Prion Propagation In Vivo. G3 Genes Genomes Genet. 2013 Aug 1;3(8):1409–18.

203. Harris JM, Nguyen PP, Patel MJ, Sporn ZA, Hines JK. Functional Diversification of Hsp40: Distinct J-Protein Functional Requirements for Two Prions Allow for Chaperone-Dependent Prion Selection. PLoS Genet [Internet]. 2014 Jul 24 [cited 2017 Feb 10];10(7). Available from: http://www.ncbi.nlm.nih.gov/pmc/articles/PMC4109904/

204. Stein KC, True HL. Structural variants of yeast prions show conformer-specific requirements for chaperone activity. Mol Microbiol. 2014 Sep 1;93(6):1156–71.

205. Higurashi T, Hines JK, Sahi C, Aron R, Craig EA. Specificity of the J-protein Sis1 in the propagation of 3 yeast prions. Proc Natl Acad Sci U S A. 2008 Oct 28;105(43):16596–601.

206. Sporn ZA, Hines JK. Hsp40 function in yeast prion propagation: Amyloid diversity necessitates chaperone functional complexity. Prion. 2015 Mar 4;9(2):80–9.

207. Stein KC, True HL. Prion Strains and Amyloid Polymorphism Influence Phenotypic Variation. PLOS Pathog. 2014 Sep 4;10(9):e1004328.

208. Hines JK, Li X, Du Z, Higurashi T, Li L, Craig EA. [SWI+], the Prion Formed by the Chromatin Remodeling Factor Swi1, Is Highly Sensitive to Alterations in Hsp70 Chaperone System Activity. PLOS Genet. 2011 Feb 17;7(2):e1001309.

209. Roberts BT, Moriyama H, Wickner RB. [URE3] prion propagation is abolished by a mutation of the primary cytosolic Hsp70 of budding yeast. Yeast Chichester Engl. 2004 Jan 30;21(2):107–17.

210. Kryndushkin D, Wickner RB. Nucleotide exchange factors for Hsp70s are required for [URE3] prion propagation in Saccharomyces cerevisiae. Mol Biol Cell. 2007 Jun;18(6):2149–54.

211. Reidy M, Masison DC. Modulation and elimination of yeast prions by protein chaperones and co-chaperones. Prion. 2011;5(4):245–9.

212. Stein KC, Bengoechea R, Harms MB, Weihl CC, True HL. Myopathy-causing mutations in an HSP40 chaperone disrupt processing of specific client conformers. J Biol Chem. 2014 Jul 25;289(30):21120–30.

213. Rospert S, Dubaquié Y, Gautschi M. Nascent-polypeptide-associated complex. Cell Mol Life Sci CMLS. 2002 Oct;59(10):1632–9.

214. Pechmann S, Willmund F, Frydman J. The Ribosome as a Hub for Protein Quality Control. Mol Cell. 2013 Feb 7;49(3):411–21.

215. Beatrix B, Sakai H, Wiedmann M. The α and β Subunit of the Nascent Polypeptide-associated Complex Have Distinct Functions. J Biol Chem. 2000 Dec 1;275(48):37838–45.

216. Wiedmann B, Sakai H, Davis TA, Wiedmann M. A protein complex required for signal-sequence-specific sorting and translocation. Nature. 1994 Aug 11;370(6489):434–40.

217. George R, Beddoe T, Landl K, Lithgow T. The yeast nascent polypeptide-associated complex initiates protein targeting to mitochondria in vivo. Proc Natl Acad Sci. 1998 Mar 3;95(5):2296–301.

218. Reimann B, Bradsher J, Franke J, Hartmann E, Wiedmann M, Prehn S, et al. Initial characterization of the nascent polypeptide-associated complex in yeast. Yeast. 1999 Mar 30;15(5):397–407.

219. Kogan GL, Gvozdev VA. Multifunctional nascent polypeptide-associated complex (NAC). Mol Biol. 2014 Mar 1;48(2):189–96.

220. Raasi S, Pickart CM. Rad23 ubiquitin-associated domains (UBA) inhibit 26 S proteasome-catalyzed proteolysis by sequestering lysine 48-linked polyubiquitin chains. J Biol Chem. 2003 Mar 14;278(11):8951–9.

221. Panasenko O, Landrieux E, Feuermann M, Finka A, Paquet N, Collart MA. The Yeast Ccr4-Not Complex Controls Ubiquitination of the Nascent-associated Polypeptide (NAC-EGD) Complex. J Biol Chem. 2006 Oct 20;281(42):31389–98.

222. Panasenko OO, David FPA, Collart MA. Ribosome Association and Stability of the Nascent Polypeptide-Associated Complex Is Dependent Upon Its Own Ubiquitination. Genetics. 2009 Feb 1;181(2):447–60.

223. Wegrzyn RD, Hofmann D, Merz F, Nikolay R, Rauch T, Graf C, et al. A conserved motif is prerequisite for the interaction of NAC with ribosomal protein L23 and nascent chains. J Biol Chem. 2006 Feb 3;281(5):2847–57.

224. Pech M, Spreter T, Beckmann R, Beatrix B. Dual Binding Mode of the Nascent Polypeptide-associated Complex Reveals a Novel Universal Adapter Site on the Ribosome. J Biol Chem. 2010 Jun 18;285(25):19679–87.

225. Franke J, Reimann B, Hartmann E, Köhlerl M, Wiedmann B. Evidence for a nuclear passage of nascent polypeptide-associated complex subunits in yeast. J Cell Sci. 2001 Jul;114(Pt 14):2641–8.

226. Raue U, Oellerer S, Rospert S. Association of protein biogenesis factors at the yeast ribosomal tunnel exit is affected by the translational status and nascent polypeptide sequence. J Biol Chem. 2007 Mar 16;282(11):7809–16.

227. Koplin A, Preissler S, Ilina Y, Koch M, Scior A, Erhardt M, et al. A dual function for chaperones SSB–RAC and the NAC nascent polypeptide–associated complex on ribosomes. J Cell Biol. 2010 Apr 5;189(1):57–68.

228. Wiedmann B, Prehn S. The nascent polypeptide-associated complex (NAC) of yeast functions in the targeting process of ribosomes to the ER membrane. FEBS Lett. 1999 Sep 10;458(1):51–4.

229. Möller I, Jung M, Beatrix B, Levy R, Kreibich G, Zimmermann R, et al. A general mechanism for regulation of access to the translocon: competition for a membrane attachment site on ribosomes. Proc Natl Acad Sci U S A. 1998 Nov 10;95(23):13425–30.

230. Fünfschilling U, Rospert S. Nascent polypeptide-associated complex stimulates protein import into yeast mitochondria. Mol Biol Cell. 1999 Oct;10(10):3289–99.

231. Zheng XM, Moncollin V, Egly JM, Chambon P. A general transcription factor forms a stable complex with RNA polymerase B (II). Cell. 1987 Jul 31;50(3):361–8.

232. Quèlo I, Hurtubise M, St-Arnaud R. alphaNAC requires an interaction with c-Jun to exert its transcriptional coactivation. Gene Expr. 2002;10(5–6):255–62.

233. Yotov WV, Moreau A, St-Arnaud R. The alpha chain of the nascent polypeptide-associated complex functions as a transcriptional coactivator. Mol Cell Biol. 1998 Mar;18(3):1303–11.

234. Liu Y, Hu Y, Li X, Niu L, Teng M. The Crystal Structure of the Human Nascent Polypeptide-Associated Complex Domain Reveals a Nucleic Acid-Binding Region on the NACA Subunit,. Biochemistry (Mosc). 2010 Apr 6;49(13):2890–6.

235. Bloss TA, Witze ES, Rothman JH. Suppression of CED-3-independent apoptosis by mitochondrial betaNAC in Caenorhabditis elegans. Nature. 2003 Aug 28;424(6952):1066–71.

236. Deng JM, Behringer RR. An insertional mutation in the BTF3 transcription factor gene leads to an early postimplantation lethality in mice. Transgenic Res. 1995 Jul;4(4):264–9.

237. Markesich DC, Gajewski KM, Nazimiec ME, Beckingham K. bicaudal encodes the Drosophila beta NAC homolog, a component of the ribosomal translational machinery*. Dev Camb Engl. 2000 Feb;127(3):559–72.

238. Keefer KM, True HL. Unpublished data.

239. Ott A-K, Locher L, Koch M, Deuerling E. Functional Dissection of the Nascent Polypeptide-Associated Complex in Saccharomyces cerevisiae. PLOS ONE. 2015 Nov 30;10(11):e0143457.

240. Kirstein-Miles J, Scior A, Deuerling E, Morimoto RI. The nascent polypeptide-associated complex is a key regulator of proteostasis. EMBO J. 2013 May 15;32(10):1451–68.

241. Arsenovic PT, Maldonado AT, Colleluori VD, Bloss TA. Depletion of the C. elegans NAC engages the unfolded protein response, resulting in increased chaperone expression and apoptosis. PloS One. 2012;7(9):e44038.

242. Pfund C, Huang P, Lopez-Hoyo N, Craig EA. Divergent Functional Properties of the Ribosome-Associated Molecular Chaperone Ssb Compared with Other Hsp70s. Mol Biol Cell. 2001 Dec 1;12(12):3773–82.

243. Yan W, Schilke B, Pfund C, Walter W, Kim S, Craig EA. Zuotin, a ribosome-associated DnaJ molecular chaperone. EMBO J. 1998 Aug 17;17(16):4809–17.

244. Gautschi M, Lilie H, Fünfschilling U, Mun A, Ross S, Lithgow T, et al. RAC, a stable ribosome-associated complex in yeast formed by the DnaK-DnaJ homologs Ssz1p and zuotin. Proc Natl Acad Sci. 2001 Mar 27;98(7):3762–7.

245. Huang P, Gautschi M, Walter W, Rospert S, Craig EA. The Hsp70 Ssz1 modulates the function of the ribosome-associated J-protein Zuo1. Nat Struct Mol Biol. 2005 Jun;12(6):497–504.

246. Conz C, Otto H, Peisker K, Gautschi M, Wölfle T, Mayer MP, et al. Functional Characterization of the Atypical Hsp70 Subunit of Yeast Ribosome-associated Complex. J Biol Chem. 2007 Nov 23;282(47):33977–84.

247. Amor AJ, Castanzo DT, Delany SP, Selechnik DM, Ooy A van, Cameron DM. The ribosome-associated complex antagonizes prion formation in yeast. Prion. 2015 Apr;9(2):144.

248. Willmund F, del Alamo M, Pechmann S, Chen T, Albanèse V, Dammer EB, et al. The Cotranslational Function of Ribosome-Associated Hsp70 in Eukaryotic Protein Homeostasis. Cell. 2013 Jan 17;152(1–2):196–209.

249. Chernoff YO, Kiktev DA. Dual role of ribosome-associated chaperones in prion formation and propagation. Curr Genet. 2016 Nov 1;62(4):677–85.

250. Kiktev DA, Melomed MM, Lu CD, Newnam GP, Chernoff YO. Feedback control of prion formation and propagation by the ribosome-associated chaperone complex. Mol Microbiol. 2015 May 1;96(3):621–32.

251. Weyer FA, Gumiero A, Gesé GV, Lapouge K, Sinning I. Structural insights into a unique Hsp70-Hsp40 interaction in the eukaryotic ribosome-associated complex. Nat Struct Mol Biol. 2017 Feb;24(2):144–51.

252. Otto H, Conz C, Maier P, Wölfle T, Suzuki CK, Jenö P, et al. The chaperones MPP11 and Hsp70L1 form the mammalian ribosome-associated complex. Proc Natl Acad Sci U S A. 2005 Jul 19;102(29):10064–9.

253. Labbadia J, Morimoto RI. The Biology of Proteostasis in Aging and Disease. Annu Rev Biochem. 2015 Jun 2;84(1):435–64.

254. Chiti F, Dobson CM. Protein Misfolding, Functional Amyloid, and Human Disease. Annu Rev Biochem. 2006;75(1):333–66.

255. Cox BS. Ψ, A cytoplasmic suppressor of super-suppressor in yeast. Heredity. 1965 Nov;20(4):505–21.

256. Paushkin SV, Kushnirov VV, Smirnov VN, Ter-Avanesyan MD. Propagation of the yeast prion-like [psi+] determinant is mediated by oligomerization of the SUP35-encoded polypeptide chain release factor. EMBO J. 1996 Jun 17;15(12):3127–34.

257. Saibil HR, Seybert A, Habermann A, Winkler J, Eltsov M, Perkovic M, et al. Heritable yeast prions have a highly organized three-dimensional architecture with interfiber structures. Proc Natl Acad Sci. 2012 Sep 11;109(37):14906–11.

258. Vishveshwara N, Bradley ME, Liebman SW. Sequestration of essential proteins causes prion associated toxicity in yeast. Mol Microbiol. 2009 Sep;73(6):1101–14.

259. McGlinchey RP, Kryndushkin D, Wickner RB. Suicidal [PSI+] is a lethal yeast prion. Proc Natl Acad Sci U S A. 2011 Mar 29;108(13):5337–41.

260. Fedorov AN, Baldwin TO. Cotranslational Protein Folding. J Biol Chem. 1997 Dec 26;272(52):32715–8.

261. Kim YE, Hipp MS, Bracher A, Hayer-Hartl M, Hartl FU. Molecular Chaperone Functions in Protein Folding and Proteostasis. Annu Rev Biochem. 2013;82(1):323–55.

262. Rospert S, Dubaquié Y, Gautschi M. Nascent-polypeptide-associated complex. Cell Mol Life Sci CMLS. 2002 Oct 1;59(10):1632–9.

263. Nelson RJ, Ziegelhoffer T, Nicolet C, Werner-Washburne M, Craig EA. The translation machinery and 70 kd heat shock protein cooperate in protein synthesis. Cell. 1992 Oct 2;71(1):97–105.

264. Pfund C, Lopez-Hoyo N, Ziegelhoffer T, Schilke BA, Lopez-Buesa P, Walter WA, et al. The molecular chaperone Ssb from Saccharomyces cerevisiae is a component of the ribosome–nascent chain complex. EMBO J. 1998 Jul 15;17(14):3981–9.

265. Peisker K, Braun D, Wölfle T, Hentschel J, Fünfschilling U, Fischer G, et al. Ribosome-associated Complex Binds to Ribosomes in Close Proximity of Rpl31 at the Exit of the Polypeptide Tunnel in Yeast. Mol Biol Cell. 2008 Dec;19(12):5279–88.

266. Chernoff YO, Kiktev DA. Dual role of ribosome-associated chaperones in prion formation and propagation. Curr Genet. 2016 Mar 11;

267. Willmund F, del Alamo M, Pechmann S, Chen T, Albanèse V, Dammer EB, et al. The cotranslational function of ribosome-associated Hsp70 in eukaryotic protein homeostasis. Cell. 2013 Jan 17;152(1–2):196–209.

268. Bukau B, Deuerling E, Pfund C, Craig EA. Getting Newly Synthesized Proteins into Shape. Cell. 2000 Apr 14;101(2):119–22.

269. Guthrie C, Fink G. Guide to Yeast Genetics and Molecular Biology. San Diego, CA: Academic Press, Inc; 1991.

270. Dulle JE, Bouttenot RE, Underwood LA, True HL. Soluble oligomers are sufficient for transmission of a yeast prion but do not confer phenotype. J Cell Biol. 2013 Oct 28;203(2):197–204.

271. Westergard L, True HL. Wild yeast harbor a variety of distinct amyloid structures with strong prion-inducing capabilities. Mol Microbiol. 2014 Apr;92(1):183–93.

272. Lin CA, Ellis SR, True HL. The Sua5 Protein Is Essential for Normal Translational Regulation in Yeast. Mol Cell Biol. 2010 Jan 1;30(1):354–63.

273. Geiler-Samerotte KA, Dion MF, Budnik BA, Wang SM, Hartl DL, Drummond DA. Misfolded proteins impose a dosage-dependent fitness cost and trigger a cytosolic unfolded protein response in yeast. Proc Natl Acad Sci. 2011 Jan 11;108(2):680–5.

274. del Alamo M, Hogan DJ, Pechmann S, Albanese V, Brown PO, Frydman J. Defining the specificity of cotranslationally acting chaperones by systematic analysis of mRNAs associated with ribosome-nascent chain complexes. PLoS Biol. 2011 Jul;9(7):e1001100.

275. Stansfield I, Akhmaloka, Tuite MF. A mutant allele of the SUP45 (SAL4) gene of Saccharomyces cerevisiae shows temperature-dependent allosuppressor and omnipotent suppressor phenotypes. Curr Genet. 1995 Apr;27(5):417–26.

276. Liebman SW, Chernoff YO. Prions in yeast. Genetics. 2012 Aug;191(4):1041–72.

277. Stansfield I, Akhmaloka null, Tuite MF. A mutant allele of the SUP45 (SAL4) gene of Saccharomyces cerevisiae shows temperature-dependent allosuppressor and omnipotent suppressor phenotypes. Curr Genet. 1995 Apr;27(5):417–26.

278. Koplin A, Preissler S, Ilina Y, Koch M, Scior A, Erhardt M, et al. A dual function for chaperones SSB–RAC and the NAC nascent polypeptide–associated complex on ribosomes. J Cell Biol. 2010 Apr 5;189(1):57–68.

279. Schirmer EC, Lindquist S. Interactions of the chaperone Hsp104 with yeast Sup35 and mammalian PrP. Proc Natl Acad Sci U S A. 1997 Dec 9;94(25):13932–7.

280. Allen KD, Wegrzyn RD, Chernova TA, Müller S, Newnam GP, Winslett PA, et al. Hsp70 chaperones as modulators of prion life cycle: novel effects of Ssa and Ssb on the Saccharomyces cerevisiae prion [PSI+]. Genetics. 2005 Mar;169(3):1227–42.

281. Shorter J, Lindquist S. Hsp104, Hsp70 and Hsp40 interplay regulates formation, growth and elimination of Sup35 prions. EMBO J. 2008 Oct 22;27(20):2712–24.

282. Gautschi M, Mun A, Ross S, Rospert S. A functional chaperone triad on the yeast ribosome. Proc Natl Acad Sci. 2002 Apr 2;99(7):4209–14.

283. Jung G, Jones G, Wegrzyn RD, Masison DC. A role for cytosolic hsp70 in yeast [PSI(+)] prion propagation and [PSI(+)] as a cellular stress. Genetics. 2000 Oct;156(2):559–70.

284. Masison DC, Kirkland PA, Sharma D. Influence of Hsp70s and their regulators on yeast prion propagation. Prion. 2009;3(2):65–73.

285. Bagriantsev SN, Gracheva EO, Richmond JE, Liebman SW. Variant-specific [PSI+] Infection Is Transmitted by Sup35 Polymers within [PSI+] Aggregates with Heterogeneous Protein Composition. Mol Biol Cell. 2008 Jun 1;19(6):2433–43.

286. James P, Pfund C, Craig EA. Functional Specificity Among Hsp70 Molecular Chaperones. Science. 1997 Jan 17;275(5298):387–9.

287. Chernoff YO, Lindquist SL, Ono B-I, Inge-Vechtomov SG, Liebman SW. Role of the chaperone protein Hsp104 in propagation of the yeast prion-like factor [psi+]. Science. 1995;268(5212):880–4.

288. Chernoff YO, Newnam GP, Kumar J, Allen K, Zink AD. Evidence for a Protein Mutator in Yeast: Role of the Hsp70-Related Chaperone Ssb in Formation, Stability, and Toxicity of the [PSI] Prion. Mol Cell Biol. 1999 Dec 1;19(12):8103–12.

289. Newnam GP, Wegrzyn RD, Lindquist SL, Chernoff YO. Antagonistic Interactions between Yeast Chaperones Hsp104 and Hsp70 in Prion Curing. Mol Cell Biol. 1999 Feb;19(2):1325–33.

290. Zakharov IA, Yarovoy BP. Cytoduction as a new tool in studying the cytoplasmic heredity in yeast. Mol Cell Biochem. 1977 Feb 4;14(1–3):15–8.

291. Ferreira PC, Ness F, Edwards SR, Cox BS, Tuite MF. The elimination of the yeast [PSI+] prion by guanidine hydrochloride is the result of Hsp104 inactivation. Mol Microbiol. 2001 Jun;40(6):1357–69.

292. Fowden L, Lewis D, Tristram H. Toxic Amino Acids: Their Action as Antimetabolites. In: Nord FF, editor. Advances in Enzymology and Related Areas of Molecular Biology [Internet]. John Wiley & Sons, Inc.; 1967 [cited 2016 Feb 26]. p. 89–163. Available from: http://onlinelibrary.wiley.com/doi/10.1002/9780470122747.ch3/summary

293. Amor AJ, Castanzo DT, Delany SP, Selechnik DM, Ooy A van, Cameron DM. The ribosome-associated complex antagonizes prion formation in yeast. Prion. 2015 Mar 4;9(2):144–64.

294. Sharma D, Masison DC. Hsp70 Structure, Function, Regulation and Influence on Yeast Prions. Protein Pept Lett. 2009;16(6):571–81.

295. Kampinga HH, Craig EA. The Hsp70 chaperone machinery: J-proteins as drivers of functional specificity. Nat Rev Mol Cell Biol. 2010 Aug;11(8):579–92.

296. Caughey B, Lansbury PT. Protofibrils, pores, fibrils, and neurodegeneration: separating the responsible protein aggregates from the innocent bystanders. Annu Rev Neurosci. 2003;26:267–98.

297. Goloudina AR, Demidov ON, Garrido C. Inhibition of HSP70: A challenging anti-cancer strategy. Cancer Lett. 2012 Dec 28;325(2):117–24.

298. Jinwal UK, Akoury E, Abisambra JF, O'Leary JC, Thompson AD, Blair LJ, et al. Imbalance of Hsp70 family variants fosters tau accumulation. FASEB J Off Publ Fed Am Soc Exp Biol. 2013 Apr;27(4):1450–9.

299. Fontaine SN, Rauch JN, Nordhues BA, Assimon VA, Stothert AR, Jinwal UK, et al. Isoform-selective Genetic Inhibition of Constitutive Cytosolic Hsp70 Activity Promotes Client Tau Degradation Using an Altered Co-chaperone Complement. J Biol Chem. 2015 May 22;290(21):13115–27.

300. Kirstein-Miles J, Scior A, Deuerling E, Morimoto RI. The nascent polypeptide-associated complex is a key regulator of proteostasis. EMBO J. 2013 May 15;32(10):1451–68.

301. Ott A-K, Locher L, Koch M, Deuerling E. Functional Dissection of the Nascent Polypeptide-Associated Complex in Saccharomyces cerevisiae. PLoS ONE. 2015 Nov 30;10(11):e0143457.

302. Derkatch IL, Chernoff YO, Kushnirov VV, Inge-Vechtomov SG, Liebman SW. Genesis and variability of [PSI] prion factors in Saccharomyces cerevisiae. Genetics. 1996 Dec;144(4):1375–86.

303. Stein KC, True HL. Extensive Diversity of Prion Strains Is Defined by Differential Chaperone Interactions and Distinct Amyloidogenic Regions. PLoS Genet. 2014 May 8;10(5):e1004337.

304. Hattendorf DA, Lindquist SL. Cooperative kinetics of both Hsp104 ATPase domains and interdomain communication revealed by AAA sensor-1 mutants. EMBO J. 2002 Jan 15;21(1–2):12–21.

305. Horton LE, James P, Craig EA, Hensold JO. The yeast hsp70 homologue Ssa is required for translation and interacts with Sis1 and Pab1 on translating ribosomes. J Biol Chem. 2001 Apr 27;276(17):14426–33.

306. Vilardell J, Warner JR. Ribosomal protein L32 of Saccharomyces cerevisiae influences both the splicing of its own transcript and the processing of rRNA. Mol Cell Biol. 1997 Apr;17(4):1959–65.

307. Tkach JM, Glover JR. Amino Acid Substitutions in the C-terminal AAA+ Module of Hsp104 Prevent Substrate Recognition by Disrupting Oligomerization and Cause High Temperature Inactivation. J Biol Chem. 2004 Aug 20;279(34):35692–701.

308. Ross-Macdonald P, Sheehan A, Roeder GS, Snyder M. A multipurpose transposon system for analyzing protein production, localization, and function in Saccharomyces cerevisiae. Proc Natl Acad Sci U S A. 1997 Jan 7;94(1):190–5.

309. Stein KC, True HL. Prion Strains and Amyloid Polymorphism Influence Phenotypic Variation. PLOS Pathog. 2014 Sep 4;10(9):e1004328.

310. Gorman JA, Clark PE, Lee MC, Debouck C, Rosenberg M. Regulation of the yeast metallothionein gene. Gene. 1986;48(1):13–22.

311. Huang VJ, Stein KC, True HL. Spontaneous Variants of the [RNQ+] Prion in Yeast Demonstrate the Extensive Conformational Diversity Possible with Prion Proteins. PLoS ONE. 2013 Oct 25;8(10):e79582.

312. Craig EA, Huang P, Aron R, Andrew A. The diverse roles of J-proteins, the obligate Hsp70 co-chaperone. Rev Physiol Biochem Pharmacol. 2006;156:1–21.

313. Sharma D, Masison DC. Hsp70 Structure, Function, Regulation and Influence on Yeast Prions. Protein Pept Lett. 2009;16(6):571–81.

314. Dragovic Z, Broadley SA, Shomura Y, Bracher A, Hartl FU. Molecular chaperones of the Hsp110 family act as nucleotide exchange factors of Hsp70s. EMBO J. 2006 Jun 7;25(11):2519–28.

315. Keefer KM, True HL. Prion-Associated Toxicity is Rescued by Elimination of Cotranslational Chaperones. PLOS Genet. 2016 Nov 9;12(11):e1006431.

316. Andréasson C, Fiaux J, Rampelt H, Mayer MP, Bukau B. Hsp110 Is a Nucleotide-activated Exchange Factor for Hsp70. J Biol Chem. 2008 Apr 4;283(14):8877–84.

317. Bukau B, Weissman J, Horwich A. Molecular Chaperones and Protein Quality Control. Cell. 2006 May 5;125(3):443–51.

318. James P, Pfund C, Craig EA. Functional specificity among Hsp70 molecular chaperones. Science. 1997 Jan 17;275(5298):387–9.

319. Cyr DM, Douglas MG. Differential regulation of Hsp70 subfamilies by the eukaryotic DnaJ homologue YDJ1. J Biol Chem. 1994 Apr 1;269(13):9798–804.

320. Shorter J, Lindquist S. Hsp104, Hsp70 and Hsp40 interplay regulates formation, growth and elimination of Sup35 prions. EMBO J. 2008 Oct 22;27(20):2712–24.

321. Rutherford SL, Lindquist S. Hsp90 as a capacitor for morphological evolution. Nature. 1998 Nov 26;396(6709):336–42.

322. Newnam GP, Wegrzyn RD, Lindquist SL, Chernoff YO. Antagonistic Interactions between Yeast Chaperones Hsp104 and Hsp70 in Prion Curing. Mol Cell Biol. 1999 Feb 1;19(2):1325–33.

323. Johnson CR, Weems AD, Brewer JM, Thorner J, McMurray MA. Cytosolic chaperones mediate quality control of higher-order septin assembly in budding yeast. Mol Biol Cell. 2015 Apr 1;26(7):1323–44.

324. Feder JH, Rossi JM, Solomon J, Solomon N, Lindquist S. The consequences of expressing hsp70 in Drosophila cells at normal temperatures. Genes Dev. 1992 Aug;6(8):1402–13.

325. Morimoto RI. Proteotoxic stress and inducible chaperone networks in neurodegenerative disease and aging. Genes Dev. 2008 Jun 1;22(11):1427–38.

326. Johnson JL, Zuehlke AD, Tenge VR, Langworthy JC. Mutation of essential Hsp90 co-chaperones SGT1 or CNS1 renders yeast hypersensitive to overexpression of other co-chaperones. Curr Genet. 2014 Nov 1;60(4):265–76.

327. Mahalingam D, Swords R, Carew JS, Nawrocki ST, Bhalla K, Giles FJ. Targeting HSP90 for cancer therapy. Br J Cancer. 2009 May 19;100(10):1523–9.

328. Ebrahimi-Fakhari D, Wahlster L, McLean PJ. Molecular Chaperones in Parkinson's Disease – Present and Future. J Park Dis. 2011 Nov;1(4):299–320.

329. Rappa F, Farina F, Zummo G, David S, Campanella C, Carini F, et al. HSP-molecular chaperones in cancer biogenesis and tumor therapy: an overview. Anticancer Res. 2012 Dec;32(12):5139–50.

330. Lindberg I, Shorter J, Wiseman RL, Chiti F, Dickey CA, McLean PJ. Chaperones in Neurodegeneration. J Neurosci. 2015 Oct 14;35(41):13853–9.

331. Sikorski RS, Hieter P. A system of shuttle vectors and yeast host strains designed for efficient manipulation of DNA in Saccharomyces cerevisiae. Genetics. 1989 May;122(1):19–27.

332. Götz J, Chen F, van Dorpe J, Nitsch RM. Formation of neurofibrillary tangles in P301l tau transgenic mice induced by Abeta 42 fibrils. Science. 2001 Aug 24;293(5534):1491–5.

333. Ono K, Takahashi R, Ikeda T, Yamada M. Cross-seeding effects of amyloid β-protein and α-synuclein. J Neurochem. 2012 Sep;122(5):883–90.

334. Derkatch IL, Liebman SW. Prion-Prion Interactions. Prion. 2007;1(3):161–9.

335. Osherovich LZ, Cox BS, Tuite MF, Weissman JS. Dissection and Design of Yeast Prions. PLOS Biol. 2004 Mar 23;2(4):e86.

336. Osherovich LZ, Weissman JS. The Utility of Prions. Dev Cell. 2002 Feb;2(2):143–51.

337. Choe Y-J, Ryu Y, Kim H-J, Seok Y-J. Increased [PSI+] Appearance by Fusion of Rnq1 with the Prion Domain of Sup35 in Saccharomyces cerevisiae. Eukaryot Cell. 2009 Jul 1;8(7):968–76.

338. Glover JR, Kowal AS, Schirmer EC, Patino MM, Liu JJ, Lindquist S. Self-seeded fibers formed by Sup35, the protein determinant of [PSI+], a heritable prion-like factor of S. cerevisiae. Cell. 1997 May 30;89(5):811–9.

339. Kalastavadi T, True HL. Analysis of the [RNQ+] Prion Reveals Stability of Amyloid Fibers as the Key Determinant of Yeast Prion Variant Propagation. J Biol Chem. 2010 Jul 2;285(27):20748–55.

340. Dulle JE, Bouttenot RE, Underwood LA, True HL. Soluble oligomers are sufficient for transmission of a yeast prion but do not confer phenotype. J Cell Biol. 2013 Oct 28;203(2):197–204.

341. Tank EMH, Harris DA, Desai AA, True HL. Prion Protein Repeat Expansion Results in Increased Aggregation and Reveals Phenotypic Variability. Mol Cell Biol. 2007 Aug 1;27(15):5445–55.

342. Kalastavadi T, True HL. Prion protein insertional mutations increase aggregation propensity but not fiber stability. BMC Biochem. 2008;9:7.

343. Lindgren M, Sörgjerd K, Hammarström P. Detection and characterization of aggregates, prefibrillar amyloidogenic oligomers, and protofibrils using fluorescence spectroscopy. Biophys J. 2005 Jun;88(6):4200–12.

344. Kurahashi H, Pack C-G, Shibata S, Oishi K, Sako Y, Nakamura Y. [PSI(+)] aggregate enlargement in rnq1 nonprion domain mutants, leading to a loss of prion in yeast. Genes Cells Devoted Mol Cell Mech. 2011 May;16(5):576–89.

345. Shibata S, Kurahashi H, Nakamura Y. Localization of prion-destabilizing mutations in the N-terminal non-prion domain of Rnq1 in Saccharomyces cerevisiae. Prion. 2009 Dec;3(4):250–8.

346. Stein KC, True HL. Extensive Diversity of Prion Strains Is Defined by Differential Chaperone Interactions and Distinct Amyloidogenic Regions. PLOS Genet. 2014 May 8;10(5):e1004337.

347. Bardill JP, True HL. Heterologous Prion Interactions Are Altered by Mutations in the Prion Protein Rnq1p. J Mol Biol. 2009 May 8;388(3):583–96.

348. Inge-Vechtomov SG, Tikhodeev ON, Karpova TS. [Selective systems for obtaining recessive ribosomal suppressors in saccharomycete yeasts]. Genetika. 1988 Jul;24(7):1159–65.

349. Masison DC, Kirkland PA, Sharma D. Influence of Hsp70s and their regulators on yeast prion propagation. Prion. 2009;3(2):65–73.

350. Toyama BH, Kelly MJS, Gross JD, Weissman JS. The structural basis of yeast prion strain variants. Nature. 2007 Sep 13;449(7159):233–7.

351. Sharma J, Liebman SW. Exploring the basis of [PIN+] variant differences in [PSI+] induction. J Mol Biol. 2013 Sep 9;425(17):3046–59.

352. Characterization of De Novo Aggregation of Prions and Protein Misfolding Disease Proteins in Yeast [Internet]. 2014. Available from: http://hdl.handle.net/10027/19351

353. Du Z, Zhang Y, Li L. The Yeast Prion [SWI+] Abolishes Multicellular Growth by Triggering Conformational Changes of Multiple Regulators Required for Flocculin Gene Expression. Cell Rep. 2015 Dec;13(12):2865–78.

354. Banning C, Votteler J, Hoffmann D, Koppensteiner H, Warmer M, Reimer R, et al. A Flow Cytometry-Based FRET Assay to Identify and Analyse Protein-Protein Interactions in Living Cells. PLoS ONE [Internet]. 2010 Feb 22 [cited 2017 Feb 22];5(2). Available from: http://www.ncbi.nlm.nih.gov/pmc/articles/PMC2825263/

355. Matsumoto G, Kim S, Morimoto RI. Huntingtin and Mutant SOD1 Form Aggregate Structures with Distinct Molecular Properties in Human Cells. J Biol Chem. 2006 Feb 17;281(7):4477–85.

356. Meriin AB, Zhang X, He X, Newnam GP, Chernoff YO, Sherman MY. Huntington toxicity in yeast model depends on polyglutamine aggregation mediated by a prion-like protein Rnq1. J Cell Biol. 2002 Jun 10;157(6):997–1004.

357. Lopez N, Aron R, Craig EA. Specificity of class II Hsp40 Sis1 in maintenance of yeast prion [RNQ+]. Mol Biol Cell. 2003 Mar;14(3):1172–81.

358. Johnson BS, McCaffery JM, Lindquist S, Gitler AD. A yeast TDP-43 proteinopathy model: Exploring the molecular determinants of TDP-43 aggregation and cellular toxicity. Proc Natl Acad Sci U S A. 2008 Apr 29;105(17):6439–44.

359. Konopka CA, Locke MN, Gallagher PS, Pham N, Hart MP, Walker CJ, et al. A yeast model for polyalanine-expansion aggregation and toxicity. Mol Biol Cell. 2011 Jun 15;22(12):1971–84.

360. Outeiro TF, Lindquist S. Yeast cells provide insight into alpha-synuclein biology and pathobiology. Science. 2003 Dec 5;302(5651):1772–5.

361. Chung CY, Khurana V, Auluck PK, Tardiff DF, Mazzulli JR, Soldner F, et al. Identification and Rescue of α-Synuclein Toxicity in Parkinson Patient–Derived Neurons. Science. 2013 Nov 22;342(6161):983–7.

362. Khurana V, Tardiff DF, Chung CY, Lindquist S. Toward stem cell-based phenotypic screens for neurodegenerative diseases. Nat Rev Neurol. 2015 Jun;11(6):339–50.